The transcription factor, FixK, plays a central role in carbon source metabolism and cellulose synthesis in *Komagataeibacter* species

by

Andrew James Varley

A Thesis Submitted in Partial Fulfillment

of the Requirements for the Degree of

Masters of Science

In

The Faculty of Science

Applied Biosciences

University of Ontario Institute of Technology

July 2017

UNIVERSITY OF ONTARIO
INSTITUTE OF TECHNOLOGY

Abstract

Komagataeibacter xylinus ATCC 53582 and *K. hansenii* ATCC 23769 are model bacterial cellulose producers. This thesis investigated both carbon source utilization and the role that a Crp/Fnr transcription factor, FixK, plays in bacterial cellulose biosynthesis. Extracellular proteins secreted by *Komagataeibacter* were assayed for degradative activity against plant cell wall compounds. Mutagenesis of *fixK*, previously associated with cellulose regulation, revealed its role in cellular metabolism. Growth, pH, gluconic acid, and cellulose yield were measured in static and agitated cultures grown in the presence of glucose, fructose or sucrose. BcsZ (formerly CmcAx) was found to be carbon-source regulated. *K. hansenii* was dependent on *fixK* for growth in fructose and sucrose, but not in glucose. Mutation of *fixK* abolished cellulose production in *K. hansenii*, but limited production in *K. xylinus*. Altogether, this study improves our understanding of carbon source utilization and bacterial cellulose synthesis in *Komagataeibacter* species.

Keywords

Komagataeibacter xylinus ATCC 53582

Komagataeibacter hansenii ATCC23769

Bacterial cellulose

bcs operon

Crp/Fnr

fixK

Reverse genetics

Carbon source metabolism

Plant cell wall degradation

Plant-microbe interaction

Gluconic acid

Biofilm

Zymography

Acknowledgements

I am deeply grateful to Dr. Janice Strap for her guidance, support, and caring mentorship over the course of my research. Both her input and faith in my approaches towards new experiments has been monumental in building my capabilities as a scientist. When the going gets tough, she's always welcoming to keep you motivated and focused. I have thoroughly enjoyed our discussions about life both in and outside of the lab. I would also like to thank my committee, Dr. Dario Bonetta and Dr. Julia Green-Johnson for their constructive comments, suggestions and time they have put in reviewing my work. They have both been welcoming with the use of their incubators, centrifuges, microscopes and small equipment that has made this research possible. Many thanks go out to my labmates throughout my time in the lab, particularly Richard Augimeri and Sierra Dargan. Richard taught me the ways of the lab and was always excited to share the knowledge he acquired during his Masters. Sierra's abilities with protein electrophoresis has provided new insights for this research will be continued in my PhD work. She has also been a wonderfully supportive girlfriend throughout my entire Masters research through proofreading, being an extra hand in the lab and keeping me nourished during stressful times. I would also like to thank Dr. Franco Gaspari and Dr. Simone Quaranta for the use and instruction of the FT-IR spectrometer. Additionally, the biology teaching staff have been very kind with lending equipment while ours has been under repair. Lastly, I would like to thank my parents for their encouragement and support throughout not only my university career, but also encouraging me to problem solve since I was a child. I am grateful for the time I have spent in the Molecular Microbial Biochemistry Laboratory here at the University of Ontario Institute of Technology and am eager to continue in academia.

Table of Contents

List of Tables

List of Figures

List of Appendices

Tables

Figures

List of Abbreviations

ATCC – American Tissue Culture Collection

ALI – Air liquid interface

BC – Bacterial cellulose

bp – Base pair

c-di-GMP – Bis-(3'→5')-cyclic diguanylate monophosphate

cAMP – Cyclic adenosine monophosphate

cDNA – Complimentary deoxyribonucleic acid

CMC – Carboxymethyl cellulose

Crp/Fnr – Cyclic AMP receptor protein and fumarate-nitrate reductase

Δ*fixK* – disruption mutant of *fixK*

DBD – DNA binding domain

DGC – Diguanylate cyclase

DMSO – Dimethyl sulfoxide

DNA – Deoxyribonucleic acid

EDTA – Ethylenediaminetetraacetic acid

gDNA – Genomic deoxyribonucleic acid

kDa – Kilodaltons

LME – Lignin modifying enzyme

MIC – Minimum inhibitory concentration

mRNA – Messenger ribonucleic acid

MW – Molecular weight

OD600 – Optical density (absorbance) at 600 nm

PCR – Polymerase chain reaction

PCWC – Plant cell wall compound

PCWDE – Plant cell wall degrading enzyme

PDE – Phosphodiesterase

RNA – Ribonucleic acid

SD – Standard deviation

SDS-PAGE – Sodium dodecyl sulfate polyacrylamide gel electrophoresis

SH – Schramm and Hestrin medium

TF – Transcription factor

TM – Transmembrane

UDP – Uridine diphosphate

WT – Wildtype

1. Introduction

1.1. Cellulose

1.1.1. Characteristics

Cellulose is the most common organic polymer on Earth. It is produced by both plants and microorganisms for an annual biomass production of approximately one million kilograms (Klemm et al., 2005). This abundant polysaccharide is a homopolymer of glucopyranose monomers connected through β-1,4-glycosidic linkages. Extensive intermolecular H-bonding between microfibril strands imparts the high crystallinity and strength observed in cellulose. Several polymorphs of cellulose exist, characterized by their stability, crystallinity, orientation, and H-bonding patterns (Kroon-Batenburg and Kroon, 1997). Native cellulose contains highly ordered H-bonding patterns (Figure 1) and is subdivided into two allomorphs cellulose I_α and I_β (Horikawa and Sugiyama, 2009). Both allomorphs coexist together within individual microfibrils (Imai and Sugiyama, 1998) and the transitions between I_α and I_β can be observed between adjacent H-bonded molecular sheets (Imai and Sugiyama, 1998). In contrast to cellulose I, cellulose II is less commonly found in nature (Brown Jr, 1996; Kuga et al., 1993), but can be artificially formed after re-crystallization or mercerization with aqueous sodium hydroxide. Cellulose II is thermodynamically more stable and as such, the chemical conversion of cellulose II back to cellulose I has been unsuccessful (Brown Jr, 1996; O'Sullivan, 1997; Yu and Atalla, 1996).

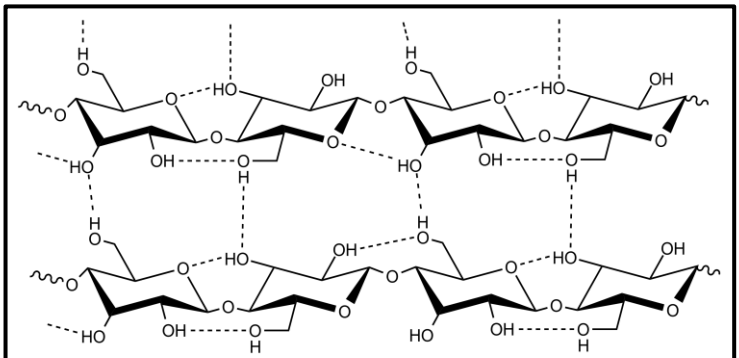

Figure 1: Native cellulose, dotted lines represent H-bonding. Adapted from Lu et al. (2014)

1.1.2. Plant cellulose

The high crystallinity and strength of cellulose provides structural support as the primary skeletal component of plant cell walls (Keegstra et al., 1973; Shokri and Adibkia, 2013; Talmadge et al., 1973). The renewability of plant-sourced cellulose provides a nearly inexhaustible raw material for a wide variety of applications. Everyday uses of plant cellulose include papers, textiles, filters, and cholesterol-regulating dietary fiber (Brown et al., 1999). In the pharmaceutical industry,

pure cellulose and its derivatives are currently utilized for drug delivery, gelling, stabilizing, filling, and taste masking agents (Shokri and Adibkia, 2013). Plant cellulose is also used extensively for biofuel production, where agricultural waste is treated to extract cellulose as a feedstock for bioethanol production. To produce ethanol from cellulose, it must first be hydrolyzed into glucose which can then fermented into ethanol by yeast (Jørgensen et al., 2007).

Plant cell walls use cellulose as a scaffolding material not only for its strength but also for its relatively high resistance to enzymatic attack (Corner, 1935; Cosgrove, 2005). To facilitate the extensibility of walls and improve resistance to disease, enzyme attack, and desiccation, plants form a lignocellulosic matrix that incorporates a range of hemicelluloses, pectins, and lignin (Cosgrove, 2005; Hammerschmidt and Kuć, 1982; Link and Walker, 1933; Vorwerk et al., 2004; Wardrop, 1971). These plant cell wall compounds (PCWC) are found complexed with cellulose and form a major roadblock for widespread biofuel production. As discussed, bioethanol is produced through the hydrolysis of cellulose; however, the recalcitrance of this lignocellulosic biomass prevents effective degradation of cellulose as PCWCs prevent enzymes from effectively degrading entrapped cellulose. The isolation of cellulose requires physical treatments and strong alkaline solutions that are both environmentally and economically costly.

1.1.3. Bacterial cellulose

Over a dozen genera of bacteria are known to produce bacterial cellulose (BC), the most prominent of which belong to the phylum *Proteobacteria* (Ausmees et al., 1999; Deinema and Zevenhuizen, 1971; Jahn et al., 2011; Matthysse et al., 1995; Napoli et al., 1975; Nobles et al., 2001; Ross et al., 1991; Zogaj et al., 2001). In contrast to plant cellulose, BC is synthesized with a higher degree of polymerization and is produced as a pure polysaccharide free from hemicelluloses, pectins, and lignin. The absence of PCWCs provides BC with unique characteristics such as a higher water holding capacity and more extensive H-bonding between cellulose strands, leading to the higher crystallinity and strength seen in BC. These advantages facilitate applications for BC in the biomedical field (wound dressing, bone grafting, etc.) and high-end manufacturing (speakers, electronic paper, organic light-emitting diodes, etc.). Like plant cellulose, BC can be enzymatically degraded into glucose; however unlike plant cellulose, there is no need for harsh pre-treatments to remove PCWC. Unfortunately, the significant financial barrier for mass production of BC largely overshadows these advantages. The model organisms for BC require a growth medium that is rich in nutrients and high in glucose, the monomer unit of cellulose.

1.2. Cellulose biosynthesis in *Komagataeibacter*

1.2.1. Characterization and habitat

The model organism for BC production is the α-*proteobacterium, Komagataeibacter xylinus* (formerly *Gluconacetobacter xylinus*, historically *Acetobacter xylinus*). *K. xylinus* and another BC model species, *K. hansenii*, are rod shaped Gram-negative bacteria that measure 0.5-0.8 x 1.0-3.0 μm; as members of the *Acetobacteraceae* family, they grow well in the presence of 0.35% (v/v) acetic acid (Asai and Shoda, 1958; Cleenwerck et al., 2009; Mamlouk and Gullo, 2013; Steel and Walker, 1957; Yamada et al., 2012a). While only some *Komagataeibacter* species require acetic acid for growth, they all produce it from the fermentation of ethanol (Yamada et al., 2012a). In 2012, twelve *Gluconacetobacter* species were subdivided into a new genus originally proposed as *Komagatabacter* (for contributions by Dr. Komagata; Yamada et al., 2012a), but later designated as *Komagataeibacter* based on phylogenetic, phenotypic, and ecological traits (Yamada et al., 2012b). A notable difference between *Komagataeibacter* and *Gluconacetobacter* is the lack of motility in *Komagataeibacter* species due to the absence of flagella. In contrast, all *Gluconacetobacter* species studied for taxonomic redistribution by Yamada et al. (Yamada et al., 2012a) produce peritrichous flagella.

Komagataeibacter xylinus are typically found living within the carposphere (fruit bearing region) of plants and thrive when the plants rot. They obtain energy and nutrients from plant exudate and the breakdown of polysaccharides during plant senescence. For the survival of the bacterial strains, this means they must relocate once their food source has been exhausted and since they do not produce flagella, *Komagataeibacter* species must rely solely on other means of transportation to colonize fruits. As acid tolerant bacteria, it has been proposed that they survive within the guts of insects such as *Drosophila* which are known to preferentially deposit bacteria on the wounds of fruit where nutrients are plentiful (Augimeri et al., 2015; Janisiewicz et al., 1999).

Amazingly, these seemingly non-motile bacteria are still able to reach the surface of a liquid when grown in aqueous media. Three possibilities for this phenomenon exist. Cellulose may adsorb carbon dioxide that is released by metabolizing cells, providing buoyancy to the cells by raising the submerged cellulose net to the liquid's surface (Schramm and Hestrin, 1954). Alternatively, I propose that they may physically propel themselves to the surface of a liquid by the synthesis of a BC network. Videos that depict cellular propulsion via cellulose synthesis (Brown Jr, 2013), and personal observations suggest that cellulose synthesis plays a role in their ability to reach the surface;

in small cultures, a cellulosic mold of the culture vessel is observed. Lastly, they may be able to adjust cellular buoyancy as studies with cyanobacteria have shown that low intracellular cyclic-diguanylate monophosphate (c-di-GMP) levels enhanced buoyancy (Agostoni et al., 2016). Regardless of how they reach the surface, once present they produce a BC pellicle at the air liquid interface (ALI) in liquid cultures (Gromet-Elhanan and Hestrin, 1963). When the pellicle at the ALI is removed, a globular cellulose network can often be found in the growth medium which, when grown in small vessels, is bound to the pellicle (observations from our lab).

Williams and Cannon (1989) proposed two roles for the cellulose-rich biofilm produced by *Komagataeibacter xylinus*. They identified a correlation between enhanced cellulose production and an improved ability to inhibit the number of colony forming units of competing organisms on apple slices. Secondly, *K. xylinus* strains that produced cellulose had a significantly improved ability to protect themselves from ultraviolet radiation. Given that cellulose is synthesized from glucose, it carries a heavy metabolic cost; biosynthesis must be controlled by environmental signals to ensure sugars are not wasted. Identifying the environmental triggers and the regulatory pathways for BC production are key steps to improving the efficiency and rate of BC biosynthesis in these organisms.

1.2.2. Carbon sources for cellulose biosynthesis

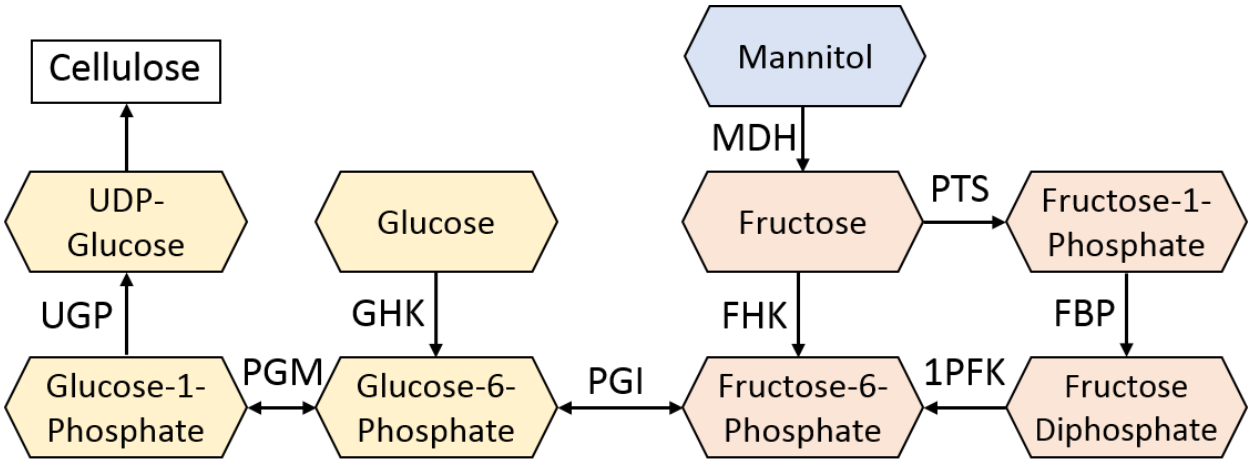

Figure 2: Cellulose biosynthesis pathways from either glucose or fructose. Abbreviated enzymes/systems are as follows: **GHK**, Glucose Hexokinase; **PGM**, Phosphogluocomutase; **UGP**, UDP-Glucose Pyrophosphorylase; **PTS**, Fructose-specific Phosphotransferase System; **FBP**, Fructose Bis-Phosphate; **1PFK**, 1-Phosphofructokinase; **FHK**, Fructose Hexokinase; **PGI**, Phosphoglucose Isomerase; **MDH**, Mannitol 2-Dehydrogenase.

Bacterial cellulose is synthesized by the polymerization of glucose from uridine diphosphate glucose (UDP-glucose) into β-1,4-glucan chains. Although glucose is the most efficient sugar for BC biosynthesis, other sugars such as fructose can be enzymatically converted into glucose

(Tonouchi et al., 1996; Figure 2). Since carbon sources used for BC production represent a large financial investment, potential feedstocks are of key interest. A study by Keshk and Sameshima (2005) investigated the cellulose yield, production efficiency, and crystallinity index of cellulose produced by *K. xylinus* as well as the carbon source consumption rate when grown in Schramm-Hestrin (SH; standard glucose rich growth medium for *K. xylinus*) medium with alternative carbon sources. They found that glycerol, glucose, fructose, and inositol produced the highest yield out of 16 carbon sources tested. When glycerol or fructose replaced glucose, 155% or 95% cellulose yield was obtained, respectively. The final pH of growth media was also quite different depending on carbon source. Cultures containing glucose resulted in the lowest pH of 3.9, while fructose, inositol, and glycerol grown cultures were near pH 5.5. Since *K. xylinus* is known to produce large amounts of gluconic acid from glucose, the similar cellulose yield in fructose and glucose media suggest that the total energy-loss of converting fructose into glucose-6-phosphate in a fructose-containing medium is nearly equal to that of oxidizing glucose into gluconic acid in a glucose-containing medium. To this end, multiple studies have shown that the rate of consumption of carbon-source plays a role in cellulose production as lower consumption rates correspond to higher efficiency (Keshk and Sameshima, 2005; Pourramezan et al., 2009). Additionally, studies have identified that the monomer sugars found in hemicelluloses and pectins (galactose, xylose, mannose, etc.) are suitable for cellulose biosynthesis (Ishihara et al., 2002; Keshk and Sameshima, 2005; Mikkelsen et al., 2009) meaning that the degradation of these polysaccharides would provide an additional nutrient source for *Komagataeibacter* species.

1.2.3. Cellulose biosynthesis

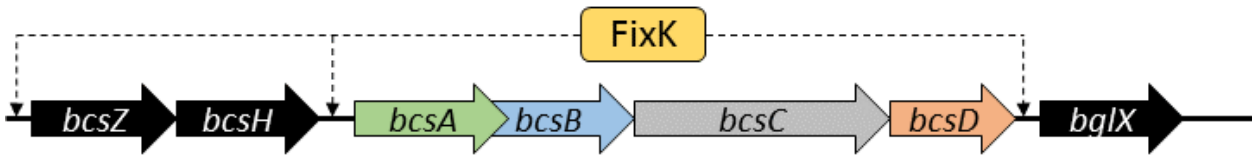

Figure 3: Bacterial cellulose synthase (*bcs*) type I operon, genes approximately to scale. In some species, *bcsA* and *bcsB* are fused to form *bcsAB*. Genes are colour coded to match Figure 5. Adapted from Augimeri & Strap (2015)

Komagataeibacter species synthesize crystalline cellulose using BcsAB, BcsC, BcsD, BcsH (cellulose-complimenting protein; previously CcpAx), BcsZ (an endoglucanase; previously CMCax), and BglX (a β-glucosidase) (Augimeri et al., 2015; Saxena et al., 1990, 1994; Wong et al., 1990). BcsAB, BcsC, and BcsD form the bacterial cellulose synthase (BCS) holoenzyme than spans

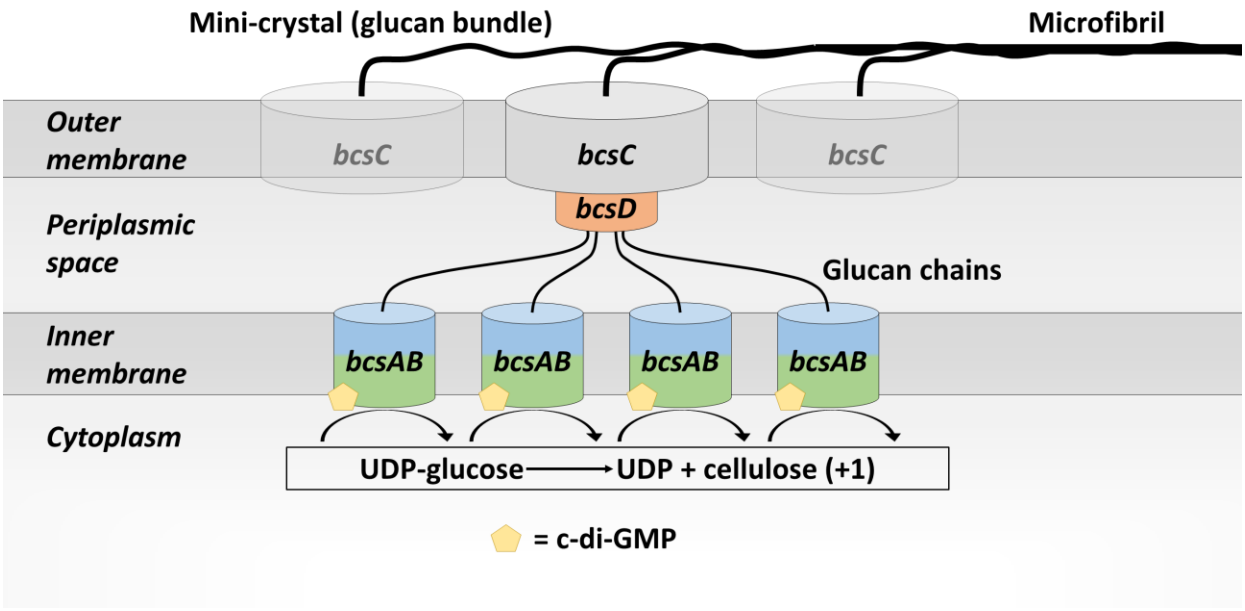

Figure 4: *K. xylinus* cellulose synthase holoenzyme complex depicting locations of individual proteins. The conversion of UDP-glucose into UDP + cellulose (+1) is regulated by the second messenger cyclic-diguanylate monophosphate (c-di-GMP). Four nascent glucan chains can pass through a single periplasmic BcsD homo octamer to form a mini-crystal. At least three mini-crystals form along linearly arranged *bcsC* to form a microfibril. Adapted from Augimeri & Strap (2015).

the inner and outer membrane (Figure 4). In *K. xylinus*, the aforementioned genes are found within the Type I bacterial cellulose synthase (*bcs*) operon and sometimes multiple operons are present in the same organism (Figure 4; Augimeri and Strap, 2015; Römling and Galperin, 2015). There are several varieties of *bcs* operons, collectively characterized as either type I, II, III, or IV based on the presence and arrangement of the genes they encode (Römling and Galperin, 2015). The distinguishing features of Type I *bcs* operons is the fusion of *bcsAB* (found in Type Ib operons) and the presence of *bcsD*, which may be responsible for the higher crystallinity of BC produced in *K. xylinus*. Type II operons are typical of *Escherichia coli* and *Salmonella enterica*, which lack *bcsD* but contain *bcsG*, *bcsE* and sometimes *bcsF* and *yhjR*. Type III operons contain *bcsA*, *bcsB*, *bcsZ* and an additional gene, *bcsK*. Lastly, Type IV are a class of *bcs*-like operons that contain *bcsA* but lack most other *bcs* genes. Additional information on these genes and their organization are outside the scope of this thesis and have been reviewed by Römling and Galperin (2015). Some strains of *K. xylinus* contain a second *bcs* operon with two additional genes of unknown function, *bcsX* and *bcsY*. BcsY could function as a transacetylase, involved in producing acetylated cellulose or another polysaccharide (Umeda et al., 1999). Notably, while only BcsAB is essential for *in vitro* cellulose

synthesis (Omadjela et al., 2013), the absence of any of these genes results in decreased BC production *in vivo* (Deng et al., 2013; Nakai et al., 2002, 2013; Wong et al., 1990). Currently, a major knowledge gap is the identity of the transcription factors (TF) responsible for promoting the *bcs* operons and regulatory proteins.

The polymerization and assembly of cellulose are tightly coupled as the *bcs* genes work in concert to simultaneously facilitate synthesis, export and crystallization (Figure 4; Augimeri and Strap, 2015; Ross et al., 1991). During synthesis, all of the extruding strands are produced 'parallel-up' with reducing ends of the cellulose chains pointing away from the bacterium (Koyama et al., 1997).

The *bcsA* gene codes for the first protein subunit of the BcsA-BcsB complex (recall that in some species, the chimeric *bcsAB* form is present). The protein product is a hydrophobic polypeptide located on the cytoplasmic face of the inner membrane with a conserved D,D,D,QXXRW motif in the catalytic glycosyltransferase subunit of cellulose synthase (Bureau and Brown, 1987; Saxena et al., 1990, 1995a; Wong et al., 1990). BcsA contains eight transmembrane domains and contains a family 2 glycosyl transferase domain (Saxena et al., 1995b). The conversion of UDP-glucose into the β-1,4-glucan chains of cellulose is allosterically activated by the ubiquitous secondary messenger c-di-GMP. Historically there has been confusion regarding the binding site of c-di-GMP. Research by Amikam & Benziman (1989) and Mayer et al. (1991) with *Agrobacterium tumefaciens* and *Komagataeibacter xylinus*, respectively, suggested that c-di-GMP binds to BcsB. Further studies identified that c-di-GMP was bound to a 200 kD membrane-bound protein complex (Weinhouse et al., 1997), and the true binding site was revealed to be a C-terminal PilZ domain on the BcsA subunit of this complex (Amikam and Galperin, 2006; Ryjenkov et al., 2006). The previous findings were explained when it was discovered that the *bcsA* and *bcsB* genes in *K. xylinus* were a fusion gene *bcsAB* that codes for the single 1500 amino acid PilZ-containing BcsAB protein (Chou and Galperin, 2016).

The *bcsB* gene codes for the second subunit of the BcsAB enzyme complex. Its product is a periplasmic protein that is anchored to the membrane by a single transmembrane (TM) helix (Morgan et al., 2013). BcsB contains two carbohydrate binding domains each linked to a flavodoxin-like fold domain (Morgan et al., 2013). The crystal structure of the BcsA-BcsB complex reveals nine TM helices, eight from BcsA and one from BcsB (Morgan et al., 2013). TM3-8 of BcsA form

a narrow channel and conserved residues on BcsA interact with an elongating glucan chain. Although some residues of BcsB have been shown to contact the polymer, they are not conserved (Morgan et al., 2013). Recently, a conserved N-terminal post-translational cleavage site for the BcsA-BcsB complex was identified between residues 757 and 758 (McManus et al., 2016).

BcsC is a 138.7 kDa protein that is homologous to bacterial proteins that code for membrane channels or pores, solidifying microscopic evidence of export sites for cellulose microfibrils (Saxena et al., 1994; Zaar, 1979). In some strains, the genes are so tightly arranged that the start codon for *bcsC* overlaps with the termination codon of the *bcsAB* gene (Saxena et al., 1994). BcsC is predicted to form a C-terminal β-barrel for nascent glucan export with a large N-terminal periplasmic tetratricopeptide repeat (TPR) domain believed to be responsible for interactions with peptidoglycan and other bacterial synthesis complex components (Daskalaki, 2008; Morgan et al., 2013; Römling and Galperin, 2015).

BcsD is a 138 kDa periplasmic protein homo-octamer (17.3 kDa monomer) with a cylindrical shape (Iyer et al., 2011). All N-termini of the octamer are within the cylinder which form four passageways for separately-extruded glucan-chains (Iyer et al., 2011). The protein has an interior right-handed twisted interface, spinning new glucan chains into higher-order cellulose fibrils (Hu et al., 2010; Saxena et al., 1994), perhaps explaining why the BcsD-containing *K. xylinus* produces fibrillary cellulose instead of the amorphous cellulose produced by other biofilm producers such as *E. coli* (Whitney and Howell, 2013). When *bcsD* is disrupted by targeted mutagenesis in *K. xylinus*, cellulose production is reduced by 40% (Wong et al., 1990), likely due to the inability to efficiently extrude cellulose past the outer membrane.

Three other genes have been identified in the *bcs* operon: *bcsZ*, *bglX*, and *bcsH*. BcsZ (also named CMCax in *Komagataeibacter* species) and BglX are an endoglucanase and β-glucosidase, respectively, and although their roles are unclear, they are known to participate in cellulose biosynthesis (Römling and Galperin, 2015). BcsZ is homologous to the secreted endoglucanase from *Rhizobium leguminosarum* which is responsible for penetration of the non-crystalline root tip hairs of plants (Koo et al., 1998; Robledo et al., 2008). It may help degrade improperly crystallized cellulose in *K. xylinus* or degrade amorphous cellulose in the environment. Alternatively, the endoglucanase may be involved in cell division or cellulose editing. Analogous to *Komagataeibacter*, *Arabidopsis* contains a membrane bound endoglucanase (*KOR*) that is required

for the correct assembly of the walls of elongating cells (Nicol et al., 1998). The absence of this endoglucanase resulted in multinucleated cells and other abnormal morphologies (Zuo et al., 2000). BcsH (previously CcpAx) affects the expression of BcsB and BcsC, interacts with BcsD, and influences crystallinity by influencing glucan chain arrangement (Deng et al., 2013; Nakai et al., 2013; Sunagawa et al., 2013).

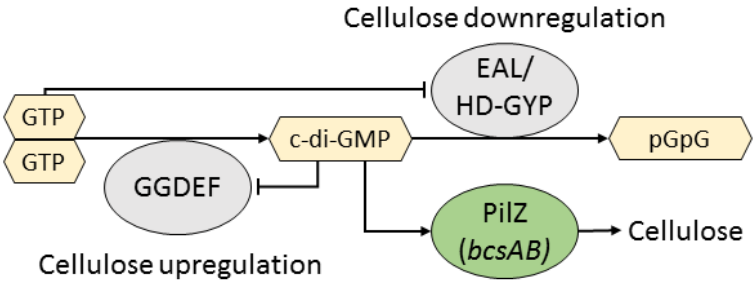

Figure 5: Turnover of c-di-GMP is antagonistically regulated by GGDEF containing DGC and EAL/HD-GYP containing PDE. Adapted from Augimeri et al. (2015)

1.2.4. Regulation of BC

Like most biofilm producers, *Komagataeibacter* species activate polysaccharide (cellulose) synthesis through the binding of the ubiquitous secondary messenger c-di-GMP. The bacterial cellulose synthase (BCS) complex is directly activated by c-di-GMP binding to the PilZ domain of BcsAB (Morgan et al., 2014). Globally, the dinucleotide is known for simultaneously triggering biofilm development (such as triggering BC synthesis) and inhibiting motility and bacterial virulence (Augimeri et al., 2015; Römling et al., 2013; Simm et al., 2004; Weinhouse et al., 1997). It is formed by the cyclization of two guanosine triphosphates (GTPs) by diguanylate cyclases (DGCs) which contain conserved GGDEF domains (Simm et al., 2004). Phosphodiesterases (PDEs) contain EAL or HD-GYP domains that facilitate the degradation of c-di-GMP into linear pGpG (Simm et al., 2004). EAL domains are also capable of hydrolyzing pGpG into monomeric pG but they do so at a much lower rate than c-di-GMP hydrolysis, indicating that alternative enzymes are primarily responsible for the degradation of pGpG (Römling et al., 2013). The complex regulation of c-di-GMP is exemplified by the discovery of bi-functional GGDEF/EAL and GGDEF/HD-GYP enzymes (Ferreira et al., 2008). Negative feedback loops from GTP and c-di-GMP control intracellular c-di-GMP levels through the inhibition of PDE and DGC, respectively. See **Figure 5** for a visual summary.

Biofilm producers can respond to environmental and internal cues by activating or inhibiting DGCs or PDEs, therefore increasing or decreasing intracellular c-di-GMP levels. Sensory domains have yet to be studied in *Komagataeibacter* species, but c-di-GMP regulating enzymes have been found to respond to O_2 levels, redox status, and light in other organisms (Chang et al., 2001; Gilles-

Gonzalez and Gonzalez, 2004; Qi et al., 2009; Tarutina et al., 2006). Considering the natural habitat for *Komagataeibacter* spp., it is likely that they are able to sense PCWC as indicators for colonization. For example, an experiment in which 3 g/l of green tea was added to the *K. xylinus* growth medium was shown to inhibit endogenous PDEs, leading to an accumulation of c-di-GMP and therefore increasing cellulose production (Nguyen et al., 2008).

Recently in our lab, the influence of PCWC on cellulose synthesis formed by *Komagataeibacter* species has been investigated. The PCWC lignin and xylan approximately doubled the weight of the pellicle product in *K. xylinus* ATCC 53582 (unpublished data). In contrast, an opposite but less profound trend was observed in *K. hansenii* ATCC 23769 (unpublished data). The addition of a small molecule, pellicin, was also shown to abolish cellulose production while increasing growth rate in *K. xylinus* (Strap et al., 2011). Surprisingly, cellulose synthase activity was not inhibited by pellicin but rather pellicin interfered with the crystallization process and its presence enhanced production of cellulose II *in vivo*. Our lab has also shown that select phytohormones affect the synthesis and crystallinity of BC (Qureshi et al., 2013). A particular phytohormone, ethylene, upregulated *bcsA, bcsB, bcsZ* (*cmcAx*), *bcsH* (*ccpAx*) and *bglAx* (Augimeri and Strap, 2015). Furthermore, enhanced transcript levels of *fixK* under ethylene conditions (previously Crp/Fnr$_{Kx}$) suggests its role as a TF involved in the regulation of these genes (Augimeri and Strap, 2015), originally implicated in cellulose synthesis by Deng et al. (2013). It is possible that PCWCs affect BC synthesis and crystallinity through this cAMP receptor protein/fumarate and nitrate reduction regulator (Crp/Fnr) family TF as well, but this remains to be investigated.

1.3. Crp/Fnr Transcription Factors

1.3.1. Crp/Fnr Family

The cAMP receptor protein/fumarate and nitrate reduction regulator (Crp/Fnr) family of transcription factors represent the paradigm of genetic regulators consisting of about 21 major groups, 14 with known functions (Körner et al., 2003). Crp and Fnr were the first two identified groups of this family and FixK represents one of the other 19 major groups.

Crp/Fnr proteins primarily function as positive transcription factors with a C-terminal helix-turn-helix nucleotide DNA binding domain (DBD), N-terminally activated by either allosteric effector binding or prosthetic group interaction (Körner et al., 2003). The DBD consensus sequences of these proteins typically contain nearly perfect four to five base pair palindromic motifs separated

by four to six base pairs (Körner et al., 2003). In *E. coli*, binding of Crp bends the DNA strand by 90 degrees due to two 40 degree kinks on each side of the dyad axis of the complex (Schultz et al., 1991). As such, gene activation is often simple without the need for additional protein factors. In *E. coli*, Crp regulated gene expression is facilitated by Crp and RNA polymerase alone (Kolb et al., 1993) yet, it has the capability of activating over 100 different promoters (Salgado et al., 2001). Furthermore, it is fairly common to discover multiple Crp/Fnr family proteins in a single species (Körner et al., 2003).

1.3.2. FixK

Originally discovered in *Rhizobium meliloti*, FixK was the third Crp/Fnr family of TFs to be identified (Batut et al., 1989). While the Crp and Fnr TFs respond to glucose levels (via cAMP) and oxygen availability (via a Fe-S cluster), respectively, FixK-like proteins lack a sensory module and respond to environmental signals via two-component regulatory systems (David et al., 1988; Gong et al., 1998; Reyrat et al., 1993). In *R. meliloti*, *fixK* is positively regulated by the two component system FixL/FixJ and negatively autoregulated by FixK via FixT (Batut et al., 1989; Foussard et al., 1997). The heme sensory protein FixL is therefore responsible for sensing oxygen and the phosphorylation of FixJ, which will ultimately activate the *fixK*-regulated symbiotic nitrogen fixation genes (Batut and Boistard, 1994; de Philip et al., 1990; Fischer, 1994). DNA binding of FixK occurs at a recognition motif of TTGA-N_6-TCAA found -40.5 from the +1 transcriptional start site (Fischer, 1994).

1.3.3. FixK in *Komagataeibacter*

The direct submission of the *K. xylinus* ATCC53582 genome by James C. Abbott (Accession number FBVP01000001) characterized the Crp/Fnr TF identified by Deng et al. (2013) as FixK by *ab initio* prediction. Protein basic local alignment search tool (BLASTp) analysis indicates that this is likely a match to FixK from *Komagataeibacter rhaeticus* where it is described to be involved in the regulation of nitrogen fixation. Notably, several other proteins annotated simply as ‘transcriptional regulators’ align to *K. xylinus* ATCC53582 FixK with higher identity over a longer query cover.

In contrast to the traditional microaerophilic sensory/nitrogen fixation response of FixK, its gene has also been shown to be phytohormonally regulated in *K. xylinus* and that it controls bacterial cellulose synthesis in *K. hansenii* (Augimeri and Strap, 2015; Deng et al., 2013). *fixK* is also

associated with the expression of *bcsH* and to a greater extent *bglX* (Deng et al., 2013). *K. xylinus* ATCC 53582 and *K. hansenii* ATCC 23769 carry a *fixK* recognition motif of TTGATTTATATCAA 143 bp upstream from *fixK* suggesting direct autoregulation of the gene (recall *fixK* is autoregulated via FixT in *R. meliloti*). A similar recognition motif TTGATATGGATCAA is present 192 bp upstream of a hypothetical protein found immediately upstream of *fixK* in *K. xylinus* ATCC 53582. The close location to *fixK* and matching DBD motif suggests that this small protein may be involved in the response to or autoregulation of *fixK*.

1.4. Plant-microbe interactions

1.4.1. Degradation of plant cell wall compounds

As discussed in section 1.1.2 (Plant cellulose), plants form a recalcitrant wall made from cellulose, hemicellulose, pectin, and lignin. As a carpospheric organism, *K. xylinus* relies on plant exudate and rotting plant material for both a carbon and nitrogen source. The production of plant cell wall degrading enzymes (PCWDE) would aid in their ability to obtain nutrients; however to our knowledge, the only PCWDEs identified in *K. xylinus* or *K. hansenii* are the carboxymethyl cellulase (CMCase) and β-glucosidase BcsZ and BglX.

The complete degradation of cellulose requires three major cellulose-hydrolyzing groups: endoglucanases, exoglucanases, and β-glucosidases (Kumar et al., 2008). These enzymes are responsible for the hydrolysis of the β-1,4-glycosidic linkages found in cellulose. Endoglucanases attack internal bonds of a cellulose chain and exoglucanases (cellobiohydrolases) cleave the last two glucose monomers on cellulose chains releasing cellobiose, a dimer of glucose. Lastly, β-glucosidases act on cellobiose to produce glucose monomers. Fungal decomposers such as *Trichoderma reesei* are the most extensively studied cellulase producers, but endoglucanases have been identified in bacteria as well (Pilz et al., 1990). An endoglucanase (BcsZ) and a β-glucosidase

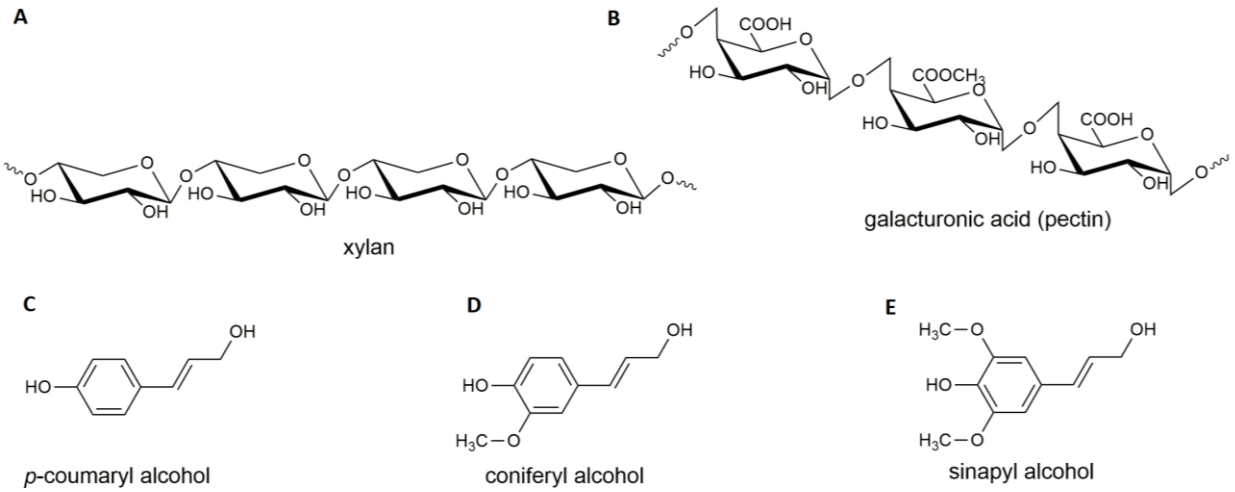

Figure 6: Structures of some typical plant cell wall compounds (PCWC). A, xylan: a common hemicellulose; B, galacturonic acid (homogalacturonan): a common pectin; C-E, lignin monomers.

(BglX) have previously been identified in both *K. xylinus* E25 (Kubiak et al., 2014) and *K. hansenii* ATCC 23769 (Standal et al., 1994; Tajima et al., 2001). According to UniProtKB, the molecular weights of BcsZ and BglX are approximately 37.5 kDa and 83.5 kDa, respectively. Neither of these proteins have a clear purpose in these species but cellulases have been shown to display bifunctionality, composed of structurally and functionally independent catalytic and cellulose-binding domains (CBD) (Pilz et al., 1990). Furthermore, there has been no published evidence that these enzymes are capable of degrading the crystalline BC produced by these organisms.

Hemicelluloses are the second most abundant renewable biopolymer (Kumar et al., 2008). The composition of these heterogeneous polysaccharides vary depending on the types of plants (particularly hardwood and softwood), but are generally composed of D-xylose, D-arabinose, D-mannose, D-glucose, D-galactose and sugar acids. As many hemicellulose structures exist, various enzymes are required for their degradation. One of the most common hemicelluloses is xylan (**Figure 6**, A), composed of a xylose backbone with a range of covalently bound side groups including acetic acid, arabinose, D-glucuronic acid, 4-*O*-methyl-D-glucuronic acid, ferulic acid, and *p*-coumaric acid (Adsul et al., 2009). Endo-1,4-β-xylanases are responsible for hydrolyzing the xylose backbone linkages in xylan; however, β-xylosidase, α-glucuronidase, α-L-arabinofuranosidase and acetylxylan esterase enzymes are required to degrade all xylan heteropolymers into monosaccharides (Kumar et al., 2008). Some xylanases (23.3 kDa according to

UniProtKB) have been discovered in bacteria such as *Bacillus subtilis* (Paice et al., 1986), but have yet to be identified in *Komagataeibacter* species.

Pectins are the third main structural polysaccharide found in plant cell walls and are classified as homogalacturonan (**Figure 6**, B), rhamnogalacturonan I, or rhamnogalaturonan II (Mohnen, 2008). Homogalacturonan is a polymer of α-1,4-D-galacturonic acid monomers with random partial methylation and acetylation. Rhamnogalacturonan I is formed through alternating α-1,2-L-rhamnosyl-α-1,4-D-galacturonosyl units with branching arabinofuranose and galactose oligomers. Similar to homogalacturonan, rhamnogalacturonan II has a backbone of α-1,4-D-galacturonic acid monomers with random partial methylation and acetylation, but also contains four types of branching composed of up to 11 different monosaccharide types.

Pectins are abundant in fruits such as apples, apricots, bananas, carrots, grapes, lemons, and oranges (Schiewer and Patil, 2008). Apricots contain some of the highest pectin content at up to 1.32% of total fruit content (Baker, 1997; Money and Christian, 1950) and grapes typically range between 0.12% to 0.8% pectin content (Kawabata et al., 1974; Silacci and Morrison, 1990). Notably, the skin of fruits are particularly rich in pectin (Schiewer and Patil, 2008). Depolymerization and solubilization of pectins begins early in ripening and serve as a potential carbon source for *Komagataeibacter*. Pectinase enzymes encompass three enzyme categories. Polygalacturonases facilitate the hydrolysis of α-1,4-D-galactosiduronic linkages. Pectolyase and pectinesterase are responsible for cleaving side chains and methyl esters, respectively (Gummadi and Panda, 2003). Bacterial pectinases are typically 50 kDa but have been identified as large as 110 kDa (UniProtKB).

Lignin is the last but the most unique component of plant cell walls. While the other PCWC are polysaccharides with defined backbones, lignin is a complex aromatic heteropolymer composed of *p*-coumaryl, coniferyl, and sinapyl alcohol (Freudenberg & Neish 1968; Figure 6, C-E). During plant development, the majority of lignin is deposited after cellulose and hemicellulose have been deposited (Boerjan et al., 2003). Lignin therefore fills in the gaps between these polysaccharides and as such, lignin must be removed before enzymes can access hemicellulose or cellulose. The degradation of lignin requires the catalytic oxidation by the enzymes lignin peroxidase, laccase, and/or manganese peroxidase (Higuchi, 2004). Many soil dwelling bacteria have been shown to produce lignin modifying enzymes (Crawford, 1978; Sørensen, 1962) and it is likely that some carpospheric bacteria also produce such enzymes.

The production of PCWDE would benefit *Komagataeibacter* by simultaneously releasing simple sugars through the degradation of polysaccharides as well as breaking down the plant cell wall to increase nutrient availability. *K. xylinus* and *K. hansenii* have already been shown to secrete CMCase and a range of decomposing bacteria are capable of degrading the PCWC discussed. Additionally, studies have indicated that PCWC can be integrated into BC during synthesis, adjusting its properties (Augimeri et al., 2015; Chanliaud and Gidley, 1999; Park et al., 2014; Tokoh et al., 1998; Uhlin et al., 1995) and potentially improving its ability to isolate a plant wound from competitors.

1.5. Hypothesis and research objectives

Extensive research has been conducted on low cost media alternatives for the production of bacterial cellulose from *Komagataeibacter* species (Castro et al., 2011; Kuo et al., 2010; Li et al., 2015; Lin et al., 2014; Moosavi-Nasab and Yousefi, 2011; non inclusive list), yet little is known about what compounds are suitable for its synthesis. Due to their abundance and cost, agricultural wastes are some of the most promising feedstocks. These compounds are rich in plant cell wall compounds such as cellulose, xylose, and pectin that may be degraded into simpler sugars by *Komagataeibacter*. Plants often produce these compounds complexed within lignin, making it resistant to enzymatic attack.

Previous research by Deng et al. (2013) revealed a unique role of *fixK* in bacterial cellulose synthesis in *K. hansenii* ATCC 23769 through transposon mutagenesis. The absence of *fixK* leads to the complete abolishment of bacterial cellulose, yet the bacterial cellulose synthesis proteins were present in the cell extract. Expression of *bcsH* and *bglX* was downregulated in the absence of *fixK* but their role in cellulose synthesis is poorly understood. In *K. xylinus* ATCC 53582, *fixK* is regulated by the phytohormones ethylene, abscisic acid, and indole acetic acid indicating its role in detecting plant ripeness (Augimeri and Strap, 2015).

The goals of this research were i) to investigate which, if any, of the primary plant cell wall compounds are degraded by *K. xylinus* and *K. hansenii* to gain insight into the plant-bacteria interaction; and ii) to investigate the role of the global transcriptional regulator FixK in *K. xylinus* and further develop our understanding of FixK in *K. hansenii* through a reverse genetics approach.

This thesis therefore tested three hypotheses: i) *K. xylinus* and *K. hansenii* produce plant cell wall degrading enzymes, ii) FixK regulates bacterial cellulose biosynthesis in *K. xylinus*, and iii) *fixK* is involved in the regulation of carbon source metabolism.

2. Methodology

2.1. Chemicals (and growth medium)

All chemicals were purchased from BioShop (Burlington, Ontario) except where stated otherwise. D-glucose, D-fructose and yeast extract were purchased from BioBasic (Markham, Ontario). All antibiotics, cOmplete™ EDTA-free protease inhibitor cocktail, cellulase from *Trichoderma reesei*, manganese peroxidase from *Nematoloma frowardii*, lignin peroxidase, pectinase from *Aspergillus niger*, and xylanase from *Trichoderma viride* were purchased from Sigma-Aldrich (Oakville, Ontario). Plant cell wall compounds CMC, xylan from Birchwood, pectin from apple, and low sulfonate lignin were also obtained from Sigma-Aldrich (Oakville, Ontario). Pellicin (([2E]-3-phenyl-1-[2,3,4,5-tetrahydro-1,6-benzodioxocin-8-yl]prop-2-en-1-one) dissolved in DMSO was a gift from Dr. Bonetta.

2.2. Bacteria and culture conditions

Komagataeibacter xylinus American Type Culture Collection (ATCC) 53582 and *K. hansenii* ATCC 23769 were maintained as frozen glycerol stocks at -80°C. Stocks were streak plated for isolated colonies on Schramm-Hestrin (SH) medium (Hestrin & Schramm 1954) containing 1.5% agar. Unless otherwise stated, starter cultures were prepared in 5 ml of SH medium supplemented with 0.2% (v/v) filter-sterilized cellulase in a 50 ml screw-capped tube. Cultures were grown at 30°C in a rotisserie incubator until the culture reached an optical density at 600 nm (OD_{600}) of 0.5-0.7 or 0.7-0.9 for *K. xylinus* or *K. hansenii*, respectively. Cells were harvested by centrifugation at 3,000 x *g* for 10 minutes or 9,000 x *g* for 1 minute for volumes over or under 2 ml, respectively.

The inoculum for agitated culture experiments were prepared by washing the cells twice in SH medium without a carbon source (SH_0; **Table 1**) supplemented with 0.2% (v/v). Static culture experiments required cellulase-free media for pellicle production. Prior to washing cells, cultures were cooled to 4°C to prevent cellulose induced aggregation. Cells were then washed twice in cold SH_0 to remove medium cellulase and remained on ice until inoculation. All experimental cultures were inoculated in triplicate to an OD_{600} of 0.005 unless otherwise stated.

K. xylinus Δ*fixK* and *K. hansenii* Δ*fixK* cultures were supplemented with 50 µg/ml and 150 µg/ml of chloramphenicol to prevent the loss of the gene disruption, respectively.

2.3. Detection of extracellular plant cell wall degradative enzymes

2.3.1. Agar plate assays

Screening for the presence of plant cell wall degrading enzymes (PCWDE) secreted by *K. xylinus* or *K. hansenii* was performed using substrate supplemented agar plate assays. Detection of cellulases, xylanases, pectinases, and lignin-modifying enzymes (LMEs) was performed on 1.0% (w/v) agar plates containing 0.2% (w/v) carboxymethyl cellulose (CMC), 0.2% (w/v) xylan, 0.2% (w/v) pectin, or 0.025% (w/v) lignin, respectively. Staining with Gram's iodine solution (Bio-Media) has previously been shown to be an effective dye for staining CMC and xylan (Meddeb-Mouelhi et al., 2014) and was evaluated for its ability to also stain pectin and lignin. Washing the stained plates with MilliQ H_2O revealed well-defined clearing zones around positive controls (cellulase, xylanase, pectinase, or manganese peroxidase) indicating degradation of substrate and was therefore used for initial screening. Manganese peroxidase, lignin peroxidase, and laccase were evaluated for lignin degrading ability. Manganese peroxidase produced the most well defined clearing zones and was used as the positive control for all lignin degradation assays.

To evaluate whether enzyme activity could be found in the growth medium or trapped within *Komagataeibacter* pellicle, cultures for the PCWDE plate assays were prepared separately. The growth medium extracts were prepared from supernatants of 2 ml agitated, three day old cultures grown in SHG_2 (canonical SH; **Table 1**) supplemented with 0.2% cellulase (v/v) at 30°C in 24 well plates. Pellicle extracts were prepared similarly except without the addition of cellulase and grown statically for seven days to facilitate the production of a robust pellicle. Pellicles were then quartered with a sterile scalpel. To encourage enzyme secretion, each culture was also separately prepared with the addition of 2% (w/v) fructose, 0.05% (w/v) xylan, 0.05% (w/v) CMC, or 0.05% (w/v) lignin. Enzyme assays were performed by the addition of 10 µl of cell-free supernatants of agitated culture or placing the quartered pellicle onto the plates and incubating the plates for up to two days at 30°C. Degradation was scored as clearing zones and were detected by staining with Gram's iodine solution and destaining with MilliQ H_2O.

2.3.2. Crude protein preparations

To improve the detection of low abundance PCWDE, proteins from culture supernatants and pellicles were concentrated as follows. Crude extracellular protein was obtained from duplicate 100 ml *K. xylinus* or *K. hansenii* cultures grown in SH medium for four or seven days. Culture broths were gravity-filtered through a #4 cone filter to remove thick amorphous cellulose then immediately vacuum-filtered through a Whatman #1 filter paper using a Büchner funnel. The broth was then centrifuged at 2,250 x *g* for 10 minutes at 4°C and the cell-free supernatant was collected for concentration via ammonium sulfate precipitation or lyophilization. Pellicles were squeezed using a flat-bottomed potato ricer to obtain the "squeezate" which was vacuum-filtered through a Whatman #1 filter paper using a Büchner funnel and centrifuged at 2,250 x *g* for 10 minutes at 4°C. The cell-free supernatant was collected for concentration via ammonium sulfate precipitation or lyophilization.

Ammonium sulfate precipitation was performed by adding ammonium sulfate to 80% saturation at 4°C and centrifuged at 2,250 x *g* for 10 minutes. Samples were then resuspended in 50 mM citric acid pH 5 buffer and dialyzed in a regenerated cellulose membrane with a 12,000 to 14,000 molecular weight cut off overnight against the same buffer at 4°C (Fisherbrand). The buffer was chosen to mimic the acidic nature of the culture at mid-log growth. Cell-free culture broth and squeezate samples were concentrated approximately 20 times and 4 times, respectively.

Samples for lyophilization were frozen in 500 ml centrifuge bottles at -80°C at an angle to optimize surface area. Frozen samples were lyophilized on a Modulyo D freeze dryer fitted with a VLP200 vacuum pump (Thermo Scientific) for approximately 30 hours until dry. The freeze-dried samples were then resuspended in 50 mM citric acid pH 5 buffer. Culture broth and squeezate samples were concentrated approximately 20 times and 4 times, respectively.

Acetone precipitation was the third protein concentration method investigated. Samples were prepared as stated above and proteins from 50 ml cultures were precipitated overnight at -20°C using four volumes of acetone. The supernatant was decanted after centrifugation at 2,250 x *g* for 10 minutes at 4°C. The resulting pellet was resuspended in 50 mM citric acid pH 5 buffer at 1/20 the initial volume.

2.3.3. Zymography detection of plant cell wall degrading enzymes

PCWDE activity was determined by zymogram analysis and individual proteins within active protein bands were identified by mass spectrometry. Sodium dodecyl sulfate polyacrylamide gel electrophoresis (SDS-PAGE) was performed as described by Laemmli (1970) using the Mini-PROTEAN® tetra electrophoresis system (Bio-Rad). Depending on the enzyme assay, 0.1% (w/v) CMC, xylan, or pectin was incorporated into the 12% resolving gel prior to polymerization with 4% stacking gels cast on top of the resolving gel. Concentrated protein samples were loaded to a concentration of 200 ng and 80 ng for culture broth and squeezate samples, respectively. Lignin interfered with the polymerization of the polyacrylamide so agarose overlays (described below) were performed.

Gel electrophoresis was performed in duplicate, one for protein profiling via Coomassie staining and one for the detection of PCWDE via substrate staining. Gels were run at 100 V for approximately 2 hours and then rinsed in MilliQ H_2O. Gels were submerged and washed by shaking in 2.5% (v/v) Triton X-100 for at least 30 minutes to replace SDS with the non-ionic detergent to renature the proteins. Gels were then rinsed with MilliQ H_2O and incubated at 30°C for 20 minutes in 50 mM acetate buffer at pH 5 to resemble the pH of mid-log culture medium. They were rinsed once again for 5 minutes in MilliQ H_2O to remove excess buffer. Staining processes were dependent on the incorporated polymer as described below.

CMC and xylan gels were stained with 0.1% (w/v) Congo red for 30 minutes and then destained in 1 M NaCl until clearing zones appeared. Contrast was increased by the addition of 1% (v/v) acetic acid as Congo red turns dark purple to blue below pH 4.

Pectin gels were rinsed three times with MilliQ H_2O for at least 5 seconds then stained with 0.05% (w/v) ruthenium red for 20 minutes. Destaining was performed using MilliQ H_2O until pale red zones appeared.

Lignin was found to prevent polymerization of polyacrylamide gels. Therefore, an alternative method wherein lignin supplemented agarose gels were overlaid on top of SDS-PAGE gels was used. Protein samples were electrophoresed and renatured *in situ* as stated above except that 2 mM H_2O_2 was added to the 50 mM acetate buffer (pH 5) as lignin peroxidase requires H_2O_2 for activity. Notably, divalent cations such as Mn^{2+} serve as an electron donor for the positive control manganese peroxidase (Himmel, 2016). Substrate overlays of 1 mm thickness were cast using PAGE

casting chambers with 1% (w/v) agarose and 0.025% (w/v) lignin. Agarose overlays were cut to match the polyacrylamide gel and notched to indicate directionality. Polyacrylamide gels were sandwiched against the agarose overlays using vice-tightened glass plates with enough pressure to ensure good contact and incubated in a humidified chamber overnight at 30°C. After incubation, agarose overlays were washed three times in MilliQ H_2O for 30 minutes to remove residual H_2O_2 as it interferes with the staining procedure. Overlays were then placed in a freshly mixed 1:1 solution of 1% (w/v) $FeCl_3$ and 1% (w/v) $K_3[Fe(CN)_3]$ in the dark for 10 minutes without disturbance. Lignin stained blue-green and clear zones indicated oxidation of the polyphenol.

Protein bands exhibiting degradation of polymers were excised from gels and preserved in 1% (v/v) acetic acid until they were sent for protein identification at the SickKids Proteomic, Analytics, Robotics & Chemical Biology Centre (Toronto, Ontario) using in-gel trypsin digestion prior to electrospray ionization and mass identification via Orbitrap Liquid Chromatography tandem Mass Spectrometry. PEAKS Studio software v7.5 was used to identify proteins with corresponding peptide identities. Proteins from *K. hansenii* ATCC 23769 were searched against *K. hansenii* ATCC 23769 predicted protein database (National Center for Biotechnology Information). Proteins from *K. xylinus* ATCC 53582 were searched at a species level since the same database for *K. xylinus* ATCC 53582 strain is not available.

2.4. Disruption of *fixK*

2.4.1. Transformation and selection optimization

There are few genetic tools available for *Komagataeibacter* and transformation efficiencies are low, probably due to the production of crystalline cellulose which acts as a barrier. Optimizing the transformation protocol was therefore a necessary step for the mutagenesis of this strain. Initially it was unclear whether cell competency or plasmid compatibility was the primary obstacle for effective transformation. Electroporation, chemical transformation, and conjugation were all attempted with several plasmid backbones in *K. xylinus* without success. Simultaneous to this research, another group successfully transformed their construct, pSEVA331Bb, into *K. xylinus* ATCC53582 (Florea et al., 2016b). Since we discovered that SEVA331Bb (Addgene plasmid # 78269 deposited by Tom Ellis; **Appendix Figure 2**) was effectively maintained in *K. hansenii* as well, this plasmid was used to optimize transformation conditions.

Prior to obtaining this pSEVA331Bb, the best antibiotic for selection of *K. xylinus* and *K. hansenii* was evaluated with the goal of finding an effective antibiotic against both strains to use as a selection agent. This knowledge would assist in the development of a plasmid that would be effective in both species. The antibiotic sensitivity assay was performed by spread plating approximately 10^6 *K. xylinus* and *K. hansenii* cells on SHG_2 agar containing 6 to 50 µg/ml kanamycin, 100 to 400 µg/ml chloramphenicol, or 50 to 300 µg/ml tetracycline. Resistance was evaluated by the number of CFU on antibiotic plates after five days incubation at 30°C. Minimum inhibitory concentration (MIC) assays were also performed by inoculating *K. xylinus* and *K. hansenii* in 200 µl of SHG_2 to a McFarland standard of 0.5 in a 96 well plate containing 0 – 175 µg/ml of chloramphenicol or 0 – 14 µg/ml of tetracycline and was incubated for three days at 30°C. Results from the spread plate assay indicated that kanamycin was a poor antibiotic for plate selection of *K. hansenii* and was therefore omitted from the MIC assay.

K. xylinus grow slowly in canonical SHG_2 medium, possibly resulting in the upregulation of stress response genes that would limit competency. Alternative growth media that improve cell fitness may be a simple solution to this problem. To this end, cells were grown in growth medium with fructose, glycerol, or acetic acid as described in **Table 1**. Fructose has been shown to improve cell growth in *K. xylinus* ATCC 53524 (Mikkelsen et al., 2009) and incubation with glycerol has been implicated in improved transformation efficiency, possibly by affecting the membrane permeability (Ravid and Freshney, 1998). Cultures were inoculated in 200

Table 1: Modified SH medium used in this study. Canonical SH medium glucose was replaced with other carbon sources. Glucose or fructose based media was supplemented with 50 mM acetic acid.

Medium	[Glucose]	[Fructose]	[Sucrose]	[Glycerol]	[Acetic Acid]
SHG_2 †	2%	-	-	-	-
SHG_2 AA	2%	-	-	-	50 mM (0.43%)
SHG_1	1%	-	-	-	-
SHG_1 AA	1%	-	-	-	50 mM (0.43%)
SHF_2	-	2%	-	-	-
SHF_2 AA	-	2%	-	-	50 mM (0.43%)
SHF_1	-	1%	-	-	-
SHF_1 AA	-	1%	-	-	50 mM (0.43%)
SHG_1 Gly_1	1%	-	-	1%	-
SHF_1 Gly_1	-	1%	-	1%	-
SH_0 Gly_2	-	-	-	2%	-
SHS_2*	-	-	2%	-	-
SHM*	0.5%	0.5%	1%	-	-

†Canonical SH is named SHG2 for the purpose of this study.

*Not used for electrocompetent cell preparations

µl of media (described in **Table 1**) in triplicate in 96 well plates with 2% (v/v) cellulase to assist in cellulose degradation. This was necessary due to the reduced turbidity in small cultures facilitating the synthesis of cellulose. Growth was measured as optical density at 600 nm (OD_{600}) three times a day until the culture reached stationary phase. Despite high cellulase concentrations, *K. xylinus* showed signs of aggregation in some cultures. The cellulase concentration was doubled in cultures where aggregation/cellulose production was noticeable. These growth curves were repeated with *K. hansenii* to complement the *K. xylinus* findings and the results were used to identify the OD_{600} of cultures at mid-logarithmic growth, important for the preparation of electrocompetent cells for cultures grown in each of these media.

Transformation of *K. xylinus* is complicated due to cellulose production. Cellulose biosynthesis rapidly creates antibiotic resistance in these species by forming a biofilm between cells and the antibiotic on selection plates. Strategies for preventing the development of this biofilm were investigated by modifying the application of cellulase to selection plates. *K. xylinus* rapidly produce highly crystalline cellulose when grown in glucose (Keshk & Sameshima 2005) and therefore plating on SHG_2 would provide a recalcitrant cellulose for this assay. Although SHG_2 would be the ideal growth medium for the preparation of high cellulose-yielding electrocompetent cells, electroporation proved very difficult. Electrocompetent cells were therefore prepared in SHF_2 and transformed with pSEVA331Bb at 2.5 kV in 1 mm cuvettes and then recovered in 1 ml SHG_2. Fifty microlitre aliquots of the electroporated cells were plated on SHG_2 Chl^{150} either i) with the direct addition of 25 µl (0.1% v/v) of cellulase to the electroporation mixture, or ii) with 50 µl (0.2% v/v) cellulase incorporated into plates prior to pouring. The efficacy of both methods was evaluated by the number of satellite colonies formed after 7 days.

An additional means to combat cellulose production was to modify the growth, recovery, and plating medium to be less favorable for cellulose synthesis. Previous work in our lab has shown that *K. xylinus* produces less cellulose when provided fructose instead of glucose (unpublished data). These findings, combined with the data obtained from the growth curves described previously, drove the selection of SHG_2, SHF_2, SHF_1, SHF_1 AA, SHF_1 Gly_1, and SH_0 Gly_2 for the preparation of electrocompetent cells. All of these media are fructose or glycerol based except for SHG_2 which was included as the current standard. Cells in each media were prepared as follows: *K. xylinus* was grown in 100 ml of each of the media listed above to an OD_{600} of approximately 0.5. Cultures were chilled to 4°C then centrifuged (2,350 x *g*; 20 min; 4°C) and the supernatant was decanted. Cell pellets were

washed once in 25 ml and twice in 10 ml 1 mM HEPES (pH 7.0) by repeated centrifugation and decanting. Cells were finally resuspended in 15% (v/v) glycerol to a calculated OD_{600} of approximately 50 to ensure equal cell numbers between preparations. Aliquots of 100 µl were stored frozen at -80°C. To evaluate electroporation efficiency, pSEVA331Bb was electroporated into 50 µl of thawed cells at 2500 V in 1 mm cuvettes using 120 ng (2.4 ng/µl) DNA. After electroporation, cells were immediately transferred into 1 ml of SHF_1 supplemented with 0.5% (v/v) cellulase and agitated at 30°C. Transformants were selected by spread plating 50 µl of electroporated cultures supplemented with 25 µl of cellulase at 75 minutes and 6.5 hours post transformation.

2.4.2. *fixK* knockout construct design and mutation in *Komagataeibacter*

fixK has previously been implicated in cellulose production in *K. hansenii* (Deng et al., 2013). Mutational analysis was focused on this gene to further understand its role at both a physiological and morphological level between species. A linear construct was designed to mutate *fixK* by inserting an in-frame stop codon and chloramphenicol cassette into the gene (**Figure 7**). Genomic DNA (gDNA) was extracted from mid-log grown cultures of *K. xylinus* and *K. hansenii* using an EZ-10 Spin Column Bacterial DNA Mini-Prep Kit (BioBasic) according to manufacturer's

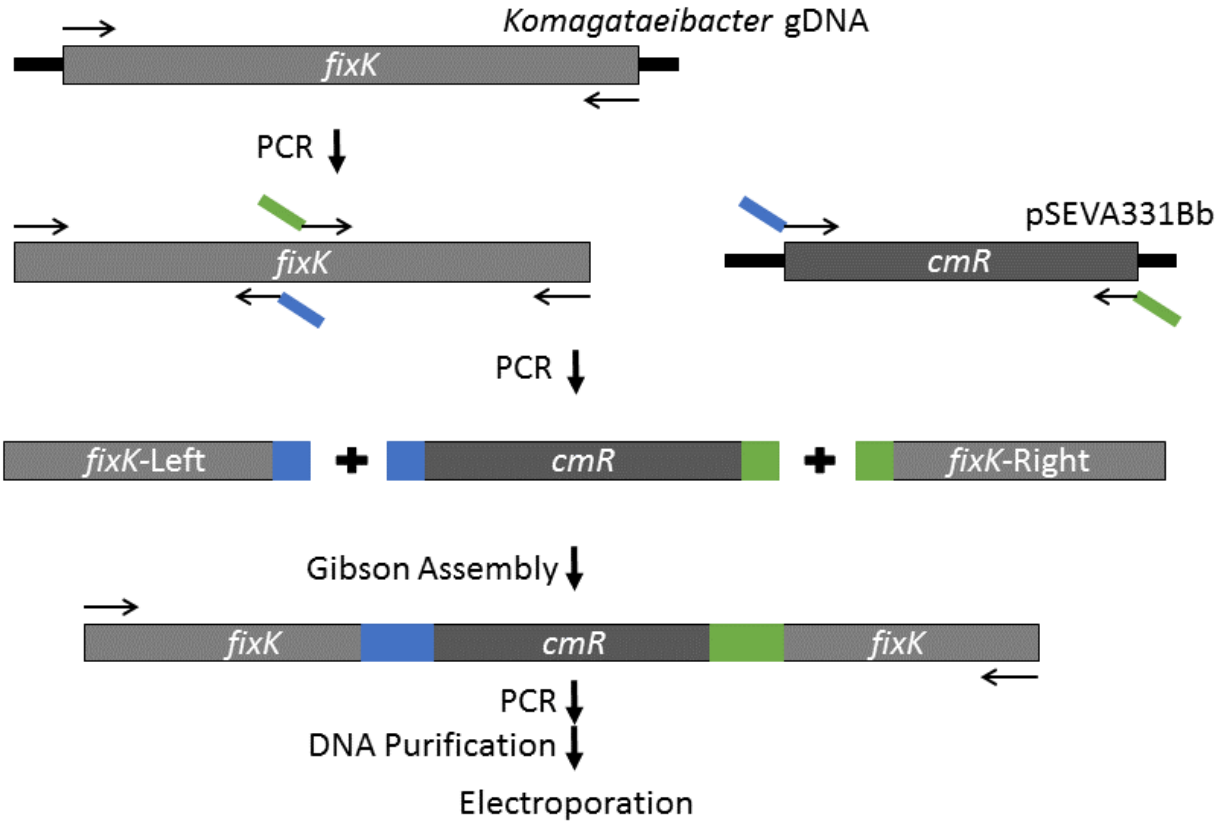

Figure 7: Construct design for *fixK* mutation. *fixK* was amplified from genomic DNA to isolate *fixK* as *fixK* interior primers may result in off-target effects with genomic DNA. Left and right sides of *fixK* were amplified using primers with complementary 5' overhangs to the chloramphenicol cassette from pSEVA331Bb. The chloramphenicol cassette was amplified with complementary 5' overhangs to the left and right sides of *fixK*. The 5' overhangs are coloured blue (left) and green (right). The three fragments were mixed and assembled using Gibson Assembly. The product was amplified to provide sufficient quantities for electroporation into *K. xylinus* and *K. hansenii*. DNA purification was performed after each PCR. Primers were designed to incorporate a stop codon for the left side of *fixK*.

instructions. PrimerBlast (Ye et al., 2012), SnapGene® software (from GSL Biotech; available at snapgene.com), and Netprimer (http://www.premierbiosoft.com/netprimer/) were used to design

and validate primers *in silico.* A 618 bp fragment of *fixK* was amplified from both *K. xylinus* and *K. hansenii*. Unless otherwise noted, all polymerase chain reactions (PCR) used Q5® High-Fidelity DNA Polymerase (New England Biolabs; NEB) with the following cycling conditions: 98°C for 30 sec; 30 cycles of 98°C for 10 sec, 66 °C for 10 sec, 72°C for 30 sec; and 72°C for 2 min. All amplicons were purified using EZ-10 Spin Column DNA Cleanup Kit (BioBasic) prior to downstream applications. SnapGene® was used to design Gibson Assembly® primers for the assembly of the 5' side of *fixK*, a chloramphenicol cassette from pSEVA331Bb, and the 3' side of *fixK* (**Figure 7**). Primers selected to ensure the incorporation of an in-frame stop codon for *fixK* and fragments were amplified by PCR. The fragments were assembled using Gibson Assembly® Master Mix (NEB) according to the manufacturer's instructions and the target construct was amplified by PCR. Agarose gel electrophoresis of the amplified assembled product revealed multiple bands. Therefore, the 1403 base pair (bp) target was gel-purified using EZ-10 Spin Column DNA Gel Extraction Miniprep Kit (BioBasic) and was used as a template to amplify a clean *fixK*-flanked chloramphenicol cassette assembly (*fixK*-Chl-*fixK*). Primers used for *fixK* mutagenesis are listed in (**Appendix Table 1**).

fixK was mutated in both *K. xylinus* and *K. hansenii* by homologous recombination with the linear construct *fixK*-Chl-*fixK*. This construct was electroporated into both species using 1800 V or 2500 V and either 0.25 ng/µl or 2.5 ng/µl DNA with no clear improvement for either condition. The mutated *fixK* was amplified from both species using Q5 DNA polymerase as described above and sent to Bio-Basic for sequence analysis. Mutants were maintained as glycerol stocks and stored at -80°C.

2.5. Mutant characterization

2.5.1. Colony morphology

As a putative global transcription factor, *fixK* likely controls several cell responses and signals. Wildtype and Δ*fixK* mutants of *K. xylinus* and *K. hansenii* were grown on glucose, fructose, and sucrose based SH medium to examine colony morphology. Cells were streak plated on SHG_1, SHG_2, SHF_1, SHF_2, or SHS_2 and incubated at 30°C. Additionally, *K. xylinus* wildtype and Δ*fixK* were streak plated on SHG_2 supplemented with 10 µM pellicin dissolved in dimethyl sulfoxide (DMSO) or an equal volume of DMSO as a negative control. Pictures were taken of colonies positioned above a 1 mm increment ruler with a USB 2.0 Digital Microscope (Plugable brand).

2.5.2. Agitated growth, pH, and gluconic acid assays

The role of *fixK* was further investigated through growth and acid metabolism assays in agitated cultures. Culture OD_{600}, pH, and gluconic acid was measured to evaluate growth and acid metabolism in agitated 0.2% (v/v) cellulase supplemented liquid cultures. To limit bias due to priming cultures with a single carbon source, starter cultures for these assays were prepared in SHM (**Table 1**). WT and Δ*fixK* mutants of *K. xylinus* and *K. hansenii* were inoculated in 50 ml SHG_1, SHG_2, SHF_2, and SHS_2 (**Table 1**) in 125 ml flasks to an OD_{600} of 0.005 and incubated at 30°C at 170 rpm for up to 14 days. Daily analysis was performed by aliquoting 200 µl into a 96 well plate for pH and growth analysis; 300 µl was frozen at -20°C for subsequent gluconic acid analysis. Growth was measured by OD_{600} in 96 well plates on an xMark™ Microplate Absorbance Spectrophotometer (BioRad) using the respective growth medium as a blank. These same samples were then used to measure culture pH using an Orion™ 9110DJWP Double Junction Micro pH Probe fitted to an Accumet® AB15 (Thermo Fisher Scientific™) pH meter. Total gluconic acid and glucono-δ-lactone from the three biological replicates at select time points were measured (single technical replicates) after completion of the growth/pH curve according to the microplate assay procedure from a D-gluconic acid/D-glucono-δ-lactone kit (Megazyme). Samples were diluted according to culture pH before performing the assay to ensure measurements were within the linear range. Concentration of gluconic acid was calculated as $\Delta A_{sample}/\Delta A_{standard}$ * standard (0.25 g/L) * dilution factor. Student's t-tests were performed between points of interest ($p<0.05$).

2.5.3. Static pH, gluconic acid, and cellulose yield

Komagataeibacter grow differently under agitated and static conditions. Therefore, the role of *fixK* was investigated through bacterial cellulose and acid metabolism assays under static conditions. Importantly, the pH between static and agitated cultures was used as a culture growth stage reference point to facilitate comparisons between the agitated and static culture conditions. Starter cultures were prepared in SHM (**Table 1**) to prevent carbon source priming. Wildtype and Δ*fixK* mutants of *K. xylinus* and *K. hansenii* were inoculated in 2 ml SHG_1, SHG_2, SHF_2, and SHS_2 (**Table 1**) in 24 well plates to an OD_{600} of 0.005 and incubated at 30°C for up to 33 days. For days including pellicle measurements, six technical replicates were inoculated for each biological replicate. Prior to pH measurements, pellicles were pierced to release fluids retained within a cellulosic sac that forms beneath the pellicle and then thoroughly mixed with the culture medium. Culture plates were then frozen for subsequent gluconic acid assays, performed as described in

section 2.5.2. Dry weight was measured on day 7, 13, and 23 as previously described (Augimeri et al., 2016). In brief, pellicles were pierced (to release retaining fluids) and dabbed 3 times on paper towel to remove excess medium. Pellicles were then heated to 80°C in 0.1 N NaOH for 20 minutes and then extensively washed in MilliQ H_2O until the wash solution remained at or below pH 7 after one hour of washing. Pellicles were dried until constant weight at 50°C and dry weights were measured.

2.5.4. Transcriptional analysis

To investigate whether *fixK* has regulatory control over the genes involved in bacterial cellulose biosynthesis, transcript abundance was investigated by endpoint PCR of cDNA generated from RNA isolated from *K. xylinus* and *K. hansenii* wildtype and compared to their respective Δ*fixK* mutants. Cultures were prepared in 50 ml SHG_2 supplemented with 0.2% (v/v) cellulase in 125 ml flasks and grown at 30°C at 170 rpm. RNA was extracted during mid-log growth using an RNA Purification Plus Kit (Norgen). RNA was reverse transcribed into complementary DNA (cDNA) using random primers with the iScript™ Select cDNA Synthesis Kit (Bio-Rad). Endpoint PCR was performed using the EZ PCR Master Mix (miniPCR) with the following conditions: 95°C for 2 min; 30 cycles of 95°C for 20 sec, 55-61°C for 25 sec, 72°C for 45 sec; and 72°C for 2 min. Gene targets and annealing temperatures for each primer pair are listed in **Appendix Table 1**. Significance and percent reduction in gene expression was determined by t-tests comparing the mean gray value (intensity) of wildtype versus Δ*fixK* mutants via ImageJ v1.49 (National Institutes of Health) analysis ($p<0.05$).

2.5.5. Protein profile analysis of whole cell extracts

Differential protein expression between wildtype (WT) and Δ*fixK* mutants was analyzed in whole cell protein extracts by SDS-PAGE. To prepare protein extracts, *K. xylinus* and *K. hansenii* and their respective Δ*fixK* mutants were inoculated in 50 ml SHG_2 in 125 ml flasks to an OD_{600} of 0.005. Cultures were agitated at 170 rpm at 30°C until reaching stationary phase at an OD_{600} of approximately 1.0-1.2. Cells were harvested, resuspended in 4 ml of 200 mM Tris-HCl pH 7.5 supplemented with cOmplete™ EDTA-free Protease Inhibitor Cocktail and frozen at -80°C. Cells were slowly thawed overnight and sonicated on ice for 90 seconds (pulsed; 15 seconds on and 45 seconds off; 70% amplitude) with a Model 120 Sonic Dismembrator fitted with a 0.12" diameter probe (Fisher Scientific™). Proteins were precipitated by the addition of 16 ml cold acetone (4 volumes) and chilled overnight at -20°C. Proteins were harvested at 4°C by centrifugation at 3000

x *g* for 10 minutes, resuspended in 1000 µl of 200 mM Tris-HCl pH 7.5, and quantified using a Pierce™ bicinchoninic acid protein assay kit (Thermo Fisher Scientific).

Protein samples (2 µg) were electrophoresed on 10% Mini-PROTEAN® TGX™ precast protein gels on a Mini-PROTEAN® Tetra System (Bio-Rad) according to Laemmli (1970) at 200 V for approximately 35 minutes. Gels were silver stained as described by Gromova & Celis (2006) and imaged on a fluorescent light box using an EOS Rebel Camera (Canon).

3. Results

3.1. *K. xylinus* and *K. hansenii* secrete *bcsZ* and a xylan modifying enzyme

To investigate the possibility that *Komagataeibacter xylinus* and *K. hansenii* degrade plant cell wall compounds, initial screens for enzyme activity were performed on polymer-supplemented agar plates stained with iodine. Clearing zones after destaining would therefore indicate enzyme activity due to the degradation of the substrate. Substrate-containing agar plates incubated with aliquots of culture supernatant did not reveal degradative halos, however clearing zones were observed for all polysaccharides when incubated with quartered pellicles (representative results; **Figure 8**). This suggests that these species are capable of degrading cellulose, xylan, pectin, and lignin, but that the PCWDE are not present at detectable levels in the cell free supernatant. It is therefore likely that there is a greater concentration of enzymes within the pellicles, allowing detection of degradative activity. Alternatively, the degradative enzyme activity could be the result of membrane-bound enzymes whereby bacteria trapped within the pellicles are brought into close association with the substrate on the surface of the agar. It is important to note that while the use of iodine is widely accepted as a detection method in these types of plate degradation assays, iodine is rapidly converted to its colourless ionic I^- form by reducing organic products such as vitamin C,

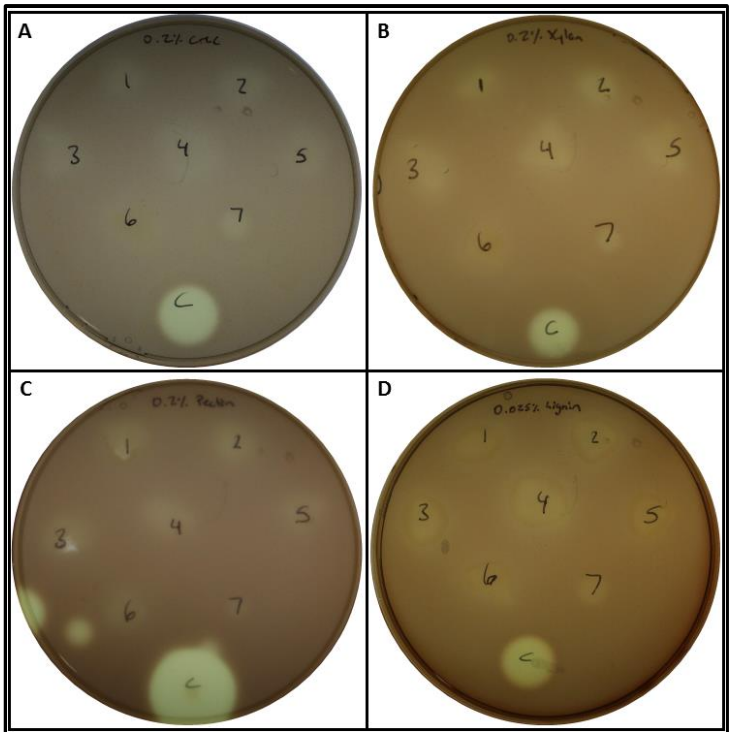

Figure 8: *K. xylinus* pellicles produce clearing zones on iodine stained (A) 0.2% CMC, (B) 0.2% xylan, (C) 0.2% pectin, and (D) 0.025% lignin supplemented agar plates. Seven-day old pellicles were placed onto polymer-supplemented plates and incubated for 2 days at 30°C. Iodine staining revealed clearing zones around all samples. Positive controls produced distinct clearing zones. *K. xylinus* cultures were grown in SHG_2 with the addition of: **1**, No additional compound; **2**, 2% fructose; **3**, 0.05% xylan; **4**, 0.05% CMC; **5**, 0.05% pectin; **6**, 0.05% lignin; **7**, 0.2% cellulase (aliquoted – no pellicle). **C** represents respective positive control (cellulase, xylanase, pectinase, or manganese peroxidase).

known to be produced by *K. oxydans* (Sugisawa et al., 1995), a related yet physiologically distinct species. Therefore, it is important to verify enzyme activity through additional analytical methods.

To further study whether the bacteria secrete PCWDE, concentrated cell free supernatant and squeezates were assayed for cellulase, xylanase, pectinase, or LMEs activity by zymography. Staining revealed substrate degradative enzymes contained within the gels; selected degradative bands were analyzed by mass spectroscopy.

In conjunction with zymography, substrate-free gels were also prepared to identify the concentration and molecular weight (MW) of secreted protein. The majority of proteins in the growth medium were below 11 kDa (**Figure 9**; representative gel). Considering most degradative enzymes are well above this MW, it is evident that *K. xylinus* and *K. hansenii* secrete these proteins at low abundance.

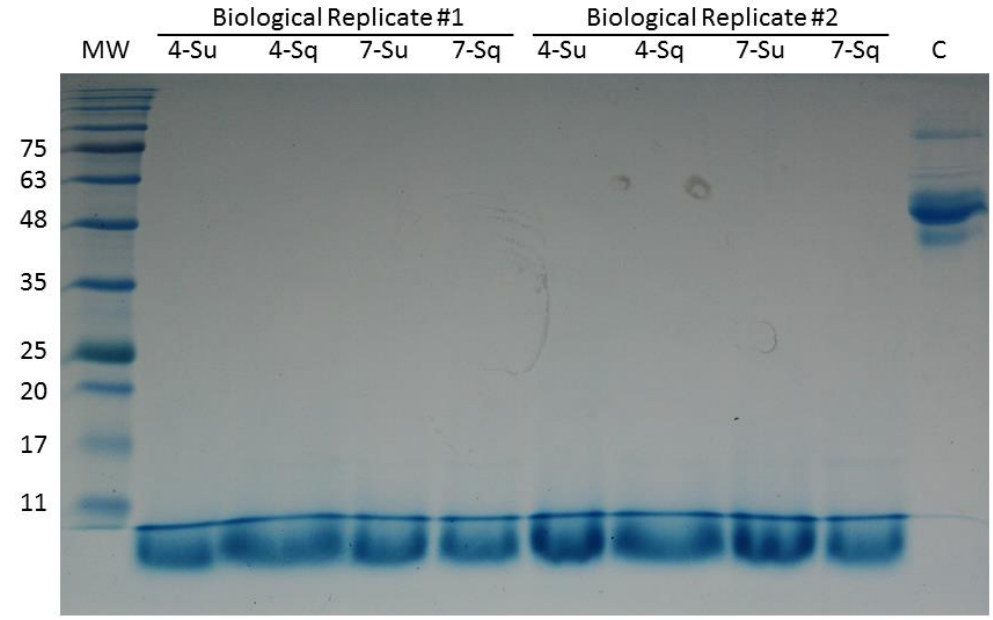

Figure 9: *K. xylinus* do not secrete >11 kDa proteins at detectable levels. Freeze-dried cell-free culture media were electrophoresed and stained with Coomassie blue. Only proteins <11kDa were detectable. **MW**, molecular weight marker; **C**, cellulase control; **4**, 4 day old culture; **7**, 7 day old culture; **Su**, supernatant (culture broth) extract; **Sq**, squeezate extract.

Zymography on CMC-supplemented polyacrylamide gels did not identify substantial CMCase activity in freeze-dried or ammonium sulfate precipitated samples. However, CMCase activity was identified in acetone-precipitated samples at a MW of 36.2 kDa (**Figure 10**). Mass spectrometric identification of proteins within excisions of the 36.2 kDa protein band for *K. hansenii* matched the 40.1 kDa BcsZ with 73% coverage and identified up to 5 oxidized methionine resides, a carbamidomethylated C329, and a possible deamidated N134 (**Appendix Figure 1**). The corresponding 36.2 kDa gel excision for *K. xylinus* matched BcsZ with 31% coverage and identified up to 2 oxidized methionine residues. Notably, the clearing zone at 36.2 kDa was only identified in samples from acetone-precipitated proteins and enzyme activity was dramatically more evident in fructose-grown cultures. Additionally, an OmpH-like outer membrane protein (ATCC53582_00683; 30.9 kDa) was identified in the 36.2 kDa protein band from the fructose-grown *K. xylinus* sample. OmpH, also known as Skp, has been characterized as a molecular chaperone for unfolded proteins as they emerge in the periplasm (Harms et al., 2001). There is no evidence that this protein interacts with BcsZ, however the knowledge that it was found secreted into the growth medium warrants further investigation.

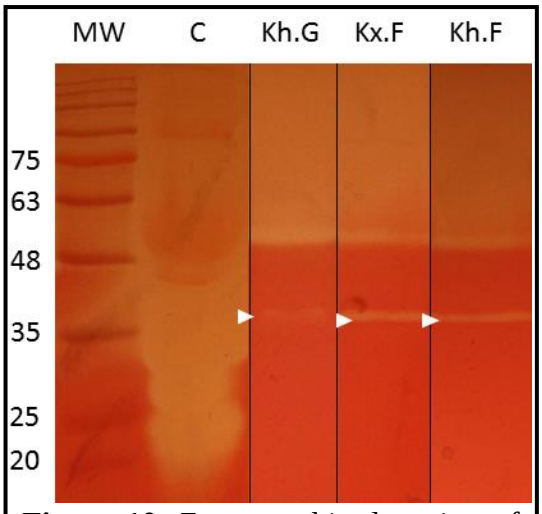

Figure 10: Zymographic detection of CMCase activity reveals a CMCase at 36.2 kDa. Acetone precipitated culture medium extracts were electrophoresed in CMC supplemented polyacrylamide gels. CMCase activity in protein extracts was identified (white arrows) by staining with Congo red. **MW**, molecular weight marker; **C**, cellulase control; **Kh.G**, *K. hansenii* from SHG_2; **Kx.F**, *K. xylinus* from SHF_2; **Kh.F**, *K. hansenii* from SHF_2.

Despite the results from preliminary agar plate screening, pectin, xylan, and lignin degrading enzymes were not detected by zymographic analysis. Whether this is due to detection limits, repression of degradative enzymes under lab conditions, or the absence of the genes required for degradation is unclear.

3.2. Chloramphenicol and tetracycline are effective selection antibiotics for *K. xylinus* and *K. hansenii*

Molecular manipulation and mutagenesis of bacteria often requires the use of antibiotic selection. Kanamycin has been an effective antibiotic for mutant selection in high yield cellulose

producing *Komagataeibacter* strains (Florea et al., 2016a), however *K. hansenii* has shown high resistance to this antibiotic (Deng et al., 2013). To improve selection methods, the sensitivity of *K. xylinus* and *K. hansenii* was determined on solid media for kanamycin, chloramphenicol, and tetracycline. *K. xylinus* was susceptible to kanamycin at 50 μg/ml but a limited number of *K. hansenii* CFUs were highly resistant (**Table 3**). As kanamycin concentration increased from 50 μg/ml to 300 μg/ml, fewer *K. hansenii* CFUs were capable of growth. Subculturing these colonies on 1000 μg/ml kanamycin revealed impressive resistance to the antibiotic (data not shown). *K. hansenii* also displayed higher resistance than *K. xylinus* against tetracycline and chloramphenicol, although complete inhibition of growth was found within reasonable concentrations as seen in **Table 2**.

The MIC assay identified 2 μg/ml and 4 μg/ml of tetracycline was inhibitory for *K. xylinus* and *K. hansenii*, respectively. Chloramphenicol was found to be inhibitory at 50 μg/ml and 150 μg/ml for *K. xylinus* and *K. hansenii*, respectively.

Table 2: *K. hansenii* is highly resistant to kanamycin. A sensitivity assay for *K. xylinus* and *K. hansenii* was performed on SHG_2 medium for kanamycin, tetracycline, and chloramphenicol. The number of resistant CFUs were counted after 5 days.

Antibiotic	Strain	μg/ml	Growth (CFUs)
Kanamycin	*K. xylinus*	50	-
		100	-
		200	-
		300	-
	K. hansenii	50	45
		100	25
		200	11
		300	2
Tetracycline	*K. xylinus*	6	-
		12.5	-
		20	-
		50	-
	K. hansenii	6	>>1000
		12.5	-
		20	-
		50	-
Chloramphenicol	*K. xylinus*	100	-
		200	-
		300	-
		400	-
	K. hansenii	100	>>1000
		200	>>200
		300	-
		400	-

3.3. Transformant selection is improved by direct cellulase application during spread plating

K. xylinus produces a recalcitrant cellulosic biofilm when grown in glucose leading to antibiotic resistance in these bacteria. Improving the cellulase-facilitated cellulose degradation was necessary for efficient transformant selection. To determine the most effective application of cellulase, *K. xylinus* electrocompetent cells were prepared from cultures grown in SHF_2 and recovered in SHG_2. Cells were plated on SHG_2 Chl^{150} with either 0.2% (v/v; 50 μl) cellulase

incorporated into the agar medium or 0.1% (v/v; 25 µl) spread on the plates with the transformation mixture. Transformants appeared within 6 to 7 days of growth with no noticeable satellite colonies for cultures that were spread plated with the addition of 0.1% (v/v) cellulase. Transformants spread on 0.2% (v/v) cellulase-supplemented medium appeared within the same timeframe however a multitude of colonies appeared as potentially false positive satellite colonies. The addition of spread plated 0.1% (v/v) cellulase was deemed to be the more effective method as it used less of the enzyme and produced less potential false positives.

3.4. Fructose facilitates faster cell growth and enhances electrocompetence of *Komagataeibacter*

Methods for the transformation of *K. xylinus* and *K. hansenii* are poorly studied. To improve electroporation, different growth media compositions were evaluated for the production of electrocompetent cells. Growth kinetics were investigated for each culture condition to determine the OD_{600} that represents mid-logarithmic growth. Despite the addition of at least 2% (v/v) cellulase to the cultures, *K. xylinus* still showed signs of aggregation when grown in 96 well plates, therefore, the possibility of exaggerated density readings due to cell clumping cannot be ruled out. Considering the high concentration of cellulase in these cultures, it is possible that this cell aggregation may be cellulose independent.

K. xylinus cultures in SHF_1 or SHF_2 (**Table 1**) grew faster and three-fold more dense than those grown in SHG_2 (**Figure 11 and Figure 12**). Surprisingly, the canonical growth medium SHG_2 resulted in poor growth for *K. xylinus* compared to other growth media as depicted by growth rate and low final culture density (**Figure 12, A and B)**. Reducing the glucose in this medium by half (SHG_1) increased culture density by stationary phase (69.5 hours) for both species (**Figure 12**). The addition of 50 mM acetic acid had little effect on growth in all conditions however substituting half or all glucose for glycerol had a positive correlation for growth (**Figure 12**). In these conditions, *K. xylinus* had a faster growth rate than *K. hansenii*, however it is important to consider that cellular aggregation may have artificially exaggerated and varied OD_{600} measurements. For instance, the culture density of *K xylinus* grown in $SH_0\,Gly_2$ dropped by approximately 30% between 52.5 and 62 hours before recovering to a similar cell density (**Figure 11, A**). Whether this is due to cell lysis or simply reduced cell aggregation by this time point is not clear.

Similar yet less dramatic trends were observed with *K. hansenii* cultures. In SHF_1 and SHF_2, *K. hansenii* grew up to 3-fold faster than in SHG_2, however there was no clear trend for final culture

density (**Figure 11, C and D**). Glycerol had no significant effects on *K. hansenii* growth rate, but the addition of 1% glycerol to SHF_1 to make SHF_1 Gly_1 seemed to improve long-term survival of fructose fed cultures as seen by sustained OD_{600} in these cultures (**Figure 11, D**).

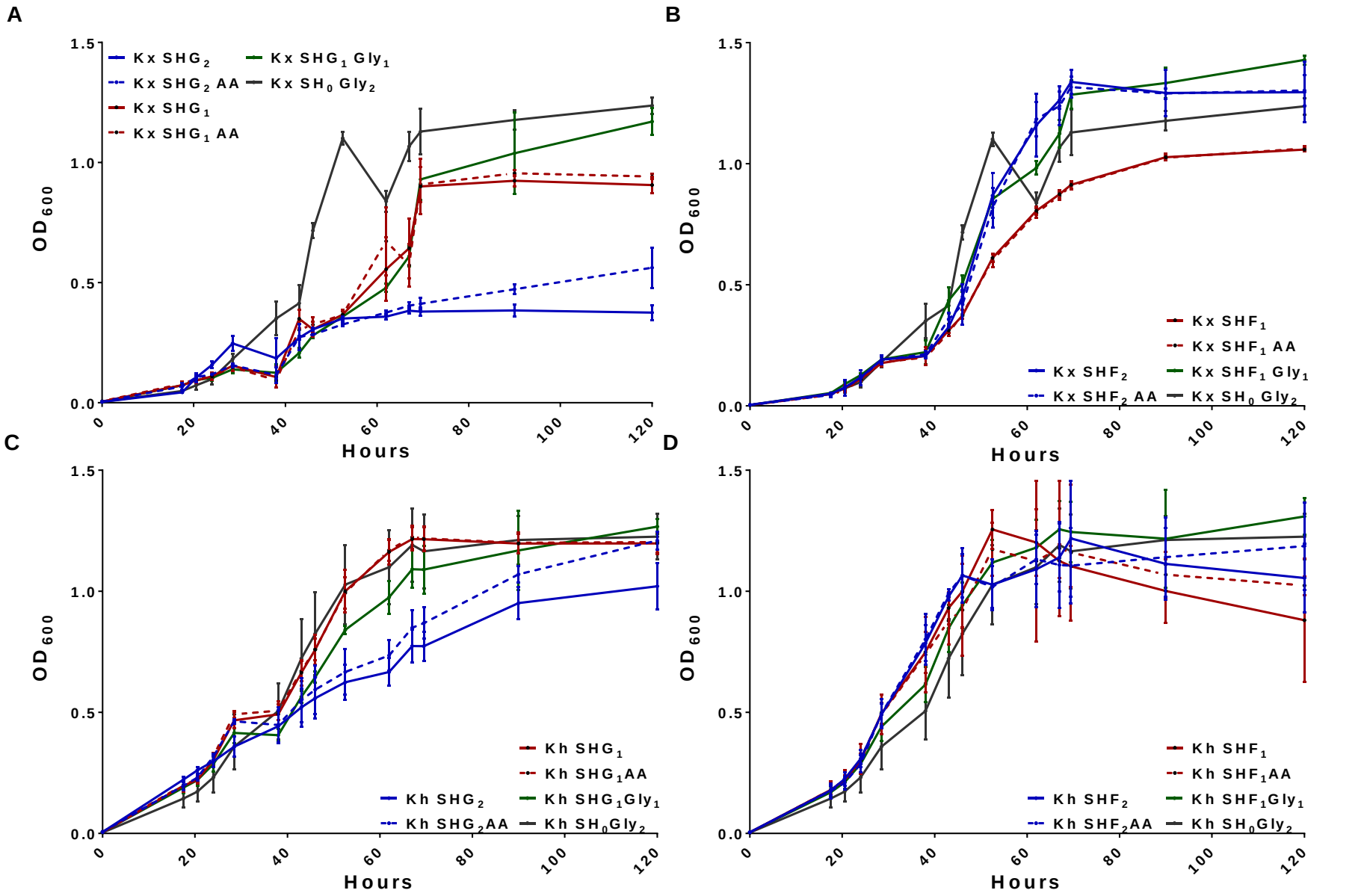

Figure 11: Growth of *K. xylinus* (A and B) and *K. hansenii* (C and D) is influenced by carbon source, but not the presence of 50 mM acetic acid. *Komagataeibacter* species were grown in the presence of various carbon sources (see **Table 1** for composition) to determine the OD_{600} of mid-logarithmic growth. *K. xylinus* SHG_1 Gly_1 facilitated rapid growth after 60 hours. *K. hansenii* cultures lose density after 60 hours when grown in fructose. Error bars show standard deviation of the mean (n = 3).

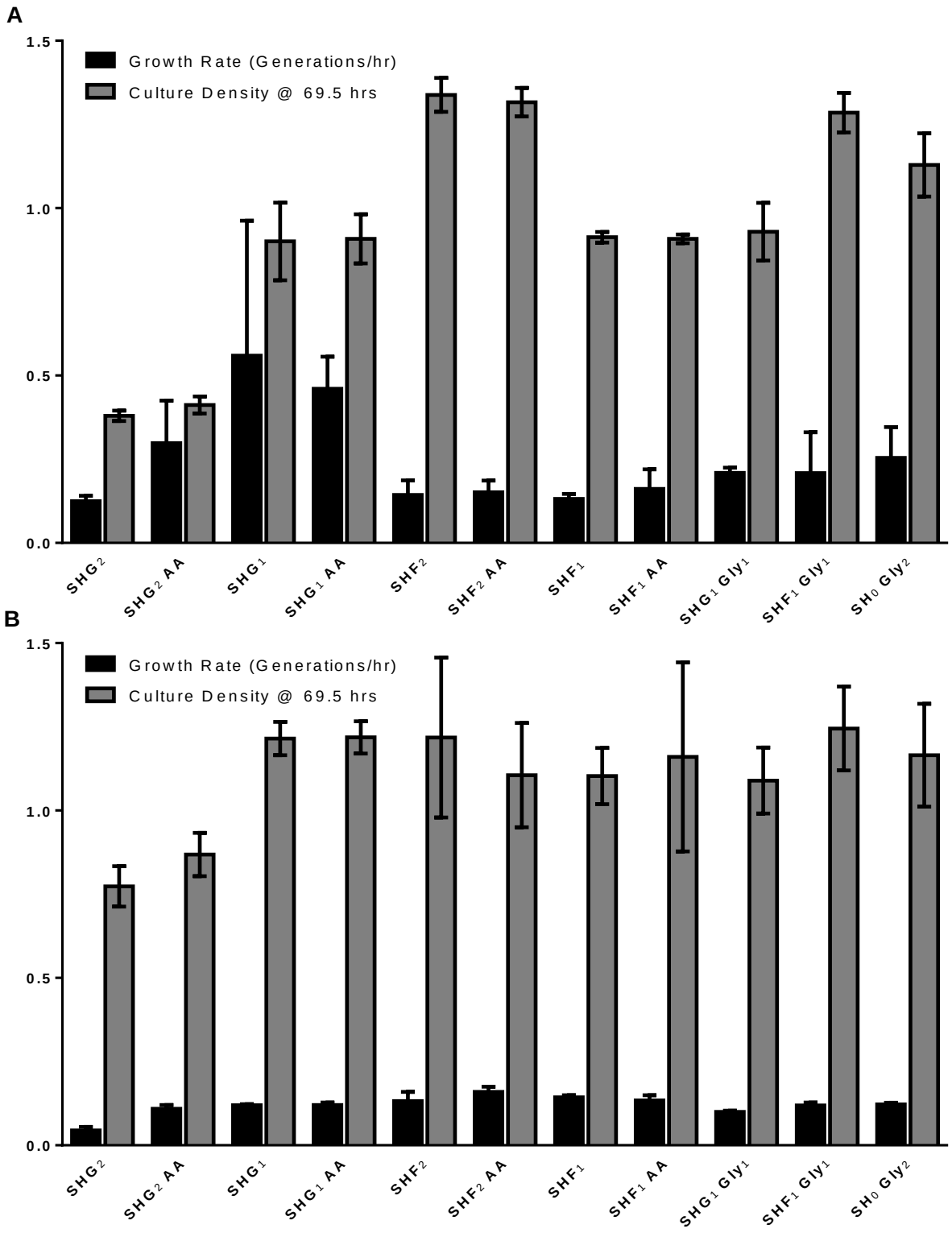

Figure 12: Growth rate (generations/hour) and OD_{600} at 69.5 hours of growth of *K. xylinus* (A) and *K. hansenii* (B) is influenced by carbon source, but not the presence of 50 mM acetic acid. *Komagataeibacter* species were grown in the presence of various growth media (see **Table 1** for composition) to determine the OD_{600} of mid-logarithmic growth. *K. xylinus* grows fastest and reaches the highest density in the presence of fructose. SHG_2, the canonical growth medium, facilitates the slowest growth of *K. xylinus*. *K.* The addition of 50 mM acetic acid had no significant change on growth for either species. Error bars show standard deviation of the mean (n = 3).

To evaluate the impact that the growth medium has on transformation efficiency, *K. xylinus* and *K. hansenii* were grown to mid-logarithmic phase in SHG_2, SHF_2, SHF_1, SHF_1 AA, SHF_1 Gly_1, and SH_0 Gly_2 and prepared for electroporation (Florea et al., 2016a). Electroporation of pSEVA331Bb into *K. xylinus* prepared in SHG_2 was unsuccessful, however pSEVA311Bb was successfully transformed into *K. xylinus* prepared in SHF_1, SHF_1 AA, SHF_1 Gly_1, and SH_0 Gly_2; transformation efficiencies are listed in **Table 3**. pSEVA331Bb was similarly electroporated into *K. hansenii* prepared in SHF_1 with an efficiency of approximately 10^7 CFU/µg DNA .

Table 3: pSEVA331Bb transformation efficiency (CFU/µg DNA) of electrocompetent *K. xylinus* prepared in various growth media (see **Table 1** for composition).

	Time	
Medium	**1.25 hours**	**6.5 hours**
SHG_2	0	0
SHF_2	0†	0†
SHF_1	$6.3x10^3$	$1.8 x10^4$
SHF_1 AA	$8.1 x10^3$	$9.8 x10^3$
SHF_1 Gly_1	$1.3 x10^4$	$9.1 x10^3$
SH_0 Gly_2	$2.7 x10^3$	$3.9 x10^3$

†SHG2 sample arced during electroporation

fixK was knocked out to understand the role that this global transcription factor plays in bacterial cellulose production and in carbon source utilization. This was accomplished by the electroporation of the *fixK* knockout construct *fixK*-Chl-*fixK* (**Figure 7**) into *K. xylinus* and *K. hansenii*. Incorporation of this construct required not only the transformation into cells but also double homologous recombination with the native *fixK*. No transformants grew on selection plates for *K. xylinus* glucose-grown cultures. For fructose-grown cultures, the transformation efficiency for the *fixK*-Chl-*fixK* construct was $2.1x10^3$ CFU/µg and $8.0x10^2$ CFU/µg when transformed at high voltage/low [DNA] (2.5 kV; 0.5 ng/µl) or low voltage/high [DNA] (1.8 kV; 1 ng/µl) voltage, respectively. The addition of acetic acid or glycerol to fructose-fed cultures did not seem to have a dramatic effect on transformation efficiency.

3.5. FixK is identical in *K. xylinus* and *K. hansenii*

Due to its role as a global transcriptional regulator, the linear construct *fixK*-Chl-*fixK* was electroporated into *K. xylinus* and *K. hansenii* to examine the role that *fixK* plays in cellulose production and other metabolic processes. Homologous recombination of the linear construct in the genome results in a truncated *fixK*, confirmed by sequence analysis. Sequencing of the *K. hansenii* ATCC 23769 Δ*fixK* mutant lead to the clarification of a miscalled inserted base pair in the published genomic sequence of *K. hansenii* ATCC 23769 at location 181,881. Removing the miscalled insertion changes the predicted amino acid sequence to be identical to *K. xylinus* ATCC 53582 with 99% identity at the nucleotide level.

3.6. *fixK* mutagenesis increases colony size and modifies colony morphology on solid media

To determine the morphological effect of the *fixK* knockout, colonial morphologies of both wildtype and Δ*fixK* mutants of *K. xylinus* and *K. hansenii* were examined in SH medium containing either glucose, fructose, or sucrose at either 10 or 20 g/L. Morphological differences appeared by 6 days of growth, with large variations by 11 days. On the carbon sources tested, Δ*fixK* mutants formed different colony morphologies than their respective wildtype (WT) strain.

K. xylinus WT and Δ*fixK* mutant form small circular convex colonies, however the WT forms projections along grooves formed during streak plating (**Figure 13, A**). These projections are likely cellulose-dependent as *K. xylinus* Δ*fixK* is incapable of producing this feature (**Figure 13, B**). Fructose and sucrose fed WT colonies appear much less opaque with poorly defined margins (**Figure 13, C and E**), especially on sucrose plates. Both the WT and Δ*fixK* mutant colonies appear morphologically distinct between halves of the same colony (**Figure 13, C-F**). One half of the colony remained relatively circular while the other became lobate in nature. In general, the extensions were unidirectional on plates indicating possible quorum sensing. Furthermore, the directionality was more pronounced in SHF_1 than SHF_2 (data not shown), indicating this is not only dependent on carbon source but also on its concentration.

On SHG_2, *K. hansenii* WT forms circular, convex colonies similar in size to *K. xylinus* (**Figure 13, G**), however the Δ*fixK* mutant colonies were much larger with an umbonate elevation (**Figure 13, H**). Interestingly, the fructose and sucrose fed WT colonies resemble the glucose fed Δ*fixK* mutant colonies (**Figure 13, H, I, and K**). The fructose and sucrose fed Δ*fixK* mutants were much larger and display a slightly undulate margin but none of the *K. hansenii* colonies display the divided culture morphology seen in *K. xylinus* (**Figure 13, J and L**).

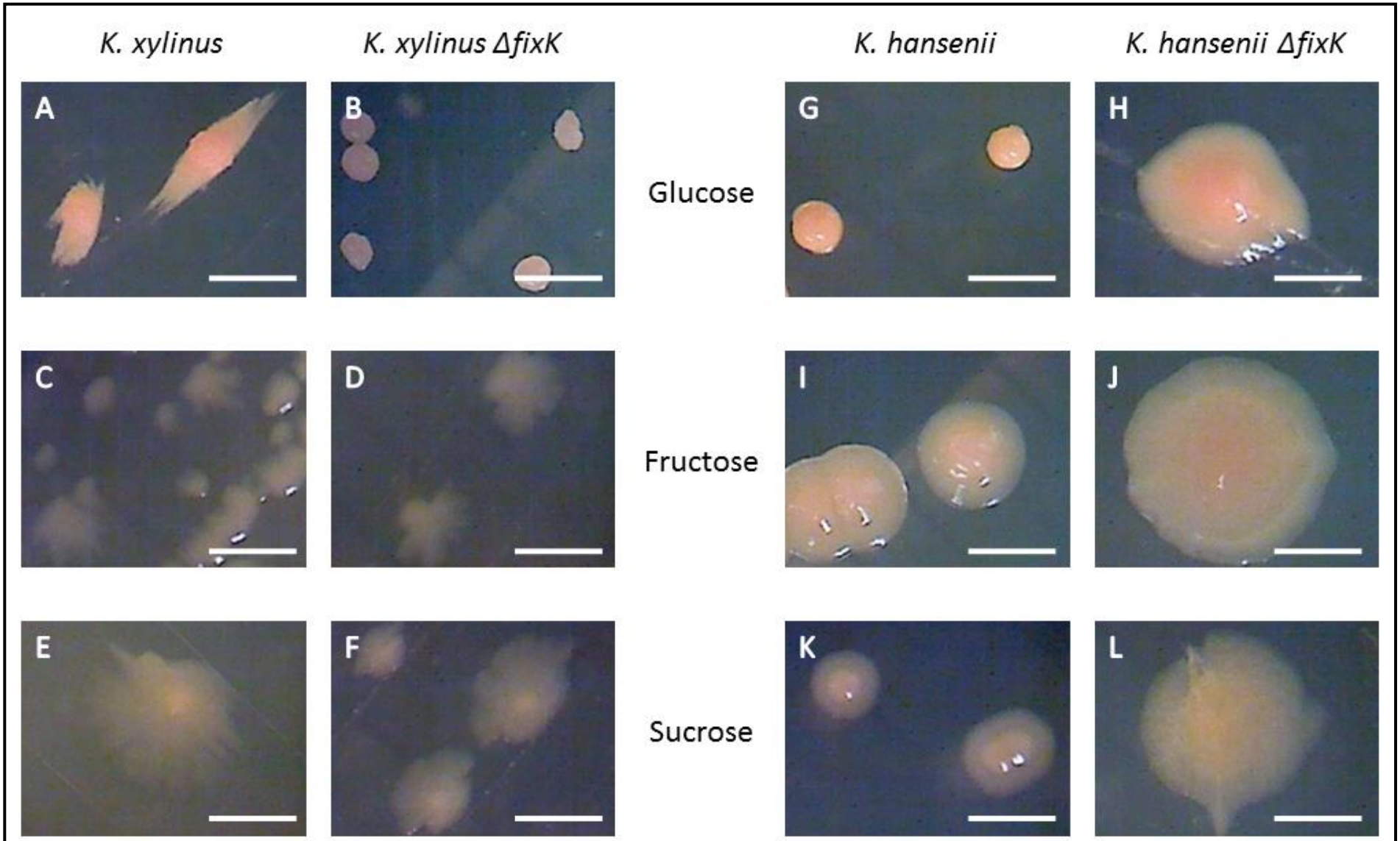

Figure 13: *K. xylinus* and *K. hansenii* colony morphology is dependent on carbon source and *fixK*. *K. xylinus* (A, C, E), *K. xylinus* Δ*fixK* (B, D, F), *K. hansenii* (G, I, K) and *K. hansenii* Δ*fixK* (H, J, L) were grown for 11 days on SHG_2 (A, B, G, H), SHF_2 (C, D, I, J), or SHS_2 (E, F, K, L). Colonies grown on SHG_2 produce far more spherical shaped colonies than on SHF_2 or SHS_2. *K. hansenii* Δ*fixK* colonies grew substantially larger than the wildtype. White scale bar = 1 mm, all pictures were taken at equal magnification.

The impact of pellicin (([2E]-3-phenyl-1-[2,3,4,5-tetrahydro-1,6-benzodioxocin-8-yl]prop-2-en-1-one), a compound known to abolish pellicle production (Strap et al., 2011), was investigated for *K. xylinus* wildtype and the Δ*fixK* mutant. Differences between the DMSO control and pellicin treated colonies became clear by 24 days of growth. The presence of pellicin in the medium resulted in increased colony size; more horizontally dispersed colonies were formed in both wildtype and mutant strains in the presence of pellicin (**Figure 14**).

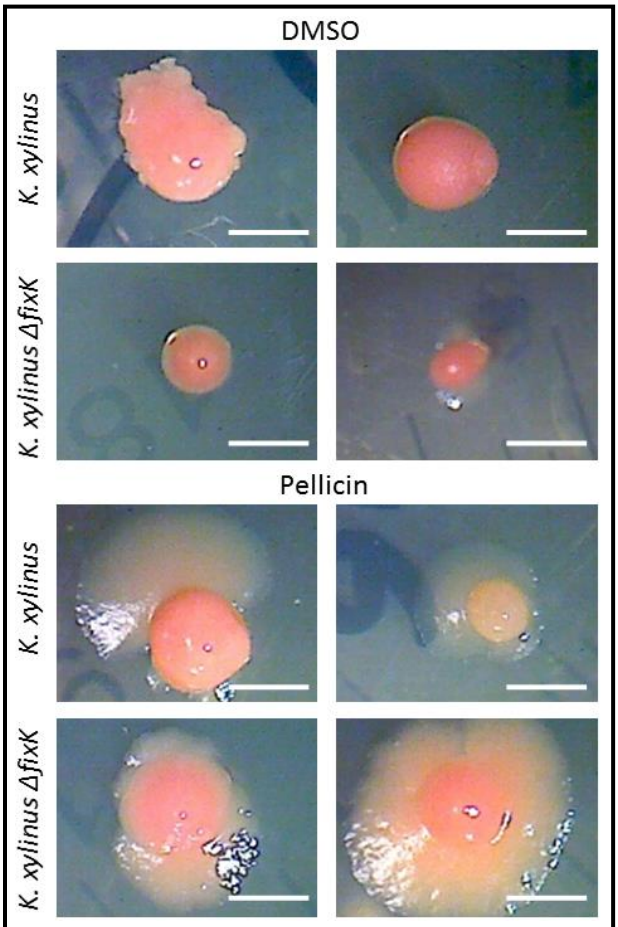

Figure 14: *K. xylinus* colony morphology is influenced by pellicin. *K. xylinus* WT and *K. xylinus* Δ*fixK* were grown for 24 days on SHG_2 containing DMSO (control) or pellicin. Colonies grown in the presence of pellicin produced horizontally dispersed colonies with less well-defined spherical shape. White scale bar = 1 mm, all pictures were taken at equal magnification. Two isolated colonies were pictured to show variation in morphology.

3.7. *fixK* is essential for fructose and sucrose metabolism in *K. hansenii* and abolishes diauxic growth in *K. xylinus*

To evaluate the role of *fixK* in the growth of *K. xylinus* and *K. hansenii*, growth kinetics were investigated during growth in agitated cultures. *fixK* was found to have subtle impacts on the growth rate and culture density of *K. xylinus* when grown in glucose, fructose, or sucrose based media (**Figure 15 and Figure 17**). Diauxic growth was observed when *K. xylinus* was grown in SHG_2; a characteristic second logarithmic growth stage that occurs when gluconic acid is metabolized. Δ*fixK* mutants did not exhibit diauxic growth (**Figure 15, A**). Limiting the glucose from 2% to 1% (as in SHG_1) improved growth by 53% for *K. xylinus* independently of *fixK* by 10 days of growth (**Figure 15, B**). A slight pH drop was observed in *K. xylinus* wildtype grown in SHF_2, likely due to the exogenously added cellulase degrading bacterial cellulose which resulted in the conversion of glucose into gluconic acid (**Figure 15, C**). No significant differences were observed when *K. xylinus* was grown in SHS_2 and the culture seemed to be minimally metabolically active (**Figure 15, D**).

K. hansenii was heavily dependent on *fixK* for optimal growth in glucose, fructose, and sucrose media (**Figure 17**). When cultured in SHG_2, *K. hansenii* Δ*fixK* had an OD_{600} less than 70% of the wildtype strain (**Figure 16, A**). This effect was concentration dependent, growth in SHG_1 limited this difference to approximately 86% (**Figure 16, B**). Dramatic dependence on *fixK* was observed during growth in SHF_2 or SHS_2 (**Figure 16**, **C and D**). *K. hansenii* Δ*fixK* was capable of reaching less than 50% growth density compared to the wildtype in both media (**Figure 16, C and D**). Surprisingly, there was no significant difference in growth rate between *K. hansenii* WT and Δ*fixK* mutants.

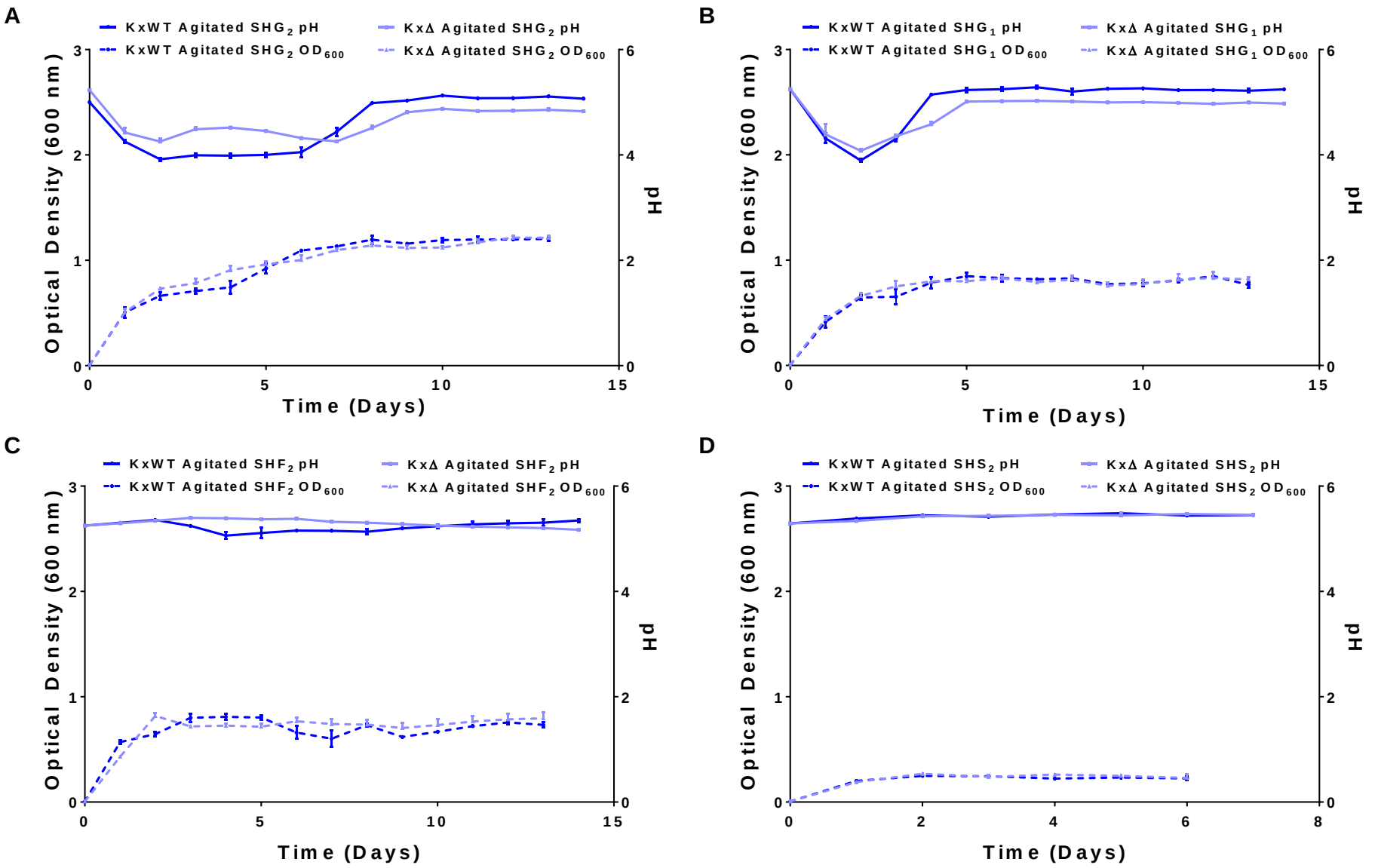

Figure 15: *fixK* influences growth and pH of *K. xylinus* in a carbon source dependent manner. OD_{600} and pH were measured in *K. xylinus* WT and *K. xylinus* Δ*fixK* in SHG_2 (A), SHG_1 (B), SHF_2 (C), and SHS_2 (D) in agitated conditions (see **Table 1** for composition). The loss of *fixK* resulted in less acid production and the loss of the diauxic growth observed in SHG_2. The transient pH drop in SHF_2 is only observed for the wildtype strain. Error bars are standard deviation of the mean (n = 3).

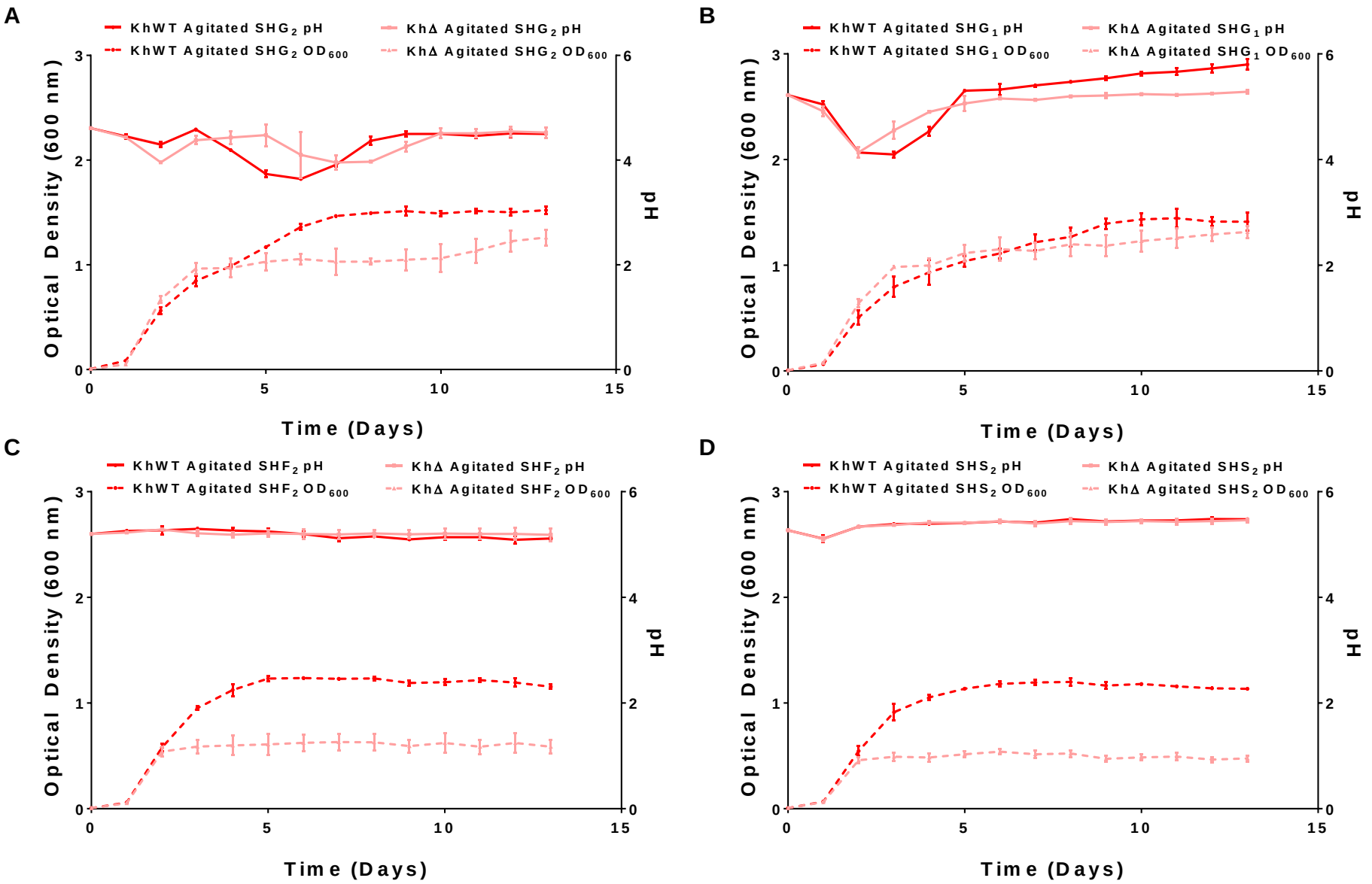

Figure 16: *fixK* influences growth and pH of *K. hansneii* in a carbon source dependent manner. OD_{600} and pH were measured in *K. hansenii* WT and *K. hansenii* Δ*fixK* in SHG_2 (A), SHG_1 (B), SHF_2 (C), and SHS_2 (D) in agitated conditions (see **Table 1** for composition). The loss of *fixK* resulted in modified acid metabolism in SHG_2 and SHG_1. Final culture density in SHG_2, SHF_2, and SHS_2 was dramatically limited in the absence of *fixK*. Error bars are standard deviation of the mean (n = 3).

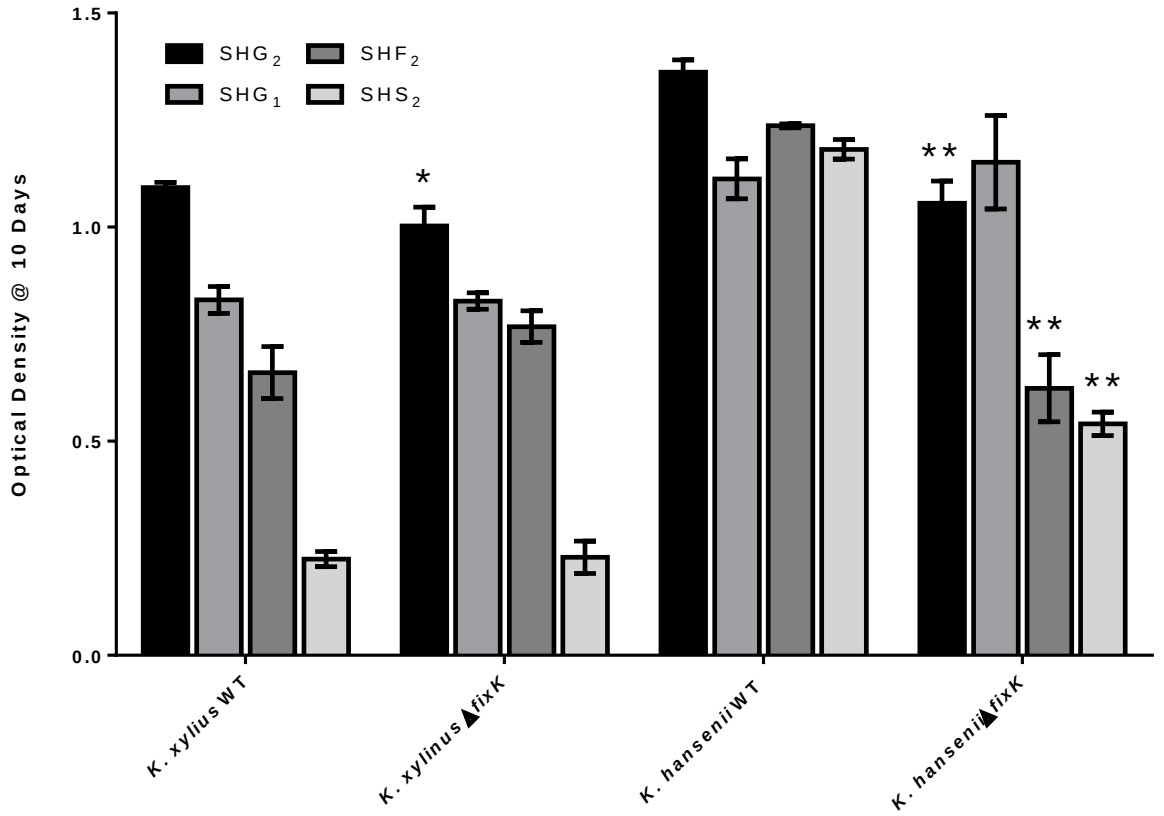

Figure 17: *fixK* influences growth and pH of *K. xylinus* and *K. hansenii* in a carbon source dependent manner. Optical density at 10 days of growth was measured in *K. hansenii* WT and *K. hansenii* Δ*fixK* in SHG_2, SHG_1, SHF_2, and SHS_2 in agitated conditions (see **Table 1** for composition). Density of *K. hansenii* in SHG_2, SHF_2, and SHS_2 was dramatically limited in the absence of *fixK*. Error bars are standard deviation of the mean (n = 3). * = significant difference from wildtype ($p < 0.05$); ** = significant difference from wildtype ($p < 0.0005$)

3.8. *fixK* is essential for optimal cellulose production in *K. hansenii* and *K. xylinus*

fixK is essential for cellulose synthesis in *K. hansenii*, however *K. xylinus* is still capable of cellulose synthesis in the absence of this gene. The cellulose produced by *K. xylinus* was therefore compared between the wildtype and Δ*fixK* knockout. At 7 days of growth, *K. xylinus* Δ*fixK* produced 19% to 40% cellulose of that of the wildtype, depending on carbon source (**Figure 18, A and B**). The greatest reduction in cellulose production due to Δ*fixK* mutagenesis was observed in glucose fed cultures, indicating an essential role for *fixK* in cellulose biosynthesis from glucose (**Figure 18,**

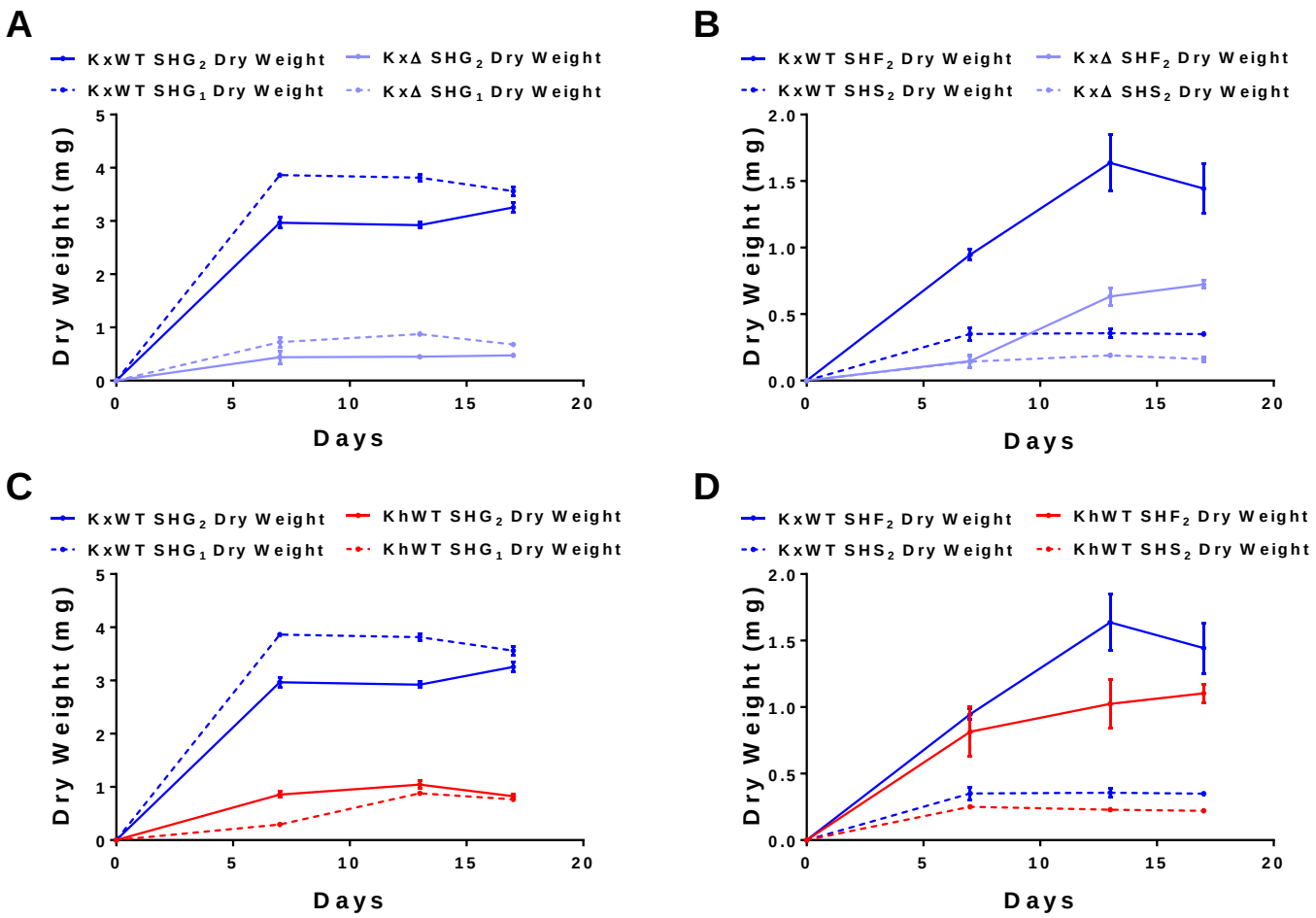

Figure 18: *fixK* regulates cellulose synthesis in *K. xylinus* and *K. hansenii*. Dehydrated pellicle weights were measured in *K. xylinus* WT, *K. xylinus* Δ*fixK* and *K. hansenii* WT. *K. xylinus* WT pellicle weight was dramatically higher than the Δ*fixK* mutant when grown in SHG_2, SHG_1 (A), SHF_2, or SHS_2 (B) (see **Table 1** for composition). *K. xylinus* WT produced dramatically more cellulose than *K. hansenii* WT in the presence of SHG_2 or SHG_1 (C), however only slightly less in the presence of SHF_2 or SHS_1 (D). Error bars show standard deviation of the mean (n = 3).

A). There was a surprising 6.6% decrease in cellulose yield ($p < 0.05$) between 13 and 17 days for *K. xylinus* WT grown in SHG_1 (**Figure 18, A**).

In *K. xylinus* and *K. hansenii* the cellulose yield decreased by 17 days in SHG_1 and SHG_2, respectively (**Figure 18, C**). In SHF_2 and SHS_2, cellulose production did not significantly change after 13 days and total yields were quite similar between species (**Figure 18, D**). In contrast, *K. hansenii* produced only about 30% of *K. xylinus* cellulose yield when glucose was the carbon source (**Figure 18, C**). *K. hansenii* Δ*fixK* mutants did not produce cellulose and therefore could not be included in this assay.

3.9. *fixK* mutants follow wildtype pH and gluconic acid trends over longer timeframes

pH and gluconic acid concentrations were measured in agitated and statically grown cultures to evaluate metabolism between WT and Δ*fixK* mutants. The pH of the growth medium was correlated with the presence of gluconic acid in both *K. xylinus* and *K. hansenii* (**Figure 19-24**). Notably, statically grown *K. hansenii* cultures grown in SHG_2 continued to acidify the growth medium while the gluconic acid concentration decreased (**Figure 22, D**), indicating that gluconic acid is a secondary metabolite for these bacteria.

The most dramatic acidification was observed in statically grown *K. xylinus* and *K. hansenii* cultures in SHG_2 with a minimum pH of 3.09 and 3.28, respectively (**Figure 19, 22**). The low pH in these media represent astonishingly high gluconic acid concentrations with up to 12 of the 20 grams of glucose being oxidized into the acid in *K. hansenii* (**Figure 22**). After the pH drop, these cultures alkylated the medium back to the initial proton concentrations. The only exception to this trend was observed for statically grown *K. xylinus* WT and *K. xylinus* Δ*fixK* in SHG_2 (**Figure 19**), however one would predict that this would have eventually occurred based on comparisons to SHG_1. Agitated *K. xylinus* grown in fructose, but not sucrose, was capable of acidifying the growth medium (**Figure 21, A**). However, agitated *K. hansenii* grown in sucrose, but not fructose, was capable of acidifying the growth medium (**Figure 24, C**). This could be due to the presence of glucose in the medium, a product of cellulose degradation. This possibility is further justified by the slow onset of similar acidification by the limited cellulose producer *K. xylinus* Δ*fixK* (**Figure 21, B**). In SHF_2 or SHS_2, *K. xylinus* produced nearly undetectable levels of gluconic acid (**Figure 21, A-D**), while *K. hansenii* could produce measureable quantities of the acid under agitated conditions (**Figure 24, A and C**).

Generally speaking, the Δ*fixK* mutants produced highly similar yet delayed pH and gluconic acid patterns compared to their respective WT strains, characterized by elongated pH curves (**Figure 19 to Figure 234**). Most notably, the agitated SHG_2 grown Δ*fixK* mutants acidified the medium to a lesser extent than their WT strains ($p<<0.001$) (**Figure 19, C and Figure 22, C**).

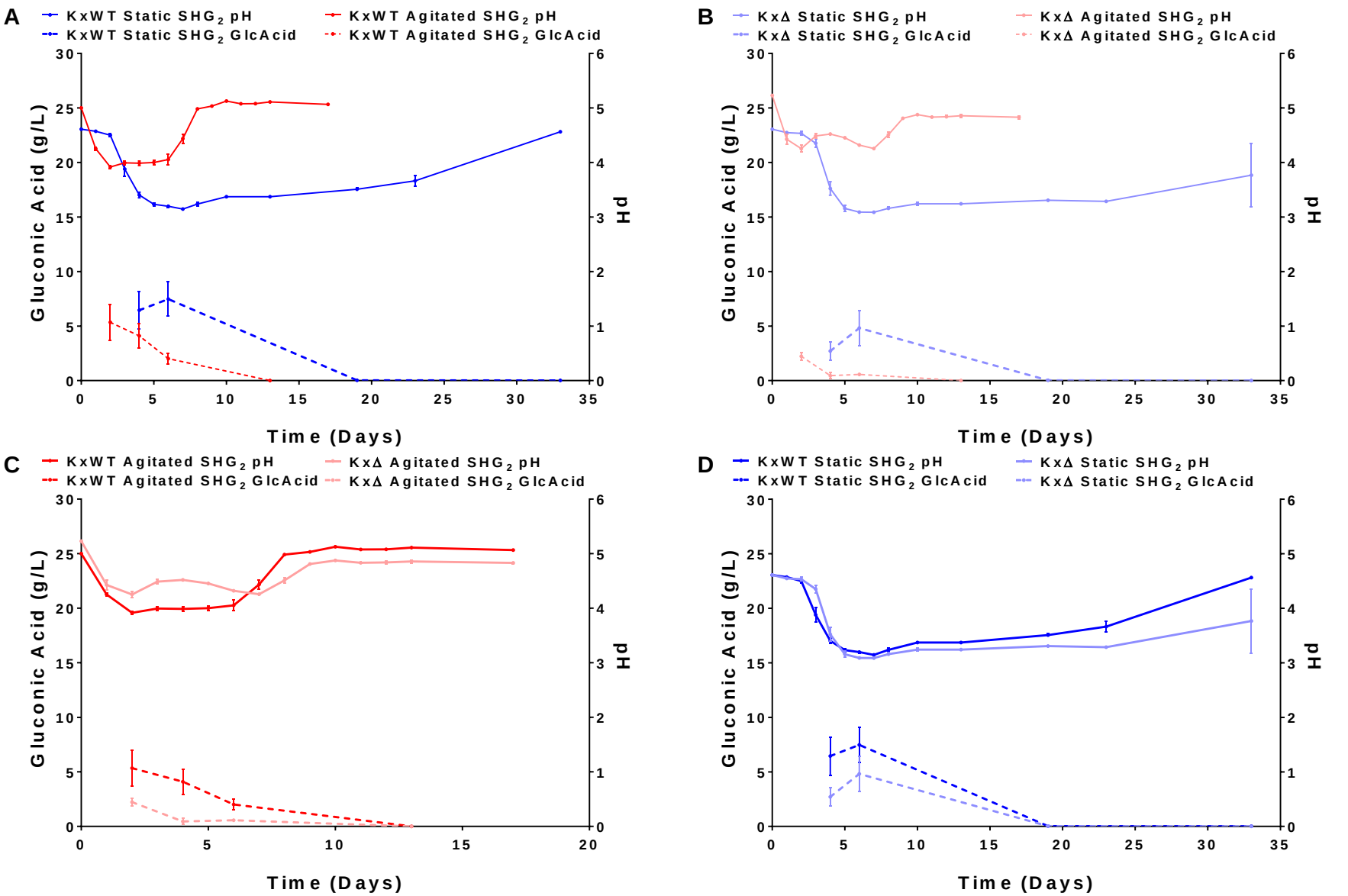

Figure 19: *fixK* is involved in acid metabolism in *K. xylinus* in agitated and statically grown SHG_2 cultures. pH and gluconic acid concentrations were measured in *K. xylinus* WT and *K. xylinus* Δ*fixK* grown in SHG_2 with and without agitation. Statically grown WT and Δ*fixK* mutants produce much more acid and take much longer to reach stationary phase under static conditions (A, B). The loss of *fixK* is associated with less acidity and less gluconic acid production under agitated conditions (C). In statically grown cultures, the Δ*fixK* mutation is associated with less gluconic acid production but greater medium acidity (D). Error bars show SD (n = 3).

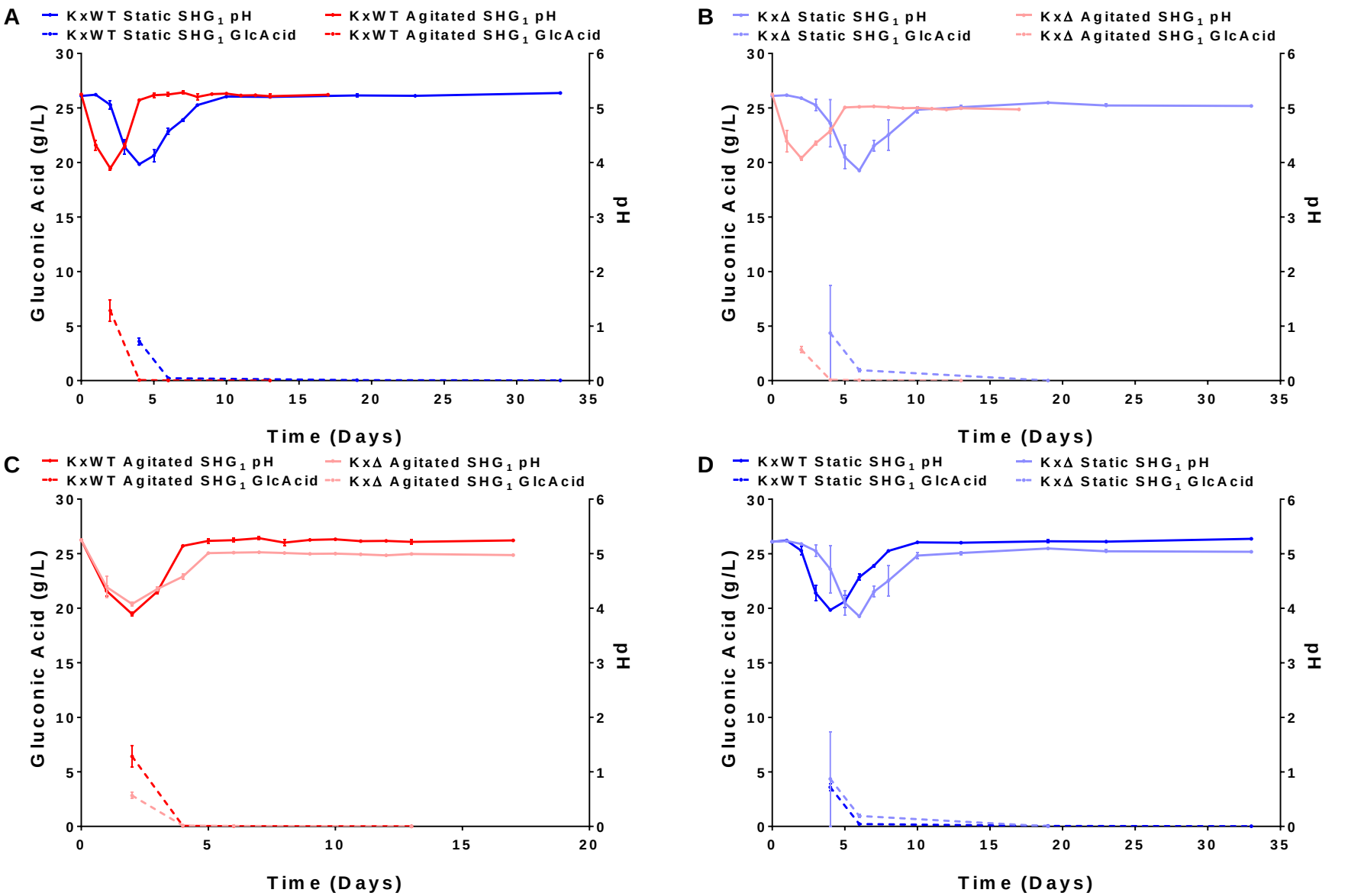

Figure 20: *fixK* is involved in acid metabolism in *K. xylinus* in agitated and statically grown SHG_1 cultures. pH and gluconic acid concentrations were measured in *K. xylinus* WT and *K. xylinus* Δ*fixK* grown in SHG_1 with and without agitation. Statically grown WT and Δ*fixK* mutants produce similar acidification profiles, however the trend is stretched over a longer time frame in static conditions (A, B). The loss of *fixK* is associated with less gluconic acid production under agitated conditions (C). In statically grown cultures, the Δ*fixK* mutation is associated with a delayed pH profile (D). Error bars show SD (n = 3).

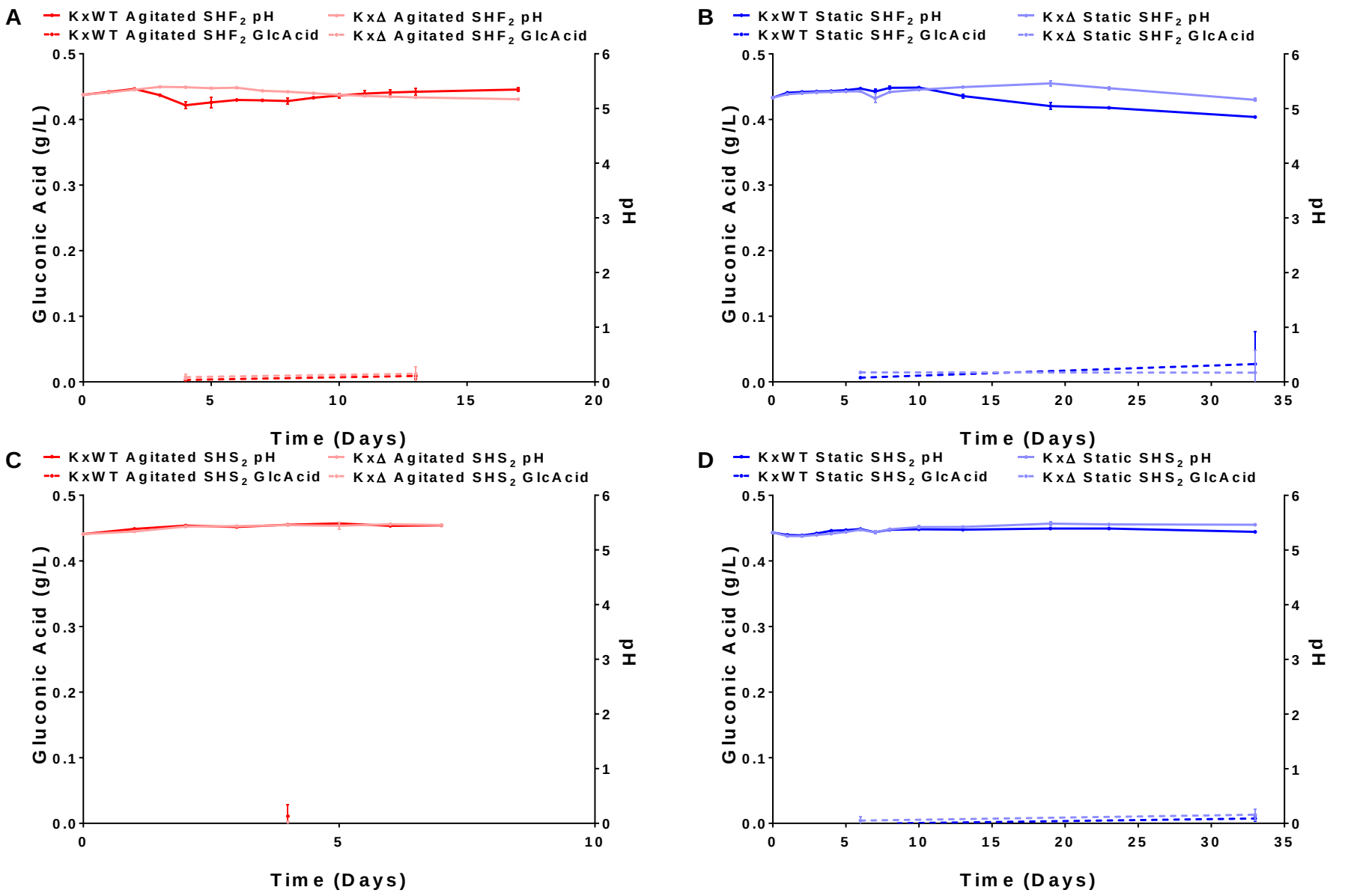

Figure 21: *fixK* has little effect on acid metabolism for *K. xylinus* in agitated and statically grown SHF_2 and SHS_2 cultures. pH and gluconic acid concentrations were measured in *K. xylinus* WT and *K. xylinus* Δ*fixK* grown in SHF_2 and SHS_2 with and without agitation. Agitated *K. xylinus* Δ*fixK* in SHF_2 was unable to acidify the growth medium to pH ~5.1 at 4 days of growth (A). None of the cultures produced measurable concentrations of gluconic acid. Note that the right y-axis ends at pH 6.5. Error bars show SD (n = 3).

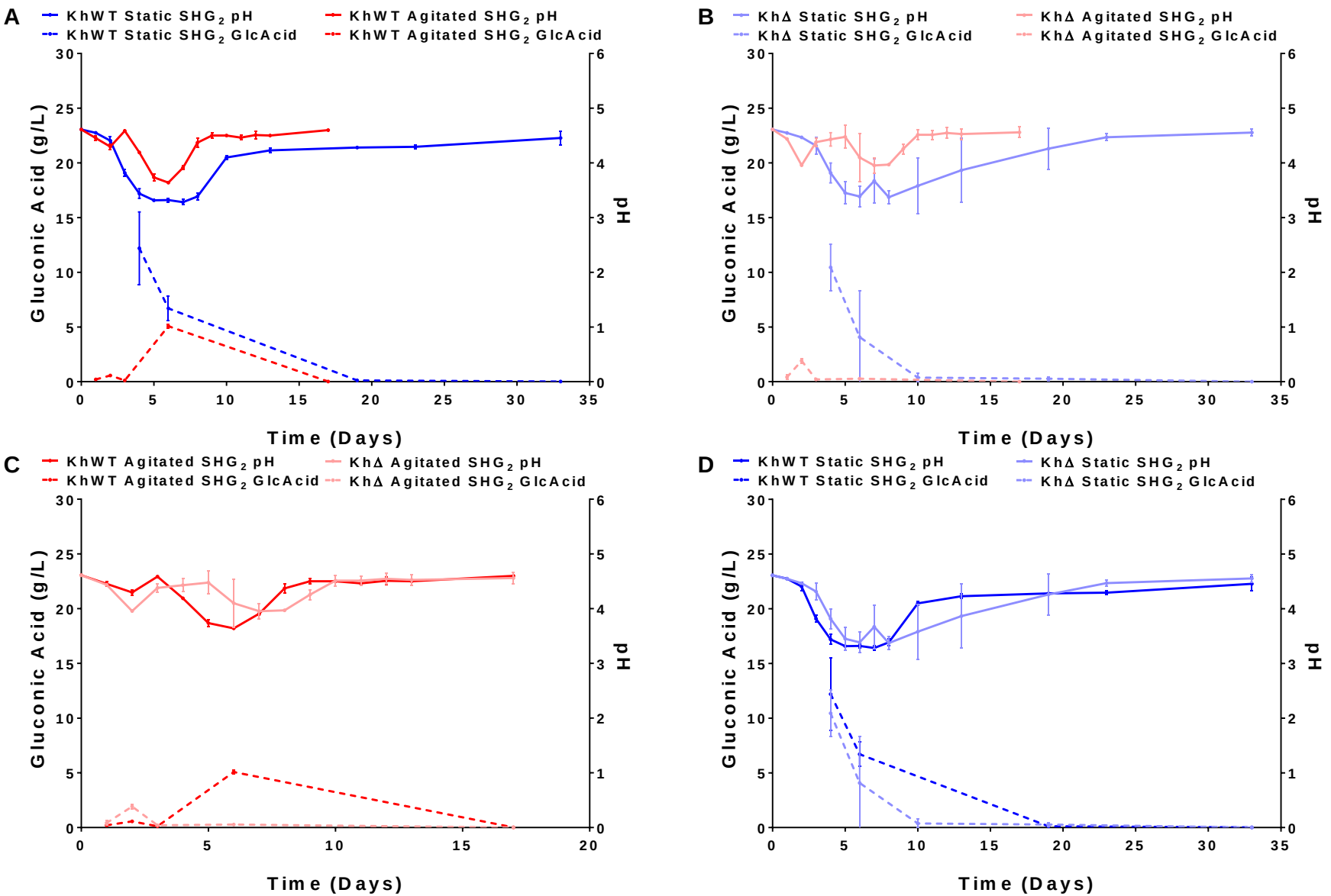

Figure 22: *fixK* is involved in acid metabolism in *K. hansenii* in agitated and statically grown SHG_2 cultures. pH and gluconic acid concentrations were measured in *K. hansenii* WT and *K. hansenii* Δ*fixK* grown in SHG_2 with and without agitation. Statically grown WT and Δ*fixK* mutants produce much more acid and take longer to reach stationary phase under static conditions (A, B). The loss of *fixK* is associated with less acidity, less gluconic acid production, and an altered pH profile under agitated conditions (C). In statically grown cultures, gluconic acid and pH profiles were similar (D). Error bars show SD (n = 3).

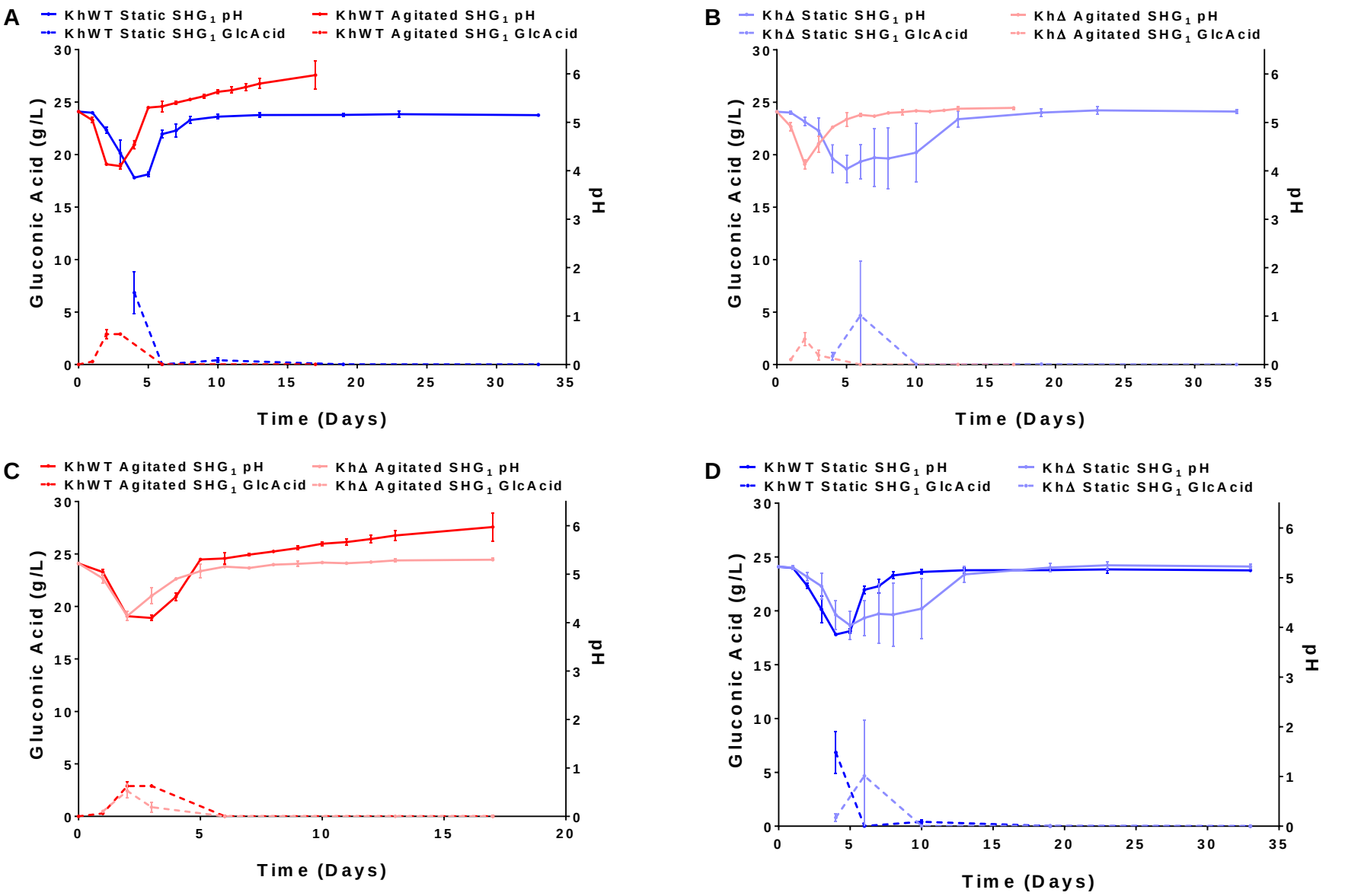

Figure 23: *fixK* is involved in acid metabolism in *K. hansenii* in agitated and statically grown SHG_1 cultures. pH and gluconic acid concentrations were measured in *K. hansenii* WT and *K. hansenii* Δ*fixK* grown in SHG_1 with and without agitation. Statically grown WT and Δ*fixK* mutants produce similar acidification profiles, however the trend is stretched over a longer time frame in static conditions (A, B). The loss of *fixK* is associated with less alkylation after 6 days of growth in SHG_1 under agitated conditions (C). In statically grown cultures, the Δ*fixK* mutation is associated with a delayed pH profile (D). Note that the right y-axis ends at pH 6.5. Error bars show SD (n = 3).

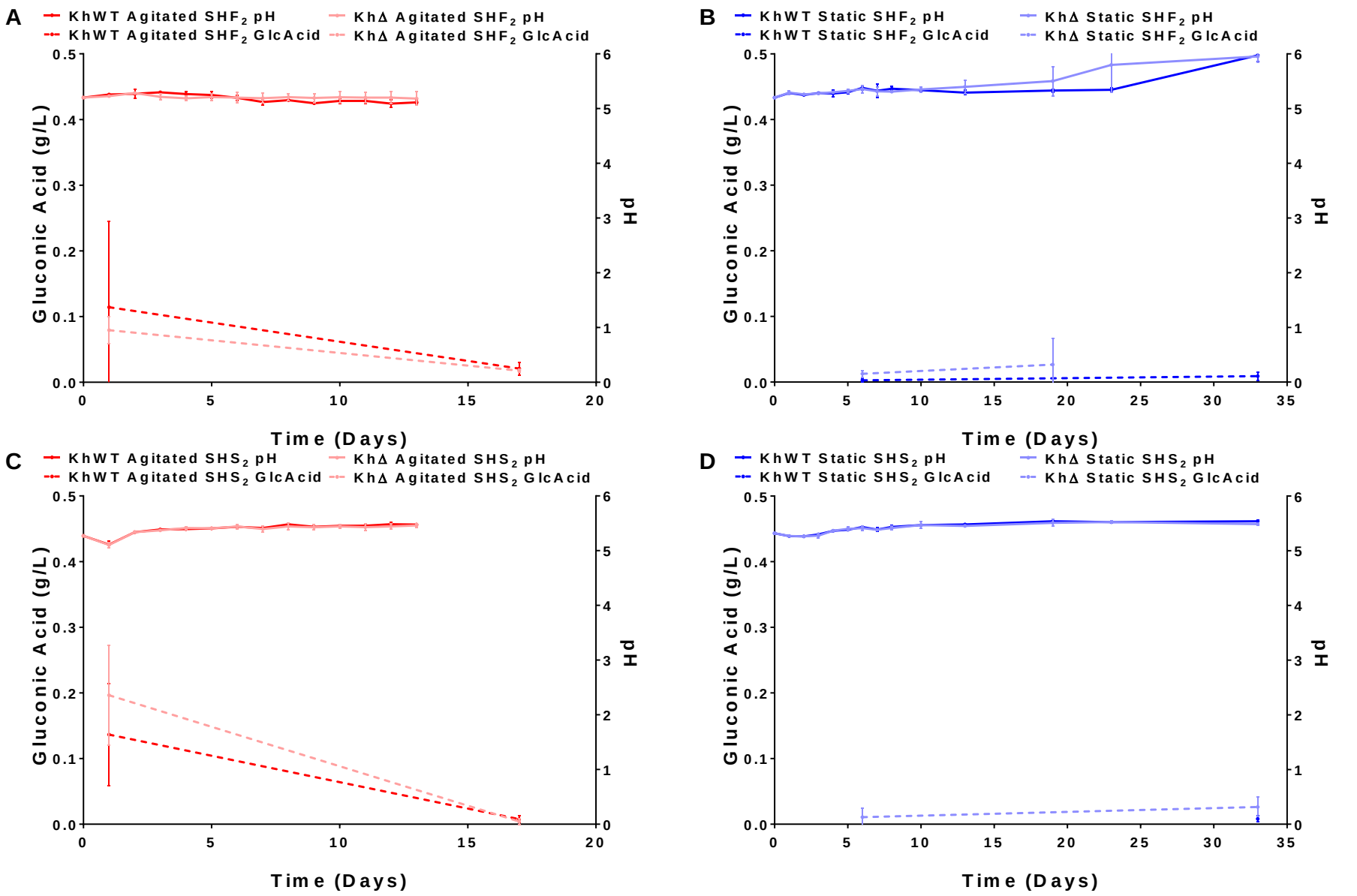

Figure 24: *fixK* has little effect on acid metabolism for *K. hansenii* in agitated and statically grown SHF_2 and SHS_2 cultures. pH and gluconic acid concentrations were measured in *K. xylinus* WT and *K. xylinus* Δ*fixK* grown in SHF_2 and SHS_2 with and without agitation. None of the cultures produced measurable concentrations of gluconic acid. Error bars show SD (n = 3).

3.10. *fixK* is involved in *bcs* operon regulation

Cellulose synthesis is dramatically influenced by the presence of *fixK* yet the gene targets for FixK remain elusive. To shed light on potential targets, the expression levels for cellulose biosynthesis genes in *K. xylinus* Δ*fixK* and *K. hansenii* Δ*fixK* were compared to *K. xylinus* WT and *K. hansenii* WT, respectively. All genes tested were expressed in both WT and both mutant strains, suggesting that *fixK* is not solely responsible for transcription of these genes (**Figure 25**). The absence of *fixK* leads to significantly reduced expression of *bcsA*, *bcsC*, *bcsH*, and *bglX* in *K. xylinus*. The same mutation in *K. hansenii* leads to reduced expression of only two genes, *bcsA* and *bcsC* (**Figure 25**).

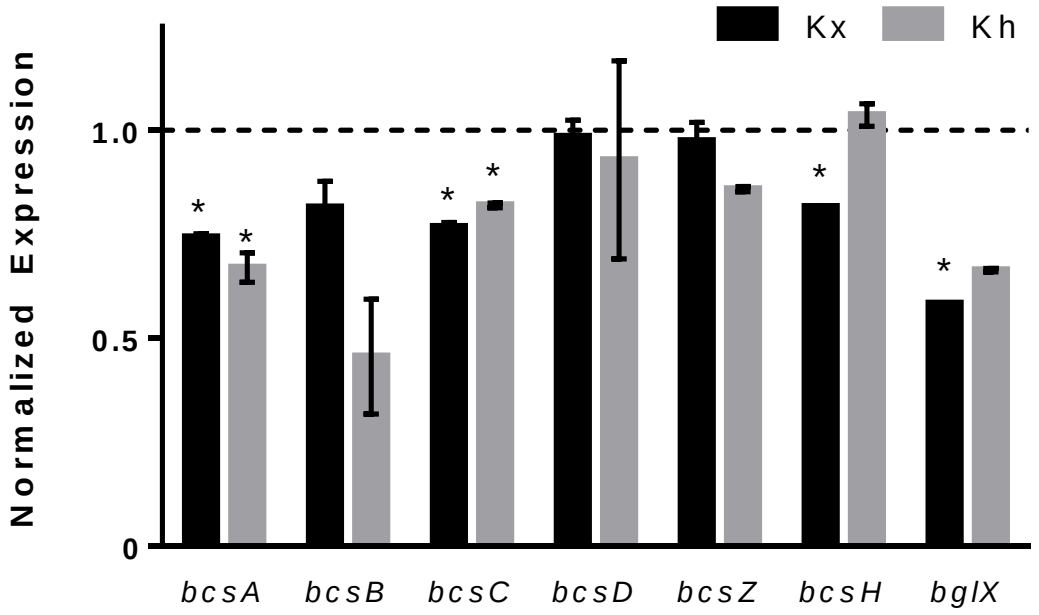

Figure 25: Endpoint PCR analysis of transcript levels of *bcsA*, *bcsB*, *bcsC*, *bcsD*, *bcsZ*, *bcsH*, and *bglX* in *K. xylinus* Δ*fixK* and *K. hansenii* Δ*fixK*. Gene expression levels are normalized against the wildtype control denoted by the dashed line at 1.0. Two independent biological replicates were used for each gene and error bars show SD (n = 2). Note that standard deviation of the wildtype is not shown, however t-test analysis considers both the wildtype and Δ*fixK* mutant sample deviations. * = significant difference from wild type ($p < 0.05$).

3.11. The absence of *fixK* abolishes expression of ~68.7 kDa protein(s) in *K. xylinus*

Protein profiles were examined to evaluate differential protein expression between WT and Δ*fixK* mutants. FixK, truncated ΔFixK, and the chloramphenicol resistance gene are predicted to be 27.8 kDa, 17.3 kDa and 25.7 kDa, respectively in both *Komagataeibacter* species. In *K. xylinus* Δ*fixK*, the protein band at 25 kDa is lost (**Figure 26, A**), which closely correlated to FixK (27.8 kDa). The loss of this band is complemented by the appearance of a protein band near 15 kDa which is likely the truncated ΔFixK protein (17.3 kDa). The absence of *fixK* abolished expression of a protein or proteins within a calculated 68.7 kDa protein band. This molecular weight does not correlate to any proteins known to be involved in cellulose biosynthesis and currently remains

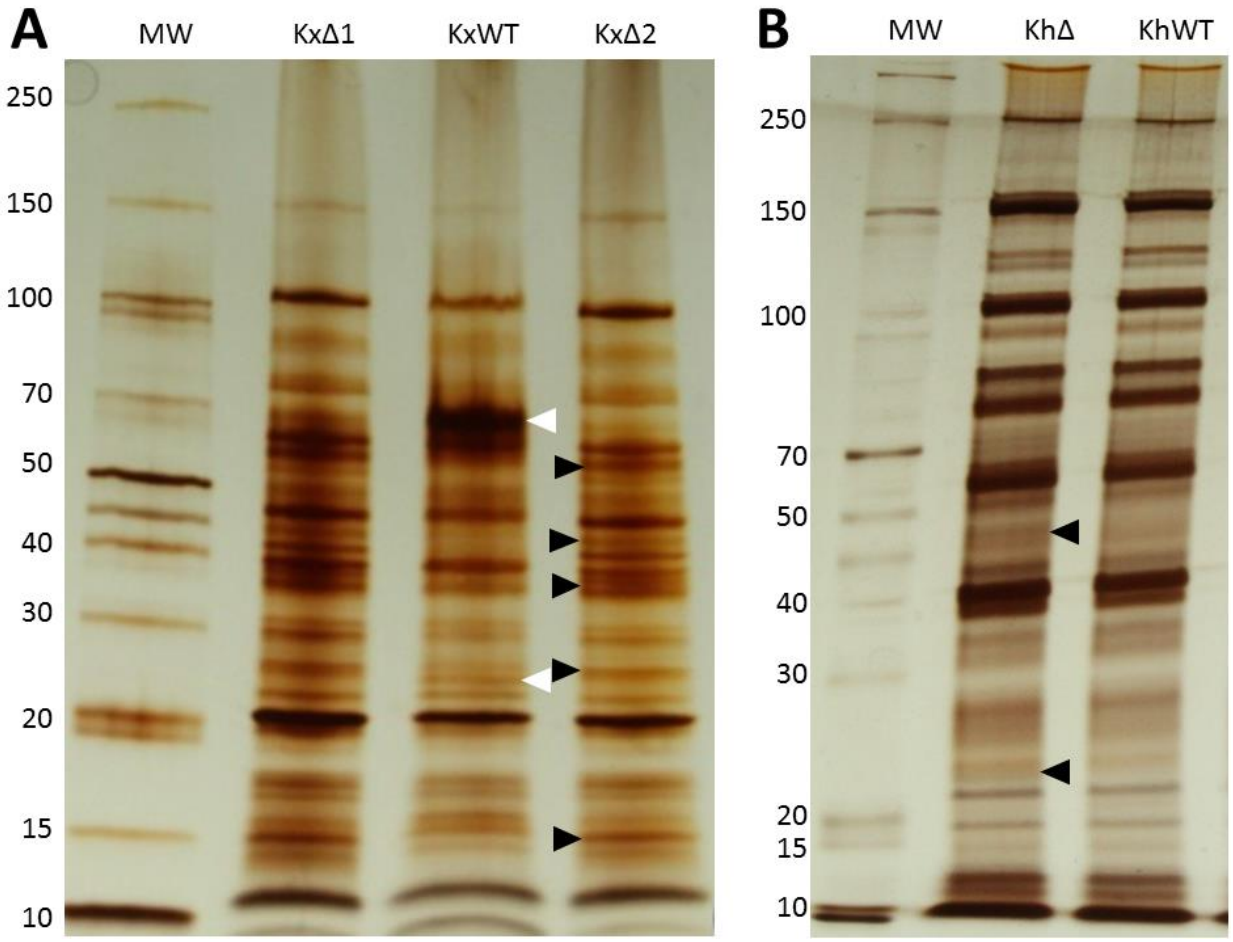

Figure 26: SDS-PAGE analysis of *K. xylinus* and *K. hansenii* and their Δ*fixK* mutants. Total protein from *K. xylinus* (A) and *K. hansenii* (B) WT and Δ*fixK* mutants grown in SHG_2 were visualized by silver staining. White arrows represent protein expression that is decreased in the Δ*fixK* mutant. Black arrows represent increased protein expression in the Δ*fixK* mutant. **MW**, molecular weight marker; **KxΔ1**, *K. xylinus* Δ*fixK* biological replicate #1; **KxWT**, *K. xylinus* WT; **KxΔ1**, *K. xylinus* Δ*fixK* biological replicate #2; **KhΔ**, *K. hansenii* Δ*fixK*; **KhWT**, *K. hansenii* WT.

unidentified. Other protein bands of increased intensity in the *K. xylinus* Δ*fixK* mutant include 58.5 kDa, 43.3 kDa, 37.1 kDa, and 26.1 kDa. The chloramphenicol resistance protein is 25.7 kDa and may be responsible for the increased intensity observed at 26.1 kDa. Protein profiles for *K. hansenii* did not reveal any dramatic differences in protein expression. A protein band at 50.1 kDa and one at 20.4 kDa were observed to have increased expression in the absence of *fixK* (**Figure 26**)*;* the latter potentially representing the truncated 17.3 kDa ΔFixK.

4. Discussion

This thesis aimed to improve our understanding of i) the ability of *Komagataeibacter* to degrade plant cell wall components and ii) the role of *fixK* on bacterial cellulose synthesis and carbon utilization in *Komagataeibacter* species. In the environment, *Komagataeibacter* live in close association with plants. The ability to degrade plant cell walls would therefore facilitate access to carbon for BC synthesis by producing simple sugars. Whether *Komagataeibacter* possess the enzymatic ability to breakdown PCWCs was evaluated. The mutagenesis of the gene for the transcription factor FixK, facilitated the investigation of its role in several cellular processes including carbon source metabolism, acid production, cell growth, and cellulose synthesis.

As already mentioned, *Komagataeibacter* grow in close association with plants. Therefore, *Komagataeibacter* would have ready access to plant cell wall compounds including cellulose, hemicelluloses, pectins, and lignin. Zymography was used to determine if *K. xylinus* or *K. hansenii* secrete enzymes that could degrade plant polymers for use in their own cellulose production. CMC was used as a soluble proxy for native cellulose and xylan was used as a representative hemicellulose. Pectin was sourced from apples, a fruit upon which *K. xylinus* thrive (Williams and Cannon, 1989). Lignin structure is diverse and undefined, as such lignin with an average molecular weight of 10,000 g/mol was chosen to represent an intact polymer. All four of these compounds can be found in fruit cell walls at highly variable ratios. The ability of *Komagataeibacter* to metabolize these plant cell wall components would provide much needed nutrients in the natural habitat of these bacteria.

Genome annotations for *K. xylinus* ATCC 53582 or *K. hansenii* ATCC 23769 lack any description of xylanase, pectinase, or lignin modifying enzymes (LME). This was not a surprise, however, as *K. hansenii* and more so *K. xylinus* are relatively poorly characterized with many annotation errors. An example of poor annotation is gene ATCC53582_00728 which is annotated as ‘Major royal jelly protein’, a protein involved in queen honeybee development. BLASTp analysis reveals that this protein is likely a gluconolactonase, an enzyme responsible for the second of two steps involved in the conversion of glucose into gluconic acid. This is a surprising find since these pathways have been a particular focus of research for over a decade (Kuo et al., 2015; Shigematsu et al., 2005; Zhong et al., 2013). Additionally, BLASTp analysis for the identification of gluconate

metabolism genes are rarely identified with the correct putative function (discussion of these proteins below).

Preliminary screens for PCWDE activity were carried out using agar plate assays. The use of iodine to detect the degradation of CMC, xylan, and pectin on agar plates was tested using commercially available enzymes as positive controls. Iodine was found to be an effective stain to detect lignin degradation. Iodine had previously been used for the study of lignin aggregation patterns (Deng et al., 2011) but, to our knowledge, this study is the first example of the use of iodine for the detection of *in situ* lignin degradation. Agar plate assays for the detection of degradative enzyme activities was performed using either culture supernatant or pellicles. The inability to detect substrate degradation with culture supernatant was unexpected, especially for CMC since BcsZ (CMCase) is known to be a secreted protein for both species. The use of pellicles as a source of enzyme in these degradation studies revealed faint yet observable substrate degradation for all four plant compounds tested. While there is the possibility that at least some of the degradative enzymes are membrane bound and therefore require the presence of *Komagataeibacter* cells, this does not explain the absence of CMCase activity in the culture supernatants. The understanding that some compounds, such as vitamin C, could produce false positives warrants the need for heat-treated or otherwise protein-denatured pellicles as a negative control if these assays are repeated elsewhere. One explanation for the absence of the CMCase is carbon source regulation since the cultures were grown in SHG_2 which contains 20 g/L of glucose. With an ample carbon source available, the production of metabolically expensive enzymes, such as CMCase, would likely be repressed since glucose was plentiful and there was no need to degrade cellulose to gain carbon. This hypothesis is further supported by zymographic analysis which revealed CMCase repression during glucose availability.

To confirm the results of the preliminary degradation assays, *K. xylinus* and *K. hansenii* secretomes were assayed by zymography for all four degradative enzyme classes: CMCase, xylanase, pectinase, and LME. BcsZ was effectively detected in acetone-precipitated protein extracts from fructose fed cultures. To our knowledge this is the first evidence that BcsZ is under glucose catabolite repression. In an environmental context, this would be an efficient means for degrading the bacterial cellulose when carbon was needed. β-glucosidase activity was effectively detected from the insoluble fraction of cell extracts of *K. hansenii* ATCC 23769 grown in SHG_2 and

the activity was predicted to be a result of BglX rather than BcsZ (Kumagai et al., 2011). Importantly, Kumagai et al. (2011) were unable to detect cellulase activity in the extracellular fraction or the cytosolic fraction of SHG_2-grown *K. hansenii*. Tahara et al. (1997) discovered CMC but not cellobiose or BC hydrolyzing activity in the extracellular extracts from *Acetobacter xylinum* BPR2001 (currently *Komagataeibacter xylinus* ATCC 700178). The growth medium used in their study was CSL-Fru (Toyosaki et al., 1995) in which fructose is the carbon source.

Xylanase, pectinase, and LME were only detected using agar plate assays with pellicle; zymographic analysis of proteins from culture supernatants failed to detect these activities under any of the conditions tested. This may be due to limited secretion of these proteins, as protein profile analysis of culture supernatants indicated that most of the secreted proteins were less than 11 kDa in size (**Figure 9**). If *K. xylinus* or *K. hansenii* contain hemicellulases, pectinases, or LME, they may require nutrient limitation to be produced. However, replacing the carbon source in SH medium with only xylan, pectin, or lignin is not conducive for static growth in either species (data not shown) and suggests SH medium is not an appropriate growth medium to emulate environmental growth conditions.

Mutagenesis of *K. xylinus* ATCC 53582 has been historically very difficult (Florea et al., 2016b). Work done on the closely related *K. rhaeticus* improved electroporation success using pSEVA331Bb. Florea et al. (2016a) were able to transform *K. xylinus* ATCC 53582 only when using a 3 kV pulse and a long post-transformation incubation time, yet efficiency remained low (~10^2 CFU/μg; compared to ~10^9 CFU/μg for *E. coli*). The plasmid pSEVA331Bb was instrumental for optimizing the transformation conditions used in this thesis. The preparation of electrocompetent cells from fructose-based medium facilitated transformation efficiency at voltages of 1.8 kV and 2.5 kV with improved efficiencies of up to $1.8x10^4$ CFU/μg with recovery times as low as 1.25 hours. The addition of acetic acid or glycerol to the growth medium used for electrocompetent cell preparation did not have an appreciable effect on transformation efficiency.

Selection of transformants was complicated by the production of cellulose as its presence led to false positive colonies forming on selection plates. Cellulose acts as a barrier to protect the cells from inhibitory concentrations of the antibiotic. Here we have overcome this problem by mixing 50 μl of transformed cells with 25 μl of cellulase (>800 units/ml) immediately prior to spread plating on selective medium. It is highly likely that the concentration of cellulase can be reduced

further by preparing electrocompetent cells from fructose-grown cultures and by selecting on fructose-based agar plates since fructose was found to reduce cellulose production. However, this has yet to be tested.

K. hansenii was found to be resistant to kanamycin. Deng et al. (2013) described this strain as completely resistant to kanamycin, however it seems that a proportion of *K. hansenii* cells display robust resistance while, inexplicably, the majority are vulnerable (**Table 2**). This discrepancy is likely due to Deng et al. (2013) conducting liquid MIC rather than agar plate based assays. In liquid cultures, the majority of the culture may be inhibited while the few kanamycin resistant cells continue to propagate. Plate assays clarify that there is either a resistance gene with very low basal level expression, usually leading to cell death before it can be upregulated, or genetic instability of *K. hansenii* leading to target adaptation. The latter of which being a distinct possibility as observations have shown genetic instability of these stains; a substantial fraction of cells naturally lose the ability to produce cellulose when grown in the laboratory (data not shown).

The growth of *K. xylinus* and, to a lesser extent, *K. hansenii* benefitted from limiting glucose concentrations in the growth medium as seen in both the fitness assays (**Figure 11 and Figure 12**) and mutant characterization (**Figure 15 and Figure 16**). Reducing glucose from 2% to 1% improves BC yield by approximately 10% (Keshk and Kazuhiko, 2005), however whether this is due to increased cell growth had not been previously investigated. Interestingly, substituting half or all of the glucose in SHG_2 with glycerol substantially improved growth and may explain the 55% increase in BC yield seen by Keshk and Kazuhiko (2005) when substituting 1% glucose for 1% glycerol. Keshk and Kazuhiko (2005) suggest that the improved production may be partially due to the rate of carbon source consumption rather than acid production. It is clear, however, that osmolarity of the growth medium is not responsible for the altered cell growth because improved growth was seen only limiting glucose and not fructose concentrations. An explanation could be that the extra glucose in the growth medium extends the time in which the cells are in an acidic ($pH < 5$) environment, inhibiting growth.

To elucidate the role of the global transcriptional regulator, FixK, in carbon source utilization and cellulose biosynthesis in *K. xylinus and K. hansenii*, *fixK* was knocked out by the homologous recombination of a linear vector targeting *fixK* for the insertion of a pSEVA331Bb-derived chloramphenicol resistance cassette. As previously discovered by Deng et al. (2013), the loss of *fixK*

resulted in the complete loss of cellulose production in *K. hansenii*. Since *fixK* was found to be identical between the two species, we expected the same phenotype in *K. xylinus*. However, *K. xylinus* was still capable of cellulose production, albeit at lower yield. Interestingly, the cellulose production in *K. xylinus* Δ*fixK* was comparable to wildtype *K. hansenii* (**Figure 18**).

Colonial morphology of the *K. hansenii* Δ*fixK* mutant was dramatically different than wild type while same mutation resulted in minor differences for *K. xylinus*. The morphological differences seem to be correlated with reduced cellulose production. Cellulose producing colonies maintained a spherical shape while spontaneous cellulose non-producing colonies remained flat (data not shown). The observed flat morphology was similarly seen in the cellulose non-producing *K. hansenii* Δ*fixK* as seen in **Figure 13**. *K. xylinus* colonies grown on fructose and sucrose display a directional phenotype with semi-circular like projections emanating from the colonies. These projections resemble cellulose non-producer morphology and are likely a result of quorum sensing as they appear to share directionality between colonies. Quorum sensing autoinducers and homologous regulatory genes have been identified in *K. intermedius* and *G. diazotrophicus* (Bertini et al., 2014; Iida et al., 2008a, 2008b, 2009; Nieto-Peñalver et al., 2012). These studies have not identified quorum sensing in bacterial cellulose producers, although there are predicted quorum sensing related genes in *K. xylinus* such as homoserine lactone efflux proteins, acetyltransferases, kinases, and dehydrogenases. Colony morphology was also impacted by pellicin, a compound known to abolish cellulose synthesis in *K. xylinus*. The presence of pellicin resulted in a cross between a cellulose producing and a cellulose non producing phenotype as they produced a convex elevation skirted by a flat morphology. The *K. xylinus* Δ*fixK* low cellulose producing mutant colonies had a larger flattened skirt than the wildtype (**Figure 14**).

Pellicle weights were measured to determine the best time frame for BC production, but revealed a surprising trend in late stage growth. The pellicle yield in some cultures decreased between 13 and 17 days of growth, indicating the presence of a BC degrading enzyme. An investigation of cellulase production in *K. xylinus* by Tahara et al. (1997) was unable to detect enzymes capable of degrading BC however the study examined extracts after only 24 hours of growth. This study showed that BcsZ is either not secreted within 24 hours of growth, or its presence is below the detection limits of the assays used (viscosity and dinitrosalicylic acid method). In this thesis, BC degradation was observed only in *K. xylinus* cultures growing in SHG_1, where carbon

source availability was half that of any other culture. The bacteria are likely producing a BC degrading enzyme, possibly BcsZ, in later growth in order to reclaim the BC for energy when soluble carbon is limited. The pellicle assays in this thesis were investigated over 17 days, whereas most published pellicle studies examine pellicle production to a maximum of 14, but usually 7 days. Notably we did not observe cellulose degradation within 13 days of growth. This underscores the importance of studying older cultures, which are more representative of environmental conditions.

Cultures were grown in both static (lacking cellulase) and agitated (cellulase added) conditions to improve our understanding of the metabolic consequences of BC. pH was measured as a reference between these two conditions to allow comparisons between culture density and cellulose production since OD_{600} measurements are not feasible when cellulose is present. Treating the pellicles with cellulase was considered as an option, however it can take hours to degrade a fully developed pellicle which complicates downstream gluconic acid measurements; cultures would be metabolically active during pellicle degradation. The pH of static cultures followed similar trends to the agitated cultures over an extended period of time. Trapped within a pellicle, cells depend on diffusion for nutrients and will therefore experience unique metabolism from the cellulase treated, agitated cultures. The delayed nutrient availability must decrease metabolism at a whole culture-level but individual cell metabolism would depend on the depth of cells within a pellicle. The pellicle therefore creates an environment in which access to nutrients is limited, affecting metabolism and growth. While the acidification and subsequent alkylation of the growth medium was expected in glucose grown cultures (Sainz et al., 2016), the reduced acidification as a result of *fixK* mutagenesis in *K. xylinus* was unexpected. If *fixK* simply upregulates cellulose production, the absence of the gene would presumably result in less glucose uptake or redirection of carbon into other processes. Less glucose uptake would imply a greater medium glucose concentration and therefore increased gluconic acid production. Quantification of glucose in the growth medium would clarify the consequences of the *fixK* mutation. Nonetheless, these findings suggest a broader role for *fixK*. In *K. hansenii,* this is evident by the dramatic role *fixK* plays in carbon source metabolism. When fed 2% (w/v) glucose, fructose, or sucrose, *fixK* facilitates a growth density to approximately twice that of the strain lacking *fixK,* underscoring the divergence between these two species. Furthermore, the pH of the growth medium does not change when fed sucrose despite an enzymatically active glucose dehydrogenase (Kornmann et al., 2003). This indicates that sucrose is imported prior to cleavage as extracellular cleavage would result in the production of gluconic acid from the available glucose.

Komagataeibacter are well known for the inverse relationship of gluconic acid production and BC biosynthesis (De Wulf et al., 1996; Krajewski et al., 2010; Shigematsu et al., 2005). The role of *fixK* was therefore investigated in gluconic acid production and pH. *fixK* showed limited effect on gluconic acid production; culture pH and gluconic acid concentration did not always directly coincide. The gluconic acid/gluconolactone (as the assay cannot differentiate between the two) is directly correlated with initial acidification of the growth medium yet the pH remains low even after the acid is metabolized. Shinagawa et al. (2009) proposed a model for the conversion of gluconic acid bond energy to a proton motive force in the closely related *K. oxydans* through the oxidation of gluconate to 2-keto-D-gluconate or 5-keto-D-gluconate. 2-keto-D-gluconate can be further oxidized to 2,5-diketo-D-gluconate, converting one or two ubiquinone molecules into ubiquinol. The reduced electron carriers ultimately facilitate the transport of protons across the inner membrane by cytochrome bo_3 (H^+-transporting ubiquinol oxidase) towards the periplasmic space and possibly into the extracellular space (**Figure 27**). This would explain the acidic nature of the growth medium well after gluconate is depleted. Contradictory to these findings, Sainz et al. (2016) found that 2-keto-D-gluconate but not 5-keto-D-gluconate was produced by *K. oxydans*.

Curation of the *K. xylinus* genome and BLASTp analysis, using previous work with *K. oxydans* as a guide (Shinagawa et al., 2009), reveals multiple enzymes that metabolize gluconate. The membrane bound glucose dehydrogenase (ATCC53582_01404) is possibly complemented by a soluble glucose dehydrogenase (ATCC53582_01271). A membrane bound (ATCC53582_01404) and a soluble (ATCC53582_00728) gluconolactonase would facilitate the extra/intracellular metabolism of glucose into gluconate. There are two gluconokinases capable of phosphorylating gluconate. Phobius (http://www.ebi.ac.uk/Tools/pfa/phobius/) analysis, which predicts transmembrane topology and signal peptides, identifies one as potentially membrane bound (ATCC53582_00279) and the other as very likely a transmembrane (ATCC53582_01594) protein.

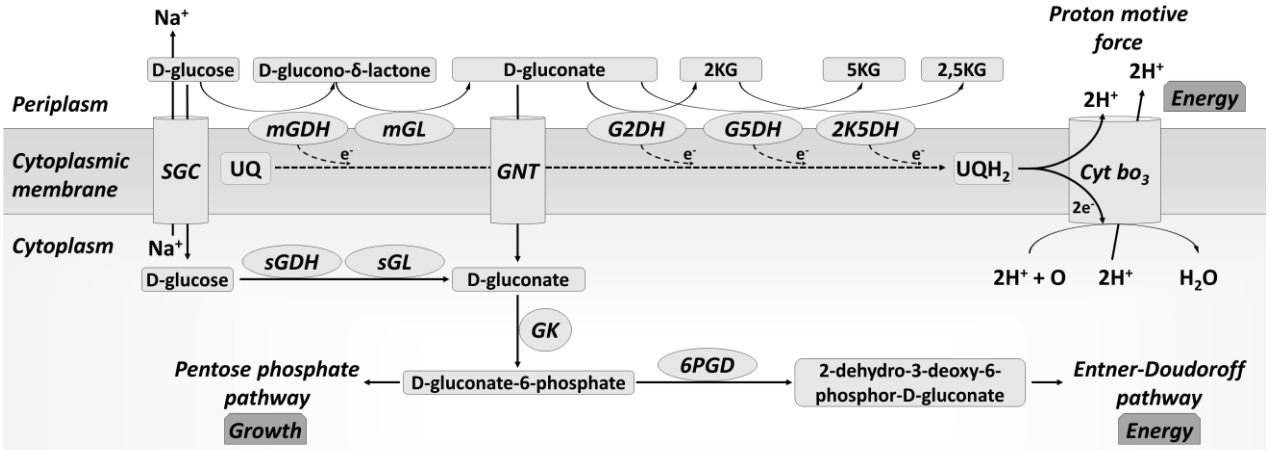

Figure 27: Proposed model of gluconate metabolism in *K. xylinus* for cellular energy or growth. **Protein abbreviations:** ***SGC***, sodium/glucose cotransporter; ***(m/s)GDH***, membrane bound/soluble glucose dehydrogenase; ***(m/s)GL***, membrane bound/soluble gluconolactonase; ***GNT***, gluconate transporter; ***G2DH***, gluconate 2-dehydrogenase; ***G5DH***, gluconate 5-dehydrogenase; ***2K5DH***, 2-keto-D-gluconate dehydrogenase; ***Cyt bo₃***, cytochrome bo_3 ubiquinol oxidase; ***GK***, gluconate kinase; 6PGD, 6-phosphogluconate dehydrogenase. **Chemical abbreviations:** **2KG**, 2-keto-D-gluconate; **5KG**, 5-keto-D-gluconate; **2,5KG**, 2,5-diketo-D-gluconate; **UQ**, ubiquinone; **UQH_2**, ubiquinol. Figure adapted from Shinagawa et al. (2009).

Once phosphorylated, D-gluconate-6-phosphate can be used in the pentose phosphate pathway or further metabolized by 6-phosphogluconate dehydrogenase to 2-dehydro-3-deoxy-6-phospho-D-gluconate similar to the Entner-Doudoroff pathway. Curiously, one of the two 6-phosphogluconolactonase enzymes carries an N-terminal signal peptide characteristic of secreted proteins, although what purpose this enzyme could serve in the extracellular space is unclear. Other gluconate metabolizing proteins are gluconate 2-dehydrogenase (ATCC53582_01786) and gluconate 5-dehydrogenase (ATCC53582_01277), capable of the conversion of gluconate into 2-keto-D-gluconate and 5-keto-D-gluconate, respectively. Finally, 2-keto-D-gluconate can be metabolized into 2,5-diketo-D-gluconate by a 2-keto-D-gluconate dehydrogenase (ATCC53582_01641). Notably, several proteins mentioned above are not annotated as described here, but BLASTp analysis reveals very high similarity to annotated homologs. *K. xylinus* likely reduces ubiquinol molecules in a similar fashion to *K. oxydans* to power the proton motive force, providing energy for the cell. Similar proteins are found in *K. hansenii* which were shown to produce more gluconic acid, yet the extracellular medium experienced less of a decrease in pH. This may be the result of *K. hansenii* directing gluconic acid into the pentose phosphate pathway, providing synthesis power for the cell, while *K. xylinus* may use gluconic acid to power a proton motive force,

resulting in proton leakage through the outer membrane and decreasing the pH. This would represent a trade-off of high energy processes such as cellulose synthesis (as seen in *K. xylinus*) for greater growth potential (as seen in *K. hansenii*).

Transcriptional analysis by endpoint PCR of cDNA revealed lower transcript levels of *bcsA* and *bcsC* compared to wildtype in both species and down regulation of *bcsH* and *bglX* in *K. xylinus*. *fixK* was previously knocked out by transposon mutagenesis by Deng et al. (2013) and qPCR was performed on *bcsZ*, *bcsH*, *bglX* and *dgc1*. Transcription levels were slightly lower for *bcsH* and much lower for *bglX* compared to the wildtype (Deng et al., 2013). Deng et al. (2013) also performed western blot analysis for BcsA, BcsB, BcsC, and BcsD and found no significant differential expression of these proteins in the absence of *fixK*. The reduced transcription of *bglX* due to the absence of *fixK* was also demonstrated in this thesis. The downregulation of *bcsA* and *bcsC* (**Figure 25**) at the transcript, but not protein level, may be due to mRNA level regulation. The protein gels comparing wildtype and Δ*fixK* mutants in this thesis coincide with Deng et al. (2013), as there were no visible changes in protein expression of similar molecular weight to BcsA, BcsB, BcsC, or BcsD.

fixK, being a member of the Crp/Fnr family of transcription factors, is likely involved in the response to extracellular signal and the control of metabolic pathways. FixK was first described as a regulator of nitrogen fixation genes in *Rhizobium meliloti* (Batut et al., 1989), however neither *K. xylinus* nor *K. hansenii* have been shown to possess nitrogen fixation capabilities. In *Bradyrhizobium*, *fixK* homologs regulate a variety of metabolic roles including microaerobic growth (Preisig et al., 1996), heme biosynthesis (Fischer et al., 2001), denitrification (Velasco et al., 2004), and hydrogen oxidation genes (Durmowicz and Maier, 1998). Furthermore, it has been shown to induce the expression of up to 17 genes while repressing 12 genes. In general, FixK is induced by microaerophilic growth via the heme containing protein FixL. Studies have not yet implicated *fixK* in fructose metabolism however the closely related Crp transcription factor is primarily involved in sensing cyclic adenosine monophosphate (cAMP) and therefore the global glucose level. Whether a new role for FixK has been revealed by this thesis or whether the *Komagataeibacter* homolog of this gene requires a new title has yet to be determined.

5. Conclusions and Future Directions

The work presented in this thesis has advanced our understanding of the role that *bcsZ* and *fixK* play in bacterial cellulose production. We provide evidence that *bcsZ* is repressed by glucose but not fructose when grown in SH medium. Furthermore, our results suggest that a cellulase is secreted into the growth medium to reclaim cellulose as an energy source. This enzyme may be BcsZ or BglX; however the expression of the protein under low glucose conditions suggests that BcsZ is more likely responsible for the observed cellulase activity. Additionally, BglX has previously been identified in the insoluble fraction of cell extracts making it even less likely to be found in the extracellular medium.

fixK was known to regulate cellulose biosynthesis in *K. hansenii* but its role in *K. xylinus* had yet to be investigated. Despite FixK having identical amino acid sequence between species, knocking out *fixK* did not abolish cellulose production in *K. xylinus*, albeit cellulose yield was dramatically reduced. While FixK does share some regulatory roles in both species (such as in affecting the expression of *bglX*), its role in the two species is strikingly different. Its role in fructose metabolism in *K. hansenii* was dramatic, with cultures lacking a functional *fixK* reaching densities of only half of the wildtype. In contrast, *K. xylinus* cultures had no significant differences in final culture densities compared to the Δ*fixK* mutants. Additionally, the expression of a highly abundant protein near 68.7 kDa was abolished in *K. xylinus* in the absence of *fixK*. Similar weight proteins in *K. hansenii* were unaffected.

Future studies should attempt to confirm whether BcsZ is indeed the enzyme responsible for the degradation of cellulose in weeks-old pellicles and to characterize the repression of the *bcsZ* promoter. Zymograms for the detection of CMCases from pellicle squeezates of 17 day or older cultures would be an effective means for revealing the enzyme responsible. While glucose is presumably a repressor for *bcsZ* expression, it is possible that fructose is an inducer of *bcsZ*. Reverse transcriptase quantitative PCR of this gene analyzed from cultures grown in fructose and glucose would clarify this.

The characterization of *fixK* has only just begun and additional studies on the regulation of *fixK* and its DNA targets are essential for understanding the regulation of bacterial cellulose synthesis. This gene plays a key role in not only bacterial cellulose production, but also in fructose metabolism and the production of 68.7 kDa proteins; yet the mechanisms have yet to be investigated.

Co-immunoprecipitation using His-tagged FixK would facilitate the identification of its DNA targets. Additionally RNA-sequencing to compare the wildtype and Δ*fixK* mutant transcriptome would reveal ancillary genes responsible for cellulose synthesis and its regulation.

6. References

Adsul, M. G., Bastawde, K. B., and Gokhale, D. V (2009). Biochemical characterization of two xylanases from yeast *Pseudozyma hubeiensis* producing only xylooligosaccharides. *Bioresour. Technol.* 100, 6488–6495.

Agostoni, M., Waters, C. M., and Montgomery, B. L. (2016). Regulation of biofilm formation and cellular buoyancy through modulating intracellular cyclic di-GMP levels in engineered cyanobacteria. *Biotechnol. Bioeng.* 113, 311–319.

Amikam, D., and Benziman, M. (1989). Cyclic diguanylic acid and cellulose synthesis in *Agrobacterium tumefaciens*. *J. Bacteriol.* 171, 6649–6655.

Amikam, D., and Galperin, M. Y. (2006). PilZ domain is part of the bacterial c-di-GMP binding protein. *Bioinformatics* 22, 3–6.

Asai, T., and Shoda, K. (1958). The taxonomy of *Acetobacter* and allied oxidative bacteria. *J. Gen. Appl. Microbiol.* 4, 289–311.

Augimeri, R. V., and Strap, J. L. (2015). The phytohormone ethylene enhances bacterial cellulose production, regulates CRP/FNRKx transcription and causes differential gene expression within the cellulose synthesis operon of *Komagataeibacter (Gluconacetobacter) xylinus* ATCC 53582. *Front. Microbiol.* 6, 1459.

Augimeri, R. V., Varley, A. J., and Strap, J. L. (2015). Establishing a role for bacterial cellulose in environmental interactions: lessons learned from diverse biofilm-producing *Proteobacteria*. *Front. Microbiol.* 6, 1282.

Augimeri, R. V, Varley, A. J., and Strap, J. L. (2016). Utilizing the ethylene-releasing compound, 2-chloroethylphosphonic acid, as a tool to study ethylene response in bacteria. e54682.

Ausmees, N., Jonsson, H., Höglund, S., Ljunggren, H., and Lindberg, M. (1999). Structural and putative regulatory genes involved in cellulose synthesis in *Rhizobium leguminosarum* bv. trifolii. *Microbiology* 145, 1253–1262.

Baker, R. (1997). Reassessment of some fruit and vegetable pectin levels. *J. Food Sci.* 62, 225–229.

Batut, J., and Boistard, P. (1994). Oxygen control in *Rhizobium*. *Antonie Van Leeuwenhoek* 66, 129–150.

Batut, J., Daveran-Mingot, M. L., David, M., Jacobs, J., Garnerone, A. M., and Kahn, D. (1989). *fixK*, a gene homologous with *fnr* and *crp* from *Escherichia coli*, regulates nitrogen fixation genes both positively and negatively in *Rhizobium meliloti*. *EMBO J.* 8, 1279.

Bertini, E. V, Peñalver, C. G. N., Leguina, A. C., Irazusta, V. P., Lucía, I., and de Figueroa, C. (2014). *Gluconacetobacter diazotrophicus* PAL5 possesses an active quorum sensing regulatory system. *Antonie Van Leeuwenhoek* 106, 497.

Boerjan, W., Ralph, J., and Baucher, M. (2003). Lignin biosynthesis. *Annu. Rev. Plant Biol.* 54, 519–546.

Brown, L., Rosner, B., Willett, W. W., and Sacks, F. M. (1999). Cholesterol-lowering effects of dietary fiber: a meta-analysis. *Am. J. Clin. Nutr.* 69, 30–42.

Brown Jr, R. M. (1996). The biosynthesis of cellulose. *J. Macromol. Sci. Part A Pure Appl. Chem.* 33, 1345–1373.

Brown Jr, R. M. (2013). Cellulose biosynthesis in *Acetobacter xylinum*.

Bureau, T. E., and Brown, R. M. (1987). *In vitro* synthesis of cellulose II from a cytoplasmic membrane fraction of *Acetobacter xylinum*. *Proc. Natl. Acad. Sci.* 84, 6985–6989.

Castro, C., Zuluaga, R., Putaux, J.-L., Caro, G., Mondragon, I., and Ganán, P. (2011). Structural characterization of bacterial cellulose produced by *Gluconacetobacter swingsii* sp. from Colombian agroindustrial wastes. *Carbohydr. Polym.* 84, 96–102.

Chang, A. L., Tuckerman, J. R., Gonzalez, G., Mayer, R., Weinhouse, H., Volman, G., et al. (2001). Phosphodiesterase A1, a regulator of cellulose synthesis in *Acetobacter xylinum*, is a heme-based sensor. *Biochemistry* 40, 3420–3426.

Chanliaud, E., and Gidley, M. J. (1999). *In vitro* synthesis and properties of pectin/*Acetobacter xylinus* cellulose composites. *Plant J.* 20, 25–35.

Chou, S.-H., and Galperin, M. Y. (2016). Diversity of cyclic di-GMP-binding proteins and mechanisms. *J. Bacteriol.* 198, 32–46.

Cleenwerck, I., De Wachter, M., González, Á., De Vuyst, L., and De Vos, P. (2009). Differentiation of species of the family *Acetobacteraceae* by AFLP DNA fingerprinting: *Gluconacetobacter kombuchae* is a later heterotypic synonym of *Gluconacetobacter hansenii*. *Int. J. Syst. Evol. Microbiol.* 59, 1771–1786.

Corner, E. J. H. (1935). Observations on resistance to powdery mildews. *New Phytol.* 34, 180–200.

Cosgrove, D. J. (2005). Growth of the plant cell wall. *Nat. Rev. Mol. Cell Biol.* 6, 850–861.

Crawford, D. L. (1978). Lignocellulose decomposition by selected *Streptomyces* strains. *Appl. Environ. Microbiol.* 35, 1041–1045.

Daskalaki, A. (2008). *Handbook of Research on Systems Biology Applications in Medicine*. IGI Global.

David, M., Daveran, M.-L., Batut, J., Dedieu, A., Domergue, O., Ghai, J., et al. (1988). Cascade regulation of nif gene expression in *Rhizobium meliloti*. *Cell* 54, 671–683.

de Philip, P., Batut, J., and Boistard, P. (1990). *Rhizobium meliloti* Fix L is an oxygen sensor and regulates *R. meliloti nifA* and *fixK* genes differently in *Escherichia coli*. *J. Bacteriol.* 172, 4255–4262.

De Wulf, P., Joris, K., and Vandamme, E. J. (1996). Improved cellulose formation by an *Acetobacter xylinum* mutant limited in (keto) gluconate synthesis. *J. Chem. Technol. Biotechnol.* 67, 376–380.

Deinema, M. H., and Zevenhuizen, L. P. T. M. (1971). Formation of cellulose fibrils by gram-negative bacteria and their role in bacterial flocculation. *Arch. Microbiol.* 78, 42–57.

Deng, Y., Feng, X., Zhou, M., Qian, Y., Yu, H., and Qiu, X. (2011). Investigation of aggregation and assembly of alkali lignin using iodine as a probe. *Biomacromolecules* 12, 1116–1125.

Deng, Y., Nagachar, N., Xiao, C., Tien, M., and Kao, T. H. (2013). Identification and characterization of non-cellulose-producing mutants of *Gluconacetobacter hansenii* generated by Tn5 transposon mutagenesis. *J. Bacteriol.* 195, 5072–5083.

Durmowicz, M. C., and Maier, R. J. (1998). The FixK2 protein is involved in regulation of symbiotic hydrogenase expression in *Bradyrhizobium japonicum*. *J. Bacteriol.* 180, 3253–3256.

Ferreira, R. B. R., Antunes, L. C. M., Greenberg, E. P., and McCarter, L. L. (2008). *Vibrio parahaemolyticus* ScrC modulates cyclic dimeric GMP regulation of gene expression relevant to growth on surfaces. *J. Bacteriol.* 190, 851–860.

Fischer, H.-M. (1994). Genetic regulation of nitrogen fixation in rhizobia. *Microbiol. Rev.* 58, 352–386.

Fischer, H.-M., Velasco, L., Delgado, M. J., Bedmar, E. J., Schären, S., Zingg, D., et al. (2001). One of two *hemN* Genes in *Bradyrhizobium japonicum* is functional during anaerobic growth and in symbiosis. *J. Bacteriol.* 183, 1300–1311.

Florea, M., Hagemann, H., Santosa, G., Abbott, J., Micklem, C. N., Spencer-Milnes, X., et al. (2016a). Engineering control of bacterial cellulose production using a genetic toolkit and a new cellulose-producing strain. *Proc. Natl. Acad. Sci.*, 201522985.

Florea, M., Reeve, B., Abbott, J., Freemont, P. S., and Ellis, T. (2016b). Genome sequence and plasmid transformation of the model high-yield bacterial cellulose producer *Gluconacetobacter hansenii* ATCC 53582. *Sci. Rep.* 6.

Foussard, M., Garnerone, A., Ni, F., Soupène, E., Boistard, P., and Batut, J. (1997). Negative autoregulation of the *Rhizobium meliloti fixK* gene is indirect and requires a newly identified regulator, FixT. *Mol. Microbiol.* 25, 27–37.

Freudenberg, K., and Neish, A. C. (1968). Constitution and biosynthesis of lignin. *Const. Biosynth. lignin.*

Gilles-Gonzalez, M.-A., and Gonzalez, G. (2004). Signal transduction by heme-containing PAS-domain proteins. *J. Appl. Physiol.* 96, 774–783.

Gong, W., Hao, B., Mansy, S. S., Gonzalez, G., Gilles-Gonzalez, M. A., and Chan, M. K. (1998). Structure of a biological oxygen sensor: a new mechanism for heme-driven signal transduction. *Proc. Natl. Acad. Sci.* 95, 15177–15182.

Gromet-Elhanan, Z., and Hestrin, S. (1963). Synthesis of cellulose by *Acetobacter xylinum* VI. Growth on citric acid-cycle intermediates. *J. Bacteriol.* 85, 284–292.

Gromova, I., and Celis, J. E. (2006). Protein detection in gels by silver staining: a procedure compatible with mass-spectrometry. *Cell Biol. A Lab. Handb.* 4, 421–429.

Gummadi, S. N., and Panda, T. (2003). Purification and biochemical properties of microbial pectinases—a review. *Process Biochem.* 38, 987–996.

Hammerschmidt, R., and Kuć, J. (1982). Lignification as a mechanism for induced systemic resistance in cucumber. *Physiol. Plant Pathol.* 20, 61–71.

Harms, N., Koningstein, G., Dontje, W., Muller, M., Oudega, B., Luirink, J., et al. (2001). The early

interaction of the outer membrane protein PhoE with the periplasmic chaperone Skp occurs at the cytoplasmic membrane. *J. Biol. Chem.* 276, 18804–18811.

Hestrin, S., and Schramm, M. (1954). Synthesis of cellulose by *Acetobacter xylinum*. 2. Preparation of freeze-dried cells capable of polymerizing glucose to cellulose. *Biochem. J.* 58, 345–352.

Higuchi, T. (2004). Microbial degradation of lignin: role of lignin peroxidase, manganese peroxidase, and laccase. *Proc. Japan Acad. Ser. B* 80, 204–214.

Himmel, M. E. (2016). *Biomass Conversion: Methods and Protocols*. Springer Customer Service Center Gmbh.

Horikawa, Y., and Sugiyama, J. (2009). Localization of crystalline allomorphs in cellulose microfibril. *Biomacromolecules* 10, 2235–2239.

Hu, S. Q., Gao, Y. G., Tajima, K., Sunagawa, N., Zhou, Y., Kawano, S., et al. (2010). Structure of bacterial cellulose synthase subunit D octamer with four inner passageways. *Proc. Natl. Acad. Sci. U. S. A.* 107, 17957–17961.

Iida, A., Ohnishi, Y., and Horinouchi, S. (2008a). An OmpA family protein, a target of the GinI/GinR quorum-sensing system in *Gluconacetobacter intermedius*, controls acetic acid fermentation. *J. Bacteriol.* 190, 5009–5019.

Iida, A., Ohnishi, Y., and Horinouchi, S. (2008b). Control of acetic acid fermentation by quorum sensing via N-acylhomoserine lactones in *Gluconacetobacter intermedius*. *J. Bacteriol.* 190, 2546–2555.

Iida, A., Ohnishi, Y., and Horinouchi, S. (2009). Identification and characterization of target genes of the GinI/GinR quorum-sensing system in *Gluconacetobacter intermedius*. *Microbiology* 155, 3021–3032.

Imai, T., and Sugiyama, J. (1998). Nanodomains of Iα and Iβ cellulose in algal microfibrils. *Macromolecules* 31, 6275–6279.

Ishihara, M., Matsunaga, M., Hayashi, N., and Tišler, V. (2002). Utilization of D-xylose as carbon source for production of bacterial cellulose. *Enzyme Microb. Technol.* 31, 986–991.

Iyer, P. R., Catchmark, J., Brown, N. R., and Tien, M. (2011). Biochemical localization of a protein involved in synthesis of *Gluconacetobacter hansenii* cellulose. *Cellulose* 18, 739–747.

Jahn, C. E., Selimi, D. A., Barak, J. D., and Charkowski, A. O. (2011). The *Dickeya dadantii* biofilm matrix consists of cellulose nanofibres, and is an emergent property dependent upon the type III secretion system and the cellulose synthesis operon. *Microbiology* 157, 2733–2744.

Janisiewicz, W. J., Conway, W. S., Brown, M. W., Sapers, G. M., Fratamico, P., and Buchanan, R. L. (1999). Fate of *Escherichia coli* O157: H7 on fresh-cut apple tissue and its potential for transmission by fruit flies. *Appl. Environ. Microbiol.* 65, 1–5.

Jørgensen, H., Kristensen, J. B., and Felby, C. (2007). Enzymatic conversion of lignocellulose into fermentable sugars: Challenges and opportunities. *Biofuels, Bioprod. Biorefining* 1, 119–134.

Kawabata, A., Sawayama, S., and Uryu, K. (1974). A study on the contents of pectic substances in fruits, vegetable fruits and nuts. *Japanese J. Nutr.*

Keegstra, K., Talmadge, K. W., Bauer, W. D., and Albersheim, P. (1973). The structure of plant cell walls III. A model of the walls of suspension-cultured sycamore cells based on the interconnections of the macromolecular components. *Plant Physiol.* 51, 188–197.

Keshk, S., and Kazuhiko, S. (2005). Evaluation of different carbon sources for bacterial cellulose production. *African J. Biotechnol.* 4, 478.

Keshk, S., and Sameshima, K. (2005). Evaluation of different carbon sources for bacterial cellulose production. *African J. Biotechnol.* 4, 478–482.

Klemm, D., Heublein, B., Fink, H.-P., and Bohn, A. (2005). Cellulose: fascinating biopolymer and sustainable raw material. *Angew. Chem. Int. Ed. Engl.* 44, 3358–93.

Kolb, A., Busby, S., Buc, I. I., Garges, S., and Adhya, S. (1993). Transcriptional regulation by cAMP and its receptor protein. *Annu. Rev. Biochem.* 62, 749–797.

Koo, H. M., Song, S. H., Pyun, Y. R., and Kim, Y. S. (1998). Evidence that a beta-1,4-endoglucanase secreted by *Acetobacter xylinum* plays an essential role for the formation of cellulose fiber. *Biosci. Biotechnol. Biochem.* 62, 2257–2259.

Körner, H., Sofia, H. J., and Zumft, W. G. (2003). Phylogeny of the bacterial superfamily of CRP-FNR transcription regulators: exploiting the metabolic spectrum by controlling alternative gene programs. *FEMS Microbiol. Rev.* 27, 559–592.

Kornmann, H., Duboc, P., Marison, I., and von Stockar, U. (2003). Influence of nutritional factors on the nature, yield, and composition of exopolysaccharides produced by *Gluconacetobacter xylinus* I-2281. *Appl. Environ. Microbiol.* 69, 6091–6098.

Koyama, M., Helbert, W., Imai, T., Sugiyama, J., and Henrissat, B. (1997). Parallel-up structure evidences the molecular directionality during biosynthesis of bacterial cellulose. *Proc. Natl. Acad. Sci.* 94, 9091–9095.

Krajewski, V., Simić, P., Mouncey, N. J., Bringer, S., Sahm, H., and Bott, M. (2010). Metabolic engineering of *Gluconobacter oxydans* for improved growth rate and growth yield on glucose by elimination of gluconate formation. *Appl. Environ. Microbiol.* 76, 4369–4376.

Kroon-Batenburg, L. M. J., and Kroon, J. (1997). The crystal and molecular structures of cellulose I and II. *Glycoconj. J.* 14, 677–690.

Kubiak, K., Kurzawa, M., Jedrzejczak-Krzepkowska, M., Ludwicka, K., Krawczyk, M., Migdalski, A., et al. (2014). Complete genome sequence of *Gluconacetobacter xylinus* E25 strain-Valuable and effective producer of bacterial nanocellulose. *J. Biotechnol.* 176, 18–19.

Kuga, S., Takagi, S., and Brown, R. M. (1993). Native folded-chain cellulose II. *Polymer (Guildf).* 34, 3293–3297.

Kumagai, A., Mizuno, M., Nozaki, K., Saxena, I. M., and Amano, Y. (2011). Comparative atudy on the ability to produce gentiobiose in cellulose-producing bacteria *Asaia bogorensis* and *Gluconacetobacter xylinus*. *J. Appl. Glycosci.* 58, 147–150.

Kumar, R., Singh, S., and Singh, O. V (2008). Bioconversion of lignocellulosic biomass: biochemical and molecular perspectives. *J. Ind. Microbiol. Biotechnol.* 35, 377–391.

Kuo, C., Lin, P., and Lee, C. (2010). Enzymatic saccharification of dissolution pretreated waste cellulosic fabrics for bacterial cellulose production by *Gluconacetobacter xylinus*. *J. Chem. Technol. Biotechnol.* 85, 1346–1352.

Kuo, C., Teng, H., and Lee, C. (2015). Knock-out of glucose dehydrogenase gene in *Gluconacetobacter xylinus* for bacterial cellulose production enhancement. *Biotechnol. Bioprocess Eng.* 20, 18–25.

Laemmli, U. K. (1970). Cleavage of structural proteins during the assembly of the head of bacteriophage T4. *Nature* 227, 680–685.

Li, Z., Wang, L., Hua, J., Jia, S., Zhang, J., and Liu, H. (2015). Production of nano bacterial cellulose from waste water of candied jujube-processing industry using *Acetobacter xylinum*. *Carbohydr. Polym.* 120, 115–119.

Lin, D., Lopez-Sanchez, P., Li, R., and Li, Z. (2014). Production of bacterial cellulose by *Gluconacetobacter hansenii* CGMCC 3917 using only waste beer yeast as nutrient source. *Bioresour. Technol.* 151, 113–119.

Link, K. P., and Walker, J. C. (1933). The isolation of catechol from pigmented Onion scales and its significance in relation to disease resistance in Onions. *J. Biol. Chem.* 100.

Lu, B., Xu, A., and Wang, J. (2014). Cation does matter: how cationic structure affects the dissolution of cellulose in ionic liquids. *Green Chem.* 16, 1326–1335.

Mamlouk, D., and Gullo, M. (2013). Acetic acid bacteria: physiology and carbon sources oxidation. *Indian J. Microbiol.* 53, 377–384.

Matthysse, A., White, S., and Lightfoot, R. (1995). Genes required for cellulose synthesis in *Agrobacterium tumefaciens*. *J. Bacteriol.* 177, 1069–1075.

Mayer, R., Ross, P., Weinhouse, H., Amikam, D., Volman, G., Ohana, P., et al. (1991). Polypeptide composition of bacterial cyclic diguanylic acid-dependent cellulose synthase and the occurrence of immunologically crossreacting proteins in higher plants. *Proc. Natl. Acad. Sci.* 88, 5472–5476.

McManus, J. B., Deng, Y., Nagachar, N., Kao, T., and Tien, M. (2016). AcsA–AcsB: The core of the cellulose synthase complex from *Gluconacetobacter hansenii* ATCC23769. *Enzyme Microb. Technol.* 82, 58–65.

Meddeb-Mouelhi, F., Moisan, J. K., and Beauregard, M. (2014). A comparison of plate assay methods for detecting extracellular cellulase and xylanase activity. *Enzyme Microb. Technol.* 66, 16–19.

Mikkelsen, D., Flanagan, B. M., Dykes, G. A., and Gidley, M. J. (2009). Influence of different carbon sources on bacterial cellulose production by *Gluconacetobacter xylinus* strain ATCC 53524. *J. Appl. Microbiol.* 107, 576–583.

Mohnen, D. (2008). Pectin structure and biosynthesis. *Curr. Opin. Plant Biol.* 11, 266–277.

Money, R. W., and Christian, W. A. (1950). Analytical data of some common fruits. *J. Sci. Food Agric.* 1, 8–12.

Moosavi-Nasab, M., and Yousefi, A. (2011). Biotechnological production of cellulose by *Gluconacetobacter xylinus* from agricultural waste. *Iran J Biotechnol* 9, 94–101.

Morgan, J. L. W., McNamara, J. T., and Zimmer, J. (2014). Mechanism of activation of bacterial cellulose synthase by cyclic di-GMP. *Nat. Struct. Mol. Biol.* 21, 489–96.

Morgan, J. L. W., Strumillo, J., and Zimmer, J. (2013). Crystallographic snapshot of cellulose synthesis and membrane translocation. *Nature* 493, 181–6.

Nakai, T., Nishiyama, Y., Kuga, S., Sugano, Y., and Shoda, M. (2002). *ORF2* gene involves in the construction of high-order structure of bacterial cellulose. *Biochem. Biophys. Res. Commun.* 295, 458–462.

Nakai, T., Sugano, Y., Shoda, M., Sakakibara, H., Oiwa, K., Tuzi, S., et al. (2013). Formation of highly twisted ribbons in a carboxymethylcellulase gene-disrupted strain of a cellulose-producing bacterium. *J. Bacteriol.* 195, 958–964.

Napoli, C., Dazzo, F., and Hubbell, D. (1975). Production of cellulose microfibrils by *Rhizobium. Appl. Microbiol.* 30, 123–131.

Nguyen, V. T., Flanagan, B., Gidley, M. J., and Dykes, G. A. (2008). Characterization of cellulose production by a *Gluconacetobacter xylinus* strain from Kombucha. *Curr. Microbiol.* 57, 449–453.

Nicol, F., His, I., Jauneau, A., Vernhettes, S., Canut, H., and Höfte, H. (1998). A plasma membrane-bound putative endo-1, 4-β-d-glucanase is required for normal wall assembly and cell elongation in *Arabidopsis*. *EMBO J.* 17, 5563–5576.

Nieto-Peñalver, C. G., Bertini, E. V, and de Figueroa, L. I. C. (2012). Identification of N-acyl homoserine lactones produced by *Gluconacetobacter diazotrophicus* PAL5 cultured in complex and synthetic media. *Arch. Microbiol.* 194, 615–622.

Nobles, D. R., Romanovicz, D. K., and Brown, R. M. (2001). Cellulose in cyanobacteria. Origin of vascular plant cellulose synthase? *Plant Physiol.* 127, 529–542.

O'Sullivan, A. (1997). Cellulose: the structure slowly unravels. *Cellulose* 4, 173–207.

Omadjela, O., Narahari, A., Strumillo, J., Mélida, H., Mazur, O., Bulone, V., et al. (2013). BcsA and BcsB form the catalytically active core of bacterial cellulose synthase sufficient for *in vitro* cellulose synthesis. *Proc. Natl. Acad. Sci. U. S. A.* 110, 17856–61.

Paice, M. G., Bourbonnais, R., Desrochers, M., Jurasek, L., and Yaguchi, M. (1986). A xylanase gene from *Bacillus subtilis*: nucleotide sequence and comparison with *B. pumilus* gene. *Arch. Microbiol.* 144, 201–206.

Park, Y. B., Lee, C. M., Kafle, K., Park, S., Cosgrove, D. J., and Kim, S. H. (2014). Effects of plant cell wall matrix polysaccharides on bacterial cellulose structure studied with vibrational sum frequency generation spectroscopy and x-ray diffraction. *Biomacromolecules* 15, 2718–2724.

Pilz, I., Schwarz, E., Kilburn, D. G., Miller Jr, R. C., Warren, R. A., and Gilkes, N. R. (1990). The tertiary structure of a bacterial cellulase determined by small-angle X-ray-scattering analysis. *Biochem. J.* 271, 277.

Pourramezan, G. Z., Roayaei, A. M., and Qezelbash, Q. R. (2009). Optimization of culture conditions for bacterial cellulose production by *Acetobacter* sp. 4B-2. *Biotechnology* 8, 150–154.

Preisig, O., Zufferey, R., and Hennecke, H. (1996). The *Bradyrhizobium japonicum fixGHIS* genes are required for the formation of the high-affinity cbb3-type cytochrome oxidase. *Arch. Microbiol.* 165, 297–305.

Qi, Y., Rao, F., Luo, Z., and Liang, Z. X. (2009). A flavin cofactor-binding PAS domain regulates c-di-GMP synthesis in AxDGC2 from *Acetobacter xylinum*. *Biochemistry* 48, 10275–10285.

Qureshi, O., Sohail, H., Latos, A., and Strap, J. L. (2013). The effect of phytohormones on the growth, cellulose production and pellicle properties of *Gluconacetobacter xylinus* ATCC 53582. *Acetic Acid Bact.* 2, 39–46.

Ravid, K., and Freshney, R. I. (1998). *DNA transfer to cultured cells*. John Wiley & Sons.

Reyrat, J. M., David, M., Blonski, C., Boistard, P., and Batut, J. (1993). Oxygen-regulated in vitro transcription of *Rhizobium meliloti nifA* and *fixK* genes. *J. Bacteriol.* 175, 6867–6872.

Robledo, M., Jiménez-Zurdo, J. I., Velázquez, E., Trujillo, M. E., Zurdo-Piñeiro, J. L., Ramírez-Bahena, M. H., et al. (2008). *Rhizobium* cellulase CelC2 is essential for primary symbiotic infection of legume host roots. *Proc. Natl. Acad. Sci. U. S. A.* 105, 7064–7069.

Römling, U., and Galperin, M. Y. (2015). Bacterial cellulose biosynthesis: diversity of operons, subunits, products, and functions. *Trends Microbiol.* 9, 545–557.

Römling, U., Galperin, M. Y., and Gomelsky, M. (2013). Cyclic di-GMP: the first 25 years of a universal bacterial second messenger. *Microbiol. Mol. Biol. Rev.* 77, 1–52.

Ross, P., Mayer, R., and Benziman, M. (1991). Cellulose biosynthesis and function in bacteria. *Microbiol. Rev.* 55, 35–58.

Ryjenkov, D. A., Simm, R., Römling, U., and Gomelsky, M. (2006). The PilZ domain is a receptor for the second messenger c-di-GMP: The PilZ domain protein YcgR controls motility in enterobacteria. *J. Biol. Chem.* 281, 30310–30314.

Sainz, F., Navarro, D., Mateo, E., Torija, M. J., and Mas, A. (2016). Comparison of D-gluconic acid production in selected strains of acetic acid bacteria. *Int. J. Food Microbiol.* 222, 40–47.

Salgado, H., Santos-Zavaleta, A., Gama-Castro, S., Millán-Zárate, D., Díaz-Peredo, E., Sánchez-Solano, F., et al. (2001). RegulonDB (version 3.2): transcriptional regulation and operon organization in *Escherichia coli* K-12. *Nucleic Acids Res.* 29, 72–74.

Saxena, I. M., Brown Jr., R. M., and acsAii (1995a). Identification of a second cellulose synthase gene (*acsAII*) in *Acetobacter xylinum*. *J. Bacteriol.* 177, 5276–5283.

Saxena, I. M., Brown Jr, R. M., Fevre, M., Geremia, R. A., and Henrissat, B. (1995b). Multidomain architecture of beta-glycosyl transferases: implications for mechanism of action. *J. Bacteriol.* 177, 1419.

Saxena, I. M., Kudlicka, K., Okuda, K., and Brown, R. M. (1994). Characterization of genes in the cellulose-synthesizing operon (*acs* operon) of *Acetobacter xylinum*: Implications for cellulose

crystallization. *J. Bacteriol.* 176, 5735–5752.

Saxena, I. M., Lin, F. C., and Brown, R. M. (1990). Cloning and sequencing of the cellulose synthase catalytic subunit gene of *Acetobacter xylinum*. *Plant Mol. Biol.* 15, 673–683.

Schiewer, S., and Patil, S. B. (2008). Pectin-rich fruit wastes as biosorbents for heavy metal removal: equilibrium and kinetics. *Bioresour. Technol.* 99, 1896–1903.

Schramm, M., and Hestrin, S. (1954). Factors affecting production of cellulose at the air/liquid interface of a culture of *Acetobacter xylinum*. *J. Gen. Microbiol.* 11, 123–129.

Schultz, S. C., Shields, G. C., and Steitz, T. A. (1991). Crystal structure of a CAP-DNA complex: the DNA is bent by 90 degrees. *Science (80-.).* 253, 1001–1007.

Shigematsu, T., Takamine, K., Kitazato, M., Morita, T., Naritomi, T., Morimura, S., et al. (2005). Cellulose production from glucose using a glucose dehydrogenase gene (*gdh*)-deficient mutant of *Gluconacetobacter xylinus* and its use for bioconversion of sweet potato pulp. *J. Biosci. Bioeng.* 99, 415–422.

Shinagawa, E., Ano, Y., Yakushi, T., Adachi, O., and Matsushita, K. (2009). Solubilization, purification, and properties of membrane-bound D-glucono-δ-lactone hydrolase from *Gluconobacter oxydans*. *Biosci. Biotechnol. Biochem.* 73, 241–244.

Shokri, J., and Adibkia, K. (2013). "Cellulose - Medical, Pharmaceutical and Electronic Applications," in, eds. T. van de Ven and L. Godbout (InTech).

Silacci, M. W., and Morrison, J. C. (1990). Changes in pectin content of Cabernet Sauvignon grape berries during maturation. *Am. J. Enol. Vitic.* 41, 111–115.

Simm, R., Morr, M., Kader, A., Nimtz, M., and Römling, U. (2004). GGDEF and EAL domains inversely regulate cyclic di-GMP levels and transition from sessibility to motility. *Mol. Microbiol.* 53, 1123–1134.

Sørensen, H. (1962). Decomposition of lignin by soil bacteria and complex formation between autoxidized lignin and organic nitrogen compounds. *J. Gen. Microbiol.* 27, 21–34.

Standal, R., Iversen, T. G., Coucheron, D. H., Fjaervik, E., Blatny, J. M., and Valla, S. (1994). A new gene required for cellulose production and a gene encoding cellulolytic activity in *Acetobacter xylinum* are colocalized with the *bcs* operon. *J. Bacteriol.* 176, 665–672.

Steel, R., and Walker, T. K. (1957). A comparative study of cellulose-producing cultures and celluloseless mutants of certain *Acetobacter* spp. *Microbiology* 17, 445–452.

Strap, J. L., Latos, A., Shim, I., and Bonetta, D. T. (2011). Characterization of pellicle inhibition in *Gluconacetobacter xylinus* 53582 by a small molecule, pellicin, identified by a chemical genetics screen. *PLoS One* 6, e28015. doi:10.1371/journal.pone.0028015.

Sugisawa, T., Ojima, S., Matzinger, P. K., and Hoshino, T. (1995). Isolation and characterization of a new vitamin C producing enzyme (l-gulono-γ-lactone dehydrogenase) of bacterial origin. *Biosci. Biotechnol. Biochem.* 59, 190–196.

Sunagawa, N., Fujiwara, T., Yoda, T., Kawano, S., Satoh, Y., Yao, M., et al. (2013). Cellulose complementing factor (Ccp) is a new member of the cellulose synthase complex (terminal

complex) in *Acetobacter xylinum*. *J. Biosci. Bioeng.* 115, 607–612.

Tahara, N., Yano, H., and Yoshinaga, F. (1997). Two types of cellulase activity produced by a cellulose-producing *Acetobacter* strain. *J. Ferment. Bioeng.* 83, 389–392.

Tajima, K., Nakajima, K., Yamashita, H., Shiba, T., Munekata, M., and Takai, M. (2001). Cloning and sequencing of the beta-glucosidase gene from *Acetobacter xylinum* ATCC 23769. *DNA Res.* 8, 263–269.

Talmadge, K. W., Keegstra, K., Bauer, W. D., and Albersheim, P. (1973). The structure of plant cell walls I. The macromolecular components of the walls of suspension-cultured sycamore cells with a detailed analysis of the pectic polysaccharides. *Plant Physiol.* 51, 158–173.

Tarutina, M., Ryjenkov, D. A., and Gomelsky, M. (2006). An unorthodox bacteriophytochrome from *Rhodobacter sphaeroides* involved in turnover of the second messenger c-di-GMP. *J. Biol. Chem.* 281, 34751–34758.

Tokoh, C., Takabe, K., Fujita, M., and Saiki, H. (1998). Cellulose synthesized by *Acetobacter xylinum* in the presence of acetyl glucomannan. *Cellulose* 5, 249–261.

Tonouchi, N., Tsuchida, T., Yoshinaga, F., Beppu, T., and Horinouchi, S. (1996). Characterization of the biosynthetic pathway of cellulose from glucose and fructose in *Acetobacter xylinum*. *Biosci. Biotechnol. Biochem.* 60, 1377–1379.

Toyosaki, H., Naritomi, T., Seto, A., Matsuoka, M., Tsuchida, T., and Yoshinaga, F. (1995). Screening of bacterial cellulose-producing *Acetobacter* strains suitable for agitated culture. *Biosci. Biotechnol. Biochem.* 59, 1498–1502.

Uhlin, K. I., Atalla, R. H., and Thompson, N. S. (1995). Influence of hemicelluloses on the aggregation patterns of bacterial cellulose. *Cellulose* 2, 129–144.

Umeda, Y., Hirano, A., Ishibashi, M., Akiyama, H., Onizuka, T., Ikeuchi, M., et al. (1999). Cloning of cellulose synthase genes from *Acetobacter xylinum* JCM 7664: implication of a novel set of cellulose synthase genes. *DNA Res.* 6, 109–115.

Velasco, L., Mesa, S., Xu, C., Delgado, M. J., and Bedmar, E. J. (2004). Molecular characterization of *nosRZDFYLX* genes coding for denitrifying nitrous oxide reductase of *Bradyrhizobium japonicum*. *Antonie Van Leeuwenhoek* 85, 229–235.

Vorwerk, S., Somerville, S., and Somerville, C. (2004). The role of plant cell wall polysaccharide composition in disease resistance. 9, 203–209.

Wardrop, A. B. (1971). Occurrence and formation in plants. *Sarkanen, KV Lignins*.

Weinhouse, H., Sapir, S., Amikam, D., Shilo, Y., Volman, G., Ohana, P., et al. (1997). C-di-GMP-binding protein, a new factor regulating cellulose synthesis in *Acetobacter xylinum*. *FEBS Lett.* 416, 207–211.

Whitney, J. C., and Howell, P. L. (2013). Synthase-dependent exopolysaccharide secretion in Gram-negative bacteria. *Trends Microbiol.* 21, 63–72.

Williams, W. S., and Cannon, R. E. (1989). Alternative environmental roles for cellulose produced by *Acetobacter xylinum*. *Appl. Environ. Microbiol.* 55, 2448–2452.

Wong, H. C., Fear, A. L., Calhoon, R. D., Eichinger, G. H., Mayer, R., Amikam, D., et al. (1990). Genetic organization of the cellulose synthase operon in *Acetobacter xylinum*. *Proc. Natl. Acad. Sci. U. S. A.* 87, 8130–8134.

Yamada, Y., Yukphan, P., Vu, H. T. L., Muramatsu, Y., Ochaikul, D., and Nakagawa, Y. (2012a). Subdivision of the genus *Gluconacetobacter* Yamada, Hoshino and Ishikawa 1998: the proposal of *Komagatabacter* gen. nov., for strains accommodated to the *Gluconacetobacter xylinus* group in the *α-Proteobacteria*. *Ann. Microbiol.* 62, 849–859.

Yamada, Y., Yukphan, P., Vu, H. T. L., Muramatsu, Y., Ochaikul, D., Tanasupawat, S., et al. (2012b). Description of *Komagataeibacter* gen. nov., with proposals of new combinations (*Acetobacteraceae*). *J. Gen. Appl. Microbiol.* 58, 397–404.

Ye, J., Coulouris, G., Zaretskaya, I., Cutcutache, I., Rozen, S., and Madden, T. L. (2012). Primer-BLAST: a tool to design target-specific primers for polymerase chain reaction. *BMC Bioinformatics* 13, 134.

Yu, X., and Atalla, R. H. (1996). Production of cellulose II by *Acetobacter xylinum* in the presence of 2,6-dichlorobenzonitrile. *Int. J. Biol. Macromol.* 19, 145–146.

Zaar, K. (1979). Visualization of pores (export sites) correlated with cellulose production in the envelope of the gram-negative bacterium *Acetobacter xylinum*. *J. Cell Biol.* 80, 773–777.

Zhong, C., Zhang, G. C., Liu, M., Zheng, X. T., Han, P. P., and Jia, S. R. (2013). Metabolic flux analysis of *Gluconacetobacter xylinus* for bacterial cellulose production. *Appl. Microbiol. Biotechnol.* 97, 6189–6199.

Zogaj, X., Nimtz, M., Rohde, M., Bokranz, W., and Römling, U. (2001). The multicellular morphotypes of *Salmonella typhimurium* and *Escherichia coli* produce cellulose as the second component of the extracellular matrix. *Mol. Microbiol.* 39, 1452–1463.

Zuo, J., Niu, Q.-W., Nishizawa, N., Wu, Y., Kost, B., and Chua, N.-H. (2000). KORRIGAN, an *Arabidopsis* endo-1, 4-β-glucanase, localizes to the cell plate by polarized targeting and is essential for cytokinesis. *Plant Cell* 12, 1137–1152.

7. Appendix

Appendix Table 1: Details of primer sets used in this study. **Bold** bases indicate 5' overhangs for Gibson Assembly. <u>Underlined</u> bases indicate the stop codon (in-frame in final assembly) inserted into *fixK*, replacing Q155.

Use	Target	Amplicon Length (bp)	Source DNA	Locus Tag	Forward Primer Sequence (5' → 3')	Reverse Primer Sequence (5' → 3')
fixK mutagenesis	*fixK*	617	*K. xylinus* *K. hansenii*	ATCC53582_00024 GXY_RS00790	GCGGTGGAAACCATCATCAC	TATCCCGTAACTGAGAGCCC
	Left side of *fixK*	315	*fixK* Amplicon	N/A	GCGGTGGAAACCATCATCAC	**GCCAATTTA**TTCGTTGGATGCCTCTTCGAGAAG
	Right side of *fixK*	319	*fixK* Amplicon	N/A	**GGCGT**AACTGGTTGCGGCCCAG	TATCCCGTAACTGAGAGCCC
	Chl Cassette	802	*pSEVA331Bb*	N/A	**<u>TCC</u>AACGAA**TAAATTGGCGAAAATGAGACGTTGATCGG	**GCAACCAG**TTACGCCCCGCCCTGCCAC
Endpoint PCR	*bcsA* side of *bcsAB*	184	*K. xylinus* *K. hansenii*	ATCC53582_00602 GXY_RS03935	ACAATGGGCTGGATGGTCGA	ACCCGCAAAAGAAGGTCGCA
	bcsB side of *bcsAB*	197	*K. xylinus* *K. hansenii*	ATCC53582_00602 GXY_RS03935	AATGCGTTCCATCTTGGGCTTGAC	ATCAGGTCAAGATAGGCGCCAACA
	bcsC	103	*K. xylinus* *K. hansenii*	ATCC53582_00603 GXY_RS03940	TACCAGTCGCATATCGGCAATCGT	GCAGGTCGTTCAACTGGCTTTCAT
	bcsD	153	*K. xylinus* *K. hansenii*	ATCC53592_00604 GXY_RS03945	TCACCCTGTTTCTTCAGACCCTGT	TCAGTTCGATCTGCAGCTTGTCCA
	bcsZ	98	*K. xylinus* *K. hansenii*	ATCC53582_00600 GXY_RS03925	CACCAACCTGCAGCATACCAATGA	CGCCATCTGTGGCATTGTTCTTGT
	bcsH	191	*K. xylinus* *K. hansenii*	ATCC53582_00601 GXY_RS15550	TGTTGCCGATGAATGGAGTCCTGT	TGTCTGTCTTGGTCATGCTGGTCA
	bglX	116	*K. xylinus* *K. hansenii*	ATCC53582_00606 GXY_RS03950	TACCGATCAGGAACTTGTCTAT	CAAAAGTGGTGTAGGTCAGG

Appendix Figure 1: Identification of possible post translational modifications of secreted BcsZ from *K. xylinus* (A) and *K. hansenii* (B) grown in SHF_2. Blue bars represent unique peptides detected by mass spectroscopy after trypsin digestion. Orange 'o' represents predicted oxidized methionine resides, red 'd' represents a predicted deamidated asparagine residue and blue 'c' represents a predicted carbamidomethylated cytosine.

Appendix Figure 2: Map of pSEVA331Bb plasmid. This plasmid was used to optimize transformation in *K. xylinus* and *K. hansenii*. The chloramphenicol resistance cassette was also used in the *fixK*-Chl-*fixK* construct to mutate *fixK*.